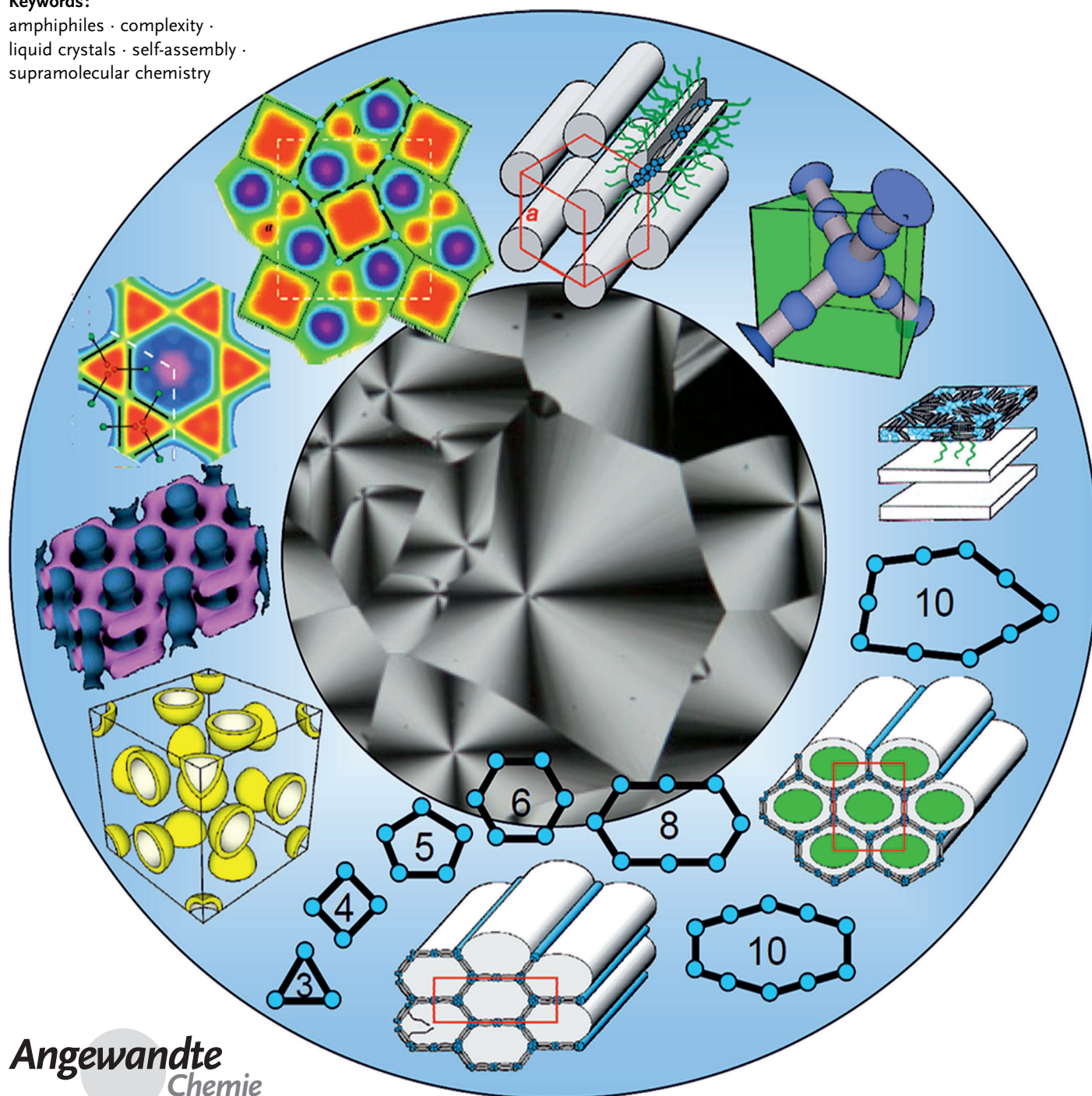


Development of Structural Complexity by Liquid-Crystal Self-assembly

Carsten Tschierske*

Keywords:

amphiphiles · complexity ·
liquid crystals · self-assembly ·
supramolecular chemistry



Since the discovery of the liquid-crystalline state of matter 125 years ago, this field has developed into a scientific area with many facets. This Review presents recent developments in the molecular design and self-assembly of liquid crystals. The focus is on new exciting soft-matter structures distinct from the usually observed nematic, smectic, and columnar phases. These new structures have enhanced complexity, including multicompartment and cellular structures, periodic and quasiperiodic arrays of spheres, and new emergent properties, such as ferroelectricity and spontaneous achiral symmetry-breaking. Comparisons are made with developments in related fields, such as self-assembled monolayers, multiblock copolymers, and nanoparticle arrays. Measures of structural complexity used herein are the size of the lattice, the number of distinct compartments, the dimensionality, and the logic depth of the resulting supramolecular structures.

1. Introduction

In his recent review in *Angewandte Chemie* on the perspectives of Chemistry, J. M. Lehn wrote: "...chemistry builds the bridge between the laws of the universe and their specific expressions in life and thoughts. The goal is to discover, understand, and implement the processes that governs the evolution of matter towards increasing complexity from particles to thoughts..."^[1] Hence, the understanding of the organization of individual molecules into supramolecular structures with specific properties at nano-, meso-, and macroscopic length scales is an important area of current science and represents an important contribution of chemistry to the general understanding of the development of complexity by self-organization and self-assembly.^[2] There are numerous different approaches to this problem involving supramolecular chemistry in isotropic solutions, periodically ordered solid-state structures, such as coordination polymers and metal-organic frameworks (MOFs), pattern formation on surfaces, and self-assembly and compartmentalization in soft matter, such as multiblock copolymers and liquid crystals (LCs), on which the focus is herein. All of these areas require the fundamental understanding of the development of ordered structures from simple building blocks.^[3,4]

The unique feature of liquid crystals is that order develops while a high degree of mobility is retained. This combination leads to the self-healing, adaptive, and stimuli-responsive behavior of these supramolecular systems, which made LCs the quintessential self-assembling molecular materials of the modern area.^[5-8] LCs are the advanced technological material found in low-power-consuming flat-panel displays (liquid-crystal displays, LCDs), which in the last decades has allowed the development of mobile data processing and communication tools with huge effects on the development of the human societies today and in the future. Although LCDs might or might not be replaced by other technologies in the future, the fundamental knowledge gained with LCs can be used for the directed self-assembly of a huge variety of other functional

materials. Moreover, research in this area is a key science for the understanding of the development of order and complexity in soft self-assembled systems in general.

In the most general sense, a condensed matter state can be considered as LC if there is orientational or positional long-range order in at least one direction and no fixed position for individual molecules. Long-range order could be orientational and positional; orientational order means that the molecules adopt a parallel alignment to minimize the excluded volume and to maximize the attractive intermolecular interactions. Figure 1 shows the simplest types of LC phases. LC phases which have exclusively orientational order are assigned as nematic (N) phases. Along with the orientational order, the mesogens can adopt a long-range or quasi long-range periodicity of their preferred positions along one direction (1D), leading to layers (smectic phases = Sm) or along two different directions (2D phases); in the latter case columns are formed and these LC phase are assigned as

From the Contents

| | |
|---|------|
| 1. Introduction | 8829 |
| 2. The Early History: From Rods to Discs | 8831 |
| 3. From Molecular Shape to Interfaces | 8832 |
| 4. Organizations of Spheroidal Aggregates | 8842 |
| 5. Packing of Spherical Nano-objects in Liquid-Crystal Templates | 8845 |
| 6. Vesicular Liquid-Crystal Phases | 8847 |
| 7. Polyphilic Liquid Crystals | 8850 |
| 8. Complex Compartmentalization Patterns of T- and X-Shaped Polyphiles | 8851 |
| 9. Tiling Patterns in Other Self-Assembled Systems | 8863 |
| 10. Bent-Core Liquid Crystals: Chirality and Polar Order | 8865 |
| 11. Summary and Conclusions | 8868 |

[*] Prof. C. Tschierske
 Institut für Chemie, Organische Chemie, Martin-Luther-Universität
 Halle-Wittenberg
 06120 Halle Saale (Germany)
 E-mail: Carsten.tschierske@chemie.uni-halle.de

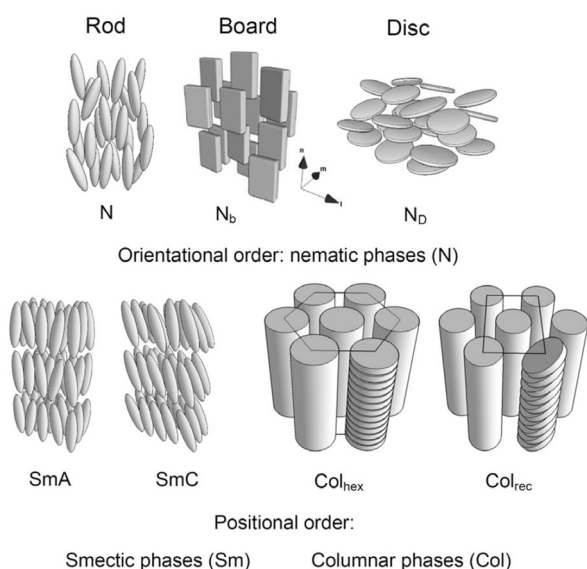


Figure 1. LC phases of rod-like, board-like (sanidic), and disc-like molecules.

columnar phases (Col). It should be pointed out that for the formation of smectic and columnar phases it is not required that orientational order is retained; that is, in these phases the molecules can be orientational ordered or not. In all LC phases the molecules or the supermolecular aggregates forming the phase do not have fixed positions and can rotate and move, which provides mobility.

Molecules, macromolecules, supermolecular aggregates, or nanoparticles can act as building blocks of liquid-crystalline phases; the focus is here on low-molecular-weight molecules. It should be noted that besides the LC phases of solvent-free molecular or supramolecular systems (thermotropic LC phases), LC phases can also be found in dilute aqueous solutions of amphiphilic molecules (lyotropic LC phases).^[9,10] These lyotropic LC phases are based on micellar aggregates with a rod-like, disc-like, or spherical shape, which form nematic, smectic, columnar, and cubic LC phases. Thus, a basic requirement for the mobility of the LC-state is either a solvent in mixed systems (lyotropic LC phases) or flexible molecular building blocks in solvent-free systems (thermotropic LC phases). As mobility is strongly temperature-dependent, LC phases occur in certain temperature ranges between the highly ordered solid crystalline state and the

disordered isotropic liquid state, and therefore LC phases are also assigned as mesophases.

There are numerous subtypes of these smectic and columnar phases in which the rotation of the molecules around their long axis can be restricted or a tilt of the molecules with respect to a major direction takes place. For example, smectic phases in which the molecules have a uniform tilt direction in the layers are assigned as SmC and those where the tilt is random or the orientation is on average perpendicular to the layer planes are assigned as SmA. In columnar phases, the columns could be arranged on a hexagonal, square, rectangular, or oblique 2D lattice, leading to Col_{hex}, Col_{squ}, Col_{rec}, and Col_{obl} phases, respectively, which can be further classified according to their plane groups (Figure 2). Furthermore, mesophases with periodicity in all three dimensions (3D phases), often with cubic symmetry (Cub), can also occur. These phases with more complex structure will be described when they are first mentioned in the text.

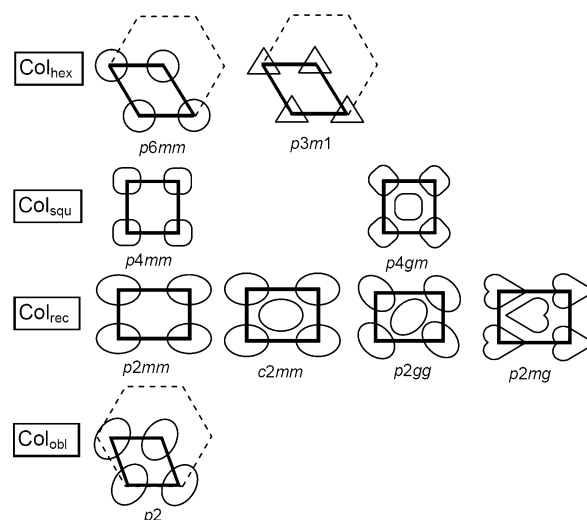


Figure 2. The fundamental types of 2D lattices currently known for columnar LC phases with their relevant plane groups.

There are three major methods used for the investigations and characterization of LC materials. Differential scanning calorimetry (DSC) provides the phase-transition temperatures and associated enthalpy values, and polarizing microscopy (PM) and X-ray diffraction (XRD) experiments provide information about the kind of order in the mesophase. Dielectric investigations, solid-state NMR spectroscopy, neutron scattering, electro-optical investigations, freeze-fracture electron microscopy, and numerous other methods are used for more detailed investigation of the structure, dynamics, and other specific properties.^[7]

Some arbitrarily chosen examples of PM and XRD patterns of the fundamental major types of LC phases are shown in Figure 3. The presence of birefringence leads to the typical PM textures of LC between crossed polarizers, indicating the presence of orientational or positional order; only the cubic phases are optically isotropic and therefore appear dark. The presence of sharp reflections in the small-



Carsten Tschierske received his Ph.D. in Organic Chemistry in 1985 at the University of Halle. After habilitation and several visitor professorships in Marburg, Würzburg, and Fukuoka (Japan), he was appointed in 1994 as Professor of Organic Chemistry/Supramolecular Chemistry at the Martin Luther University Halle-Wittenberg, Halle, Germany. He is coauthor of over 300 scientific publications and received the "Dozentenstipendium" and the Frederiks medal.

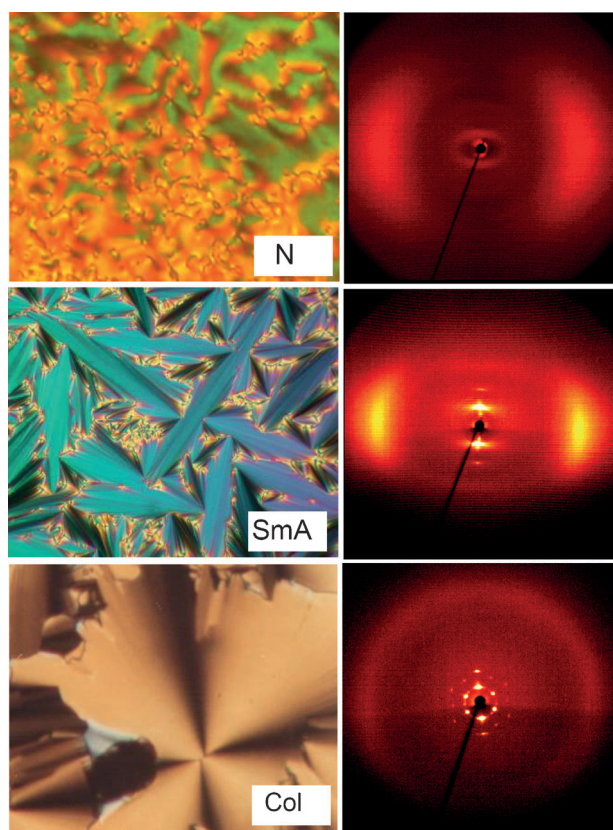


Figure 3. Typical textures (left) and representative 2D XRD patterns (right) of nematic (N), smectic (SmA), and columnar (Col_{hex}) LC phases (aligned samples).

angle region of the XRD patterns indicates long range 1D, 2D, or 3D periodicity. In contrast to simple smectic and columnar LC phases, the structural analysis of more complex mesophases requires additional XRD methods, among them synchrotron XRD, allowing detection of diffraction peaks with very weak intensity and a precise determination of diffraction intensities. This is required for the reconstruction of electron-density maps, which visualize the organization of their molecules in the LC phases. The intensities are related to the electron-density distribution $E(x,y)$ by Fourier transformation, for the case of 2D structures according to Equation (1), where $F(hk)$ is the structure factor of a diffraction peak with index (hk) . The electron-density distribution is related to the experimentally observed relative diffraction intensity $I(hk)$ through Equation (2).

$$E(xy) = \sum_{hk} F(hk) \exp[i2\pi(hx + ky)] \quad (1)$$

$$E(xy) = \sum_{hk} \sqrt{I(hk)} \exp[i2\pi(hx + ky) + \varphi_{hk}] \quad (2)$$

As the structure factor $F(hk)$ is a complex number, the phase angle cannot be determined directly. However, the centrosymmetric structure of most LC phases simplifies the problem by the fact that φ can only take up the values of 0 or π . This allows all possible phase combinations to be examined based on the three or four most intense reflections. Combined with additional knowledge (molecular shape, length, top-

ology, volume of each part, distribution of electron density among the different parts, changes on varying size, or electron density of a particular moiety), the choice of a combination can be made on the merit of each reconstructed electron density map, followed by further refinement including additional reflections.^[11,12b,13] Furthermore, grazing incidence XRD (GISAXS) of aligned thin films allows recording of 2D-resolved XRD patterns of monodomains, which are often required for proper indexation of the XRD patterns of complex LC phases that usually have only a limited number of small-angle reflections.^[14] The diffuse scattering in the wide angle range (ca. 0.45 nm) provides information about the mean lateral distance between the individual molecules and is considered as evidence for the local disorder in LC phases, whereas crystalline phases have numerous sharp reflections in this region. Confirmation of mobility is gained by shearing the sample under the PM, where the typical birefringent textures of LCs are changed and flow already by applying relatively weak shearing forces, whereas the textures of crystalline materials and LC glasses are retained without changes.

The field of LC research started 125 years ago with the astonishing observation of birefringence and selective light reflection in a chiral liquid formed by cholesteryl benzoate. This was discovered and investigated by Friedrich Reinitzer and Otto Lehmann and classified as a new state of matter between the solid crystals and the disordered isotropic liquids.^[15,16] However, at that time there was no knowledge about the connections between molecular structure and the formation of LC phases; even the structure of cholesterol was unknown.^[17] Daniel Vorländer (1867–1941), who was Professor of Chemistry at the University Halle (Saale), Germany between 1902 and 1935, was the first who investigated the relations between molecular structure and LC self-assembly in a systematic way. Before him there were about 35 LC compounds; after his retirement there were more than two thousand such compounds,^[18,19] which even in the beginning of the 1960s represented the majority of known LC materials.^[20–23] Starting with Vorländer in 1903, during the 125 years of LC research, 110 years have been performed at the Institute of Chemistry of the University Halle, and thus this is that unique place in the world with the longest continuous expertise in investigation of this state of matter, which was only interrupted by the period around World War II. This review gives a personal view of the recent development of the field of liquid crystal self-assembly. Focus is on the design of new exciting phase structures distinct from the usually observed and well investigated nematic, smectic, and columnar phases shown in Figure 1 and having enhanced complexity. The measures of complexity used herein are the size of the lattice, the number of distinct compartments, the dimensionality and the logic depth^[24] of the resulting structures.^[25]

2. The Early History: From Rods to Discs

Already in 1907, Vorländer recognized that “...the liquid-crystalline state results from a molecular structure which is as linear as possible...” and this was the guideline for LC design for the next 70 years.^[26] Vorländer introduced a number of

building blocks, among them several heterocycles^[27] and the first metallomesogens (**1** and **2** in Figure 4).^[28,29] He also obtained first compounds with other than nematic phases and with more than only one LC phase, synthesized the first chiral smectic compounds, which later turned out to show ferroelectricity,^[30] and reported about “circular infection”, nowadays known and broadly used as the induction of helical superstructures by chiral dopands. Vorländer prepared first examples of mesogenic dimers (**3**) and already in 1919 he asked the question if infinitely long molecules would be able to form extraordinary stable LC phases^[31] and he indeed prepared the first LC main-chain polymers (**4**).^[32] It is

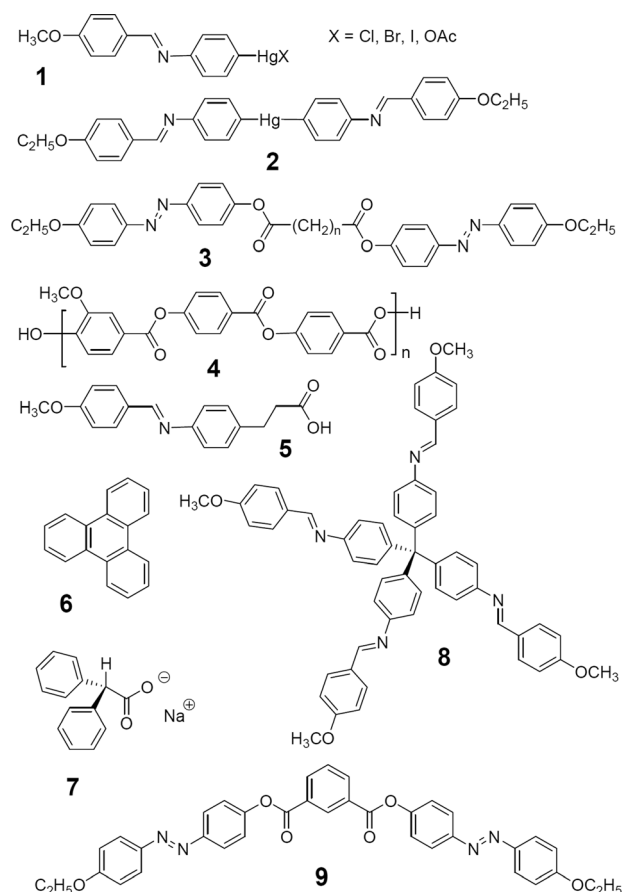


Figure 4. Examples of LCs (**1–5**, **7**, **9**) and potentially LC materials (**6**, **8**) investigated by Vorländer,^[23] and a selection of his samples stored in his famous cigar boxes (courtesy of W. Weissflog, University of Halle).

interesting to note that Vorländer thought about LC polymers at about the same time that Staudinger, who graduated at Halle University under Vorländer, was starting polymer science in Freiburg i. Br. around 1920.

Although Vorländer recognized the rigid and linear molecular shape as the basic principle of LC phase design, he kept always asking if there would be other molecular shapes leading to LC self-assembly. He synthesized numerous molecules with different shapes. Among them molecules with a bent shape (**9**), for which much later, in 1996, the formation of polar order and spontaneous achiral symmetry-breaking was discovered (bent-core mesogens; see Section 10).^[33] Star-shaped molecules (**8**) were also considered, a concept which was later developed by Eidenschink,^[34] Malthete,^[35] Tschierske,^[36] Lehmann,^[37] and others. Most interestingly, he also speculated that disc-like molecules could organize in LC phases composed of stacks of these molecules, similar to “Volta’s columns”. Although he investigated flat aromatic compounds such as triphenylene (**6**) and perylene in this respect, at that time he was unable to detect LC properties for these compounds. However, without recognizing it, he indeed discovered the first thermotropic columnar LC phase in a very different ionic compound, sodium diphenylacetate (**7**).^[38] He described more than 150 other ionic liquid crystals, a field which much later received significant attention in connection with ionic liquids,^[39] ionic liquid crystals,^[40,41] and the concept of ionic self-assembly.^[42] Moreover, sodium diphenylacetate (**7**) is the prototype of LC compounds without the usually used flexible alkyl chains, which quite recently has been rediscovered.^[43] Besides ionic LC, he also described about 200 supramolecular hydrogen bonded LC (for example **5**), which are nowadays considered as the first examples of supramolecular mesogens.^[44]

The proposal of disc-like molecules forming columnar LC phases has presumably been forgotten and for the next decades research in LC was nearly exclusively focussed on rod-like molecules, especially owing to the growing importance of these LC for application in displays. However, in 1977, Chandrasekhar, Sadashiva, and Suresh from the Raman Research Institute Bangalore reported LC hexaalkanoates of hexahydroxybenzene, which, based on XRD data, form a columnar LC phase.^[45,46] Since that time, the field of discotic mesogens and columnar LC phases has developed into a broad field,^[47] and presently columnar phases formed by molecules with π -conjugated disc-like cores is a major promising group of materials for organic semiconductors in application as organic photoconductors, field-effect transistors, and for photovoltaics.^[48]

3. From Molecular Shape to Interfaces

3.1. Polycatenar Molecules and Bicontinuous Cubic Phases

A major effect of the discovery of disc-like mesogens was that scientists started searching for alternative design concepts for mesogenic materials, as Vorländer already did several decades before. At first, attention was focused on the transition between rod-like and disc-like molecular shapes by

attaching more than only one alkyl chain to the ends of rod-like molecules (Figure 5), pioneered by Malthete, Destrade, Levelut, and Tinh.^[49] These molecules were assigned as phasmidic (having in total six chains) or polycatenar (any number of chains more than two). Weissflog et al. extended this concept to so-called swallow-tail compounds with branched end chains, having two branches with approximately equal length (for example, compound **13** in Figure 5).^[50] Alternatively, the number of chains attached to

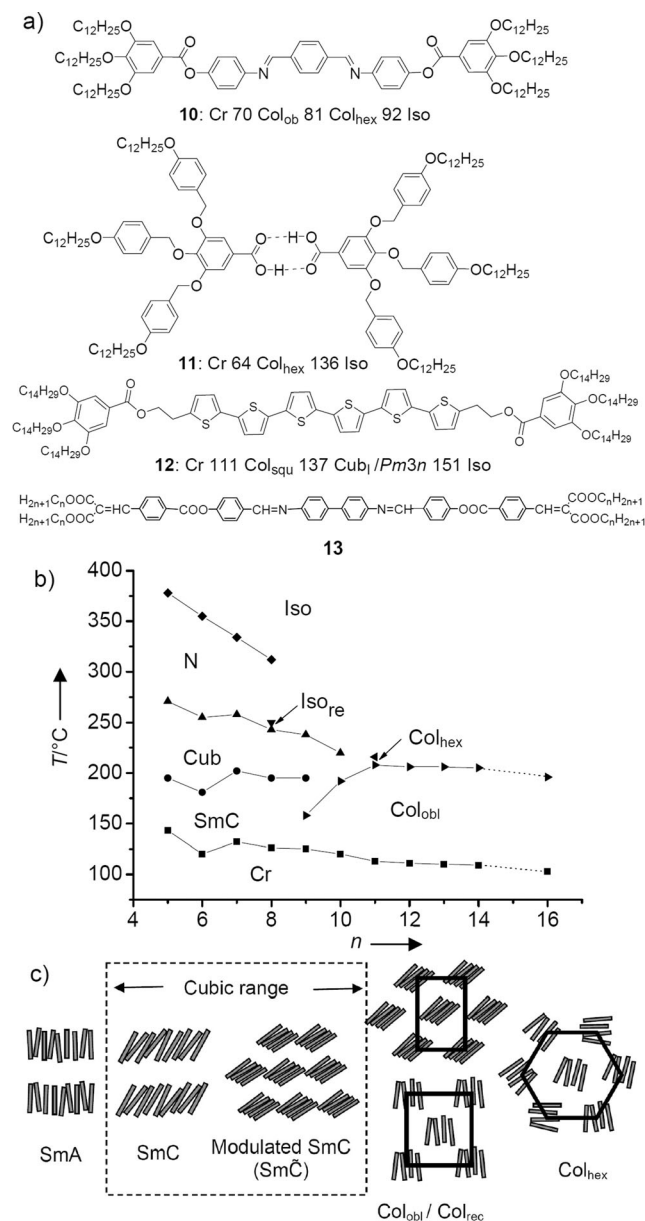


Figure 5. a) Examples of polycatenar mesogens ($T/^\circ C$).^[49, 85, 139] b) phase diagram of the homologous series of double-swallow-tailed compounds **13** depending on chain length^[50] (Iso_{re} = re-entrant isotropic liquid phase); c) molecular organization in the mesophases of polycatenar compounds; the cubic range indicates the range in which smectic or modulated smectic phases can coexist with or be replaced by bicontinuous cubic phases. b) Courtesy of W. Weissflog, University of Halle, to be published in ref. [7b], c) was reproduced with modifications from ref. [120b] with permission of The Royal Society of Chemistry.

disc-like mesogens was decreased, leading to board-like (sanidic) molecules.^[51] This research has also been driven by the search for biaxial nematic phases (N_b , see Figure 1), which were expected to be formed by board-like molecules.^[52] Although the biaxial nematic phase has not yet been achieved with polycatenar or sanidic compounds, this research lead to the discovery of new LC phases and to a new concept of LC design.

One type of these new mysterious phases was an optically isotropic phase, for which XRD indicated a cubic lattice. For polycatenar molecules, the phase sequences involving the cubic phases in the sequence nematic–smectic–cubic–columnar (N–SmC–Cub–Col) were often observed on increasing the length and the number of alkyl chains attached to the rod-like core,^[49, 53] as shown in Figure 5b for compound **13**.^[50]

In this way these molecules provided a transition between the smectic phases, typically formed by rod-like molecules, and the columnar phases, typical for disc-like molecules. The cubic phases, occurring at this transition, are a special mode of molecular self-assembly of mesogenic molecules with a periodicity in three dimensions instead of only in one (smectic) or two (columnar). The same phase sequence lamellar–cubic–columnar was previously known from lyotropic LC systems formed by amphiphilic molecules in the presence of water,^[9] but also for anhydrous soaps, as shown by the work of Luzzati and Skoulios.^[40, 54] Already before the work on polycatenar mesogens, thermotropic cubic LC phases have been observed for polar rod-like molecules incorporating hydrogen bonding groups, as the dimers of 4'-alkoxy-3'-nitrophenyl-4-carboxylic acids (compound **14** in Figure 6), first reported by Gray et al.,^[55] analogous 3'-cyano-biphenyl-4-carboxylic acids with long chains ($n > 15$)^[56–58] and 1,2-bis(4-alkoxybenzoyl)hydrazines discovered by Schubert and Demus et al.^[58, 59] Formation of cubic phases by these molecules was not in line with the theories of LC self-assembly at that time based on the shape anisometry of the molecules, and therefore not well understood before cubic phases were discovered in polycatenar mesogens.^[60, 61]

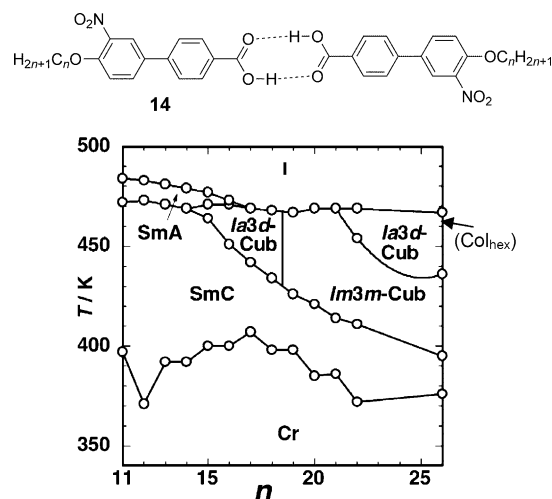


Figure 6. Cubic phases of compounds **14** depending on alkyl chain length (the Col_{hex} phase is observed as a metastable phase on cooling of compound **14** with $n = 26$).^[58] Reproduced from Ref. [58], copyright 2012, Wiley-VCH.

The similarity of the phase sequences and morphologies of anhydrous soaps, surfactant-water systems, and diblock copolymers^[62] with the smectic, columnar, and cubic ordering in polycatenar liquid crystals became obvious, and amphiphilic character and micro-segregation were recognized as key features of mesomorphic self-assembly.^[63–68] In principle, almost all mesogenic molecules capable of forming positional ordered mesophases (e.g.: Sm, Col, Cub) can be regarded as amphiphiles; that is, these molecules are composed of at least two distinct and to a certain degree incompatible segments, either rigid cores and flexible chains, or polar and non-polar groups, or combinations of both. Accordingly, their mesophases can be described by the shape of nanoscale segregated compartments and the interfaces separating them.^[65] In smectic phases, the interfaces are flat layers, in columnar phases they are honeycombs (Voronoi honeycombs,^[69] see Figure 7a,c), whereas in the cubic phases considered here, two networks of branched columns are separated by infinite minimal surfaces (Figure 7b).^[70] In analogy to self-assembling amphiphiles, these cubic phases^[58,71] occurring at the Sm–Col cross-over of polycatenar mesogens can be considered as bicontinuous cubic phases, abbreviated as Cub_v.^[72]

The understanding of mesophase formation has thus turned from simply considering the molecular shape to nanoscale segregations and the shape of the interfaces resulting during self-assembly,^[65] the curvature of which increases in the order lamellar–bicontinuous cubic–columnar. As this sequence is often observed by increasing the alkyl chain volume or by an increase in the temperature (Figure 5b), it appears that in the Cub_v phases the aromatic units are organized in the branched networks, whereas the alkyl chains form the continuum and the infinite minimal surfaces can be considered to separate the two interwoven labyrinths and to be located between the ends of the alkyl chains.

As shown in Figure 8, there are three distinct types of infinite minimal surfaces, related to the valence (ν) of the nodes in the interwoven networks of branched columns: $\nu = 3$: Schoen's gyroid ($Ia\bar{3}d$), $\nu = 4$: Schwarz's D-surface ($Pn\bar{3}m$);

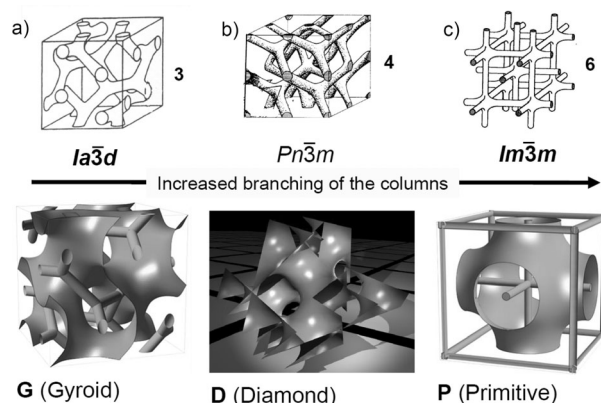


Figure 8. The three bicontinuous cubic phases with their labyrinths of branched columns (top) and the infinite minimal surfaces separating these labyrinths (bottom). D: see http://anusf.anu.edu.au/anusf_visualization/viz_showcase/stephen_hyde/; G and P are reproduced with permission from Ref. [58], copyright 2008, American Chemical Society.

$\nu = 6$: Schwarz's P-surface ($Im\bar{3}m$). The $Ia\bar{3}d$ cubic phase with a valence of the branches of $\nu = 3$ (Figure 8a) is the most often observed type. The gyroid infinite minimal surfaces, introduced by Schoen^[73] separates these two networks. Recent studies by Kutsumizu et al. suggest that the threefold nodes in the $Ia\bar{3}d$ phase of rod-like and polycatenar compounds appear to dominate the structure and actually could be considered as layer fragments with a twisted triangular shape (Figure 9), representing the majority of the interwoven networks.^[74] It thus seems that the rod-like molecular shape has a modifying effect on the structure of the $Ia\bar{3}d$ cubic phase (compare Figure 8a and 9a).

The $Pn\bar{3}m$ phase (Figure 8b) involving tetrahedral branches with $\nu = 4$ (double diamond) is often observed in lyotropic systems, but rarely found for thermotropic LCs and is less well-investigated in these systems. In thermotropic LC systems it was first reported for a rod-like amphiphile^[75] and then found to be more often formed by disc-like molecules (see Section 3.3.3).^[76–78]

The $Im\bar{3}m$ phase is the second frequently observed cubic phase, but for polycatenar and other rod-like mesogens it does not have the simple structure, known for this type of cubic phases in lyotropic systems and shown in Figure 8c. The lattice parameters are much larger than expected for such a simple structure formed by two interwoven networks with branchings having a valence of $\nu = 6$. Different models were proposed for this type of cubic phase (Figure 10). The first model, proposed by Levelut et al.^[79a] and then modified by Kutsumizu et al. and Saito et al.^[79b–d] has additional surfaces between the networks (**A**), i.e. there are molecules in the networks as well as between them. However, these structures are not in line with experimental electron density maps and therefore can be excluded. The other two models **B** and **C** are backed up by electron

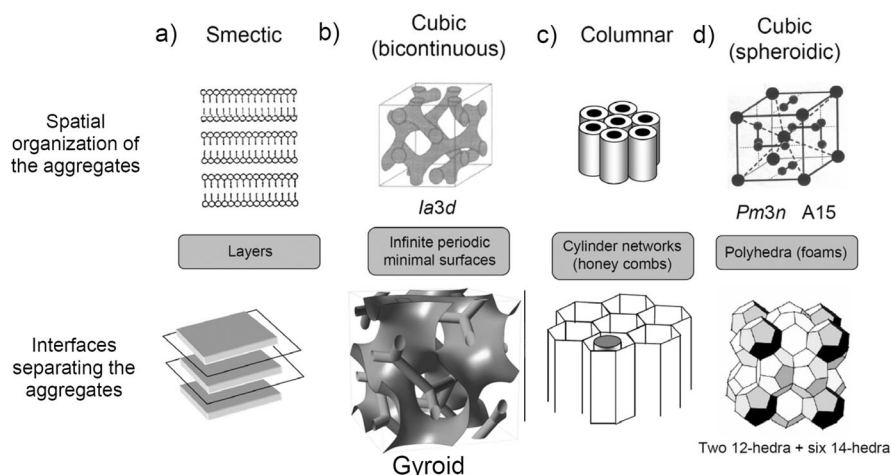


Figure 7. Interfaces in LC phases; the upper line shows the aggregate cores and the lower one their interaggregate interfaces.^[120d] Reproduced from Ref. [120d] copyright 2012, Wiley-VCH; the gyroid was reproduced with permission from Ref. [58], copyright 2008, American Chemical Society.

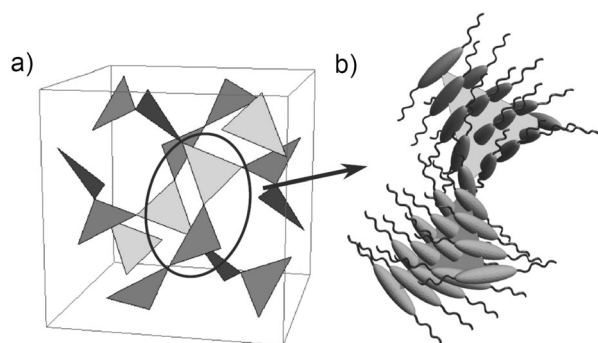


Figure 9. Model of the $Ia\bar{3}d$ phase as proposed for rod-like and polycatenar molecules: a) unit cell with triangles forming the two branched networks; b) shows the proposed tilted and twisted arrangement of the molecules on these triangles.^[74] Reprinted with permission from Ref. [74], copyright 2012, the Physical Society of Japan.

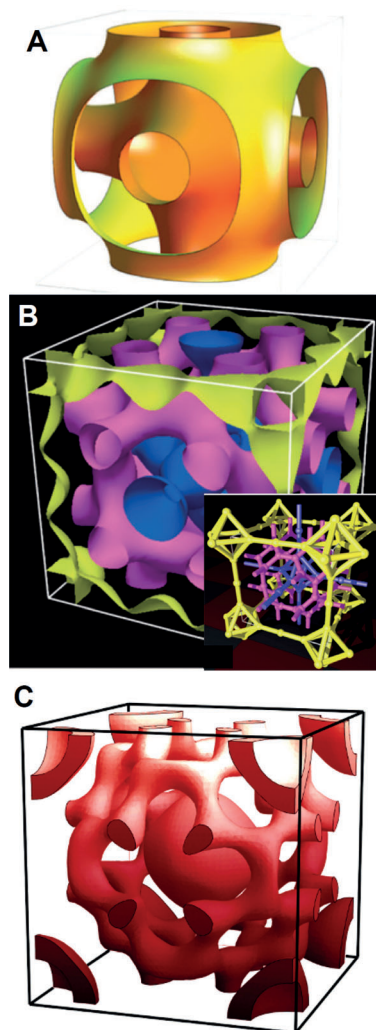


Figure 10. Three distinct models **A–C** of the $Im\bar{3}m$ phase of rod-like and polycatenar mesogens; in **A** the molecules are located between the interfaces with the ends of the alkyl chains on these surfaces; the inset in **B** shows the three labyrinths of branched columns involving the aromatic cores; in **C** the aromatic cores are in the red areas.^[79,81] **A, C)** Reprinted with permission from Ref. [58], copyright 2008, American Chemical Society; **B)** reproduced from Ref. [80] with permission of The Royal Society of Chemistry.

density calculations using different methods for the choice of phase combinations and differ in structural details. In the model **B**, proposed by Ungar et al.,^[80] there are three networks, leading to an overall tricontinuous structure. In model **C**, proposed by Kutsumizu et al.,^[58,81] there are small vesicles in the center and at the corners of the unit cell formed by the rod-like aromatics cores and filled with alkyl chains. These vesicles are separated by a network of branched columns. Although model **C** is composed of regions with different degree of curvature, this structure avoids any nodes with valences $\nu > 3$. The complete absence of the classical $Im\bar{3}m$ structure (Figure 8c) with $\nu = 6$ and the rare occurrence of the $Pn\bar{3}m$ lattice with $\nu = 4$ in thermotropic cubic phases of rod-like molecules suggests that such high-valence nodes are disfavored for these compounds, which is most likely due to the unfavorable non-parallel arrangement of the rod-like cores required by these high valence nodes. As such high valence nodes are absent in model **C** and the formation of vesicular spheroids has recently been reported for cubic phases of other compounds (see Section 6),^[82,83] this structure appears to be possible. This hybrid structure **C**, combining a net formed by threefold branched columns separating vesicles located on the $Im\bar{3}m$ cubic lattice, would have increased complexity compared to all previously reported bicontinuous cubic phases formed by flexible binary amphiphiles, namely surfactants and diblock copolymers. It seems that the rod-like segments provide restrictions which compete with the interface curvature required by nano-segregation and thus increase the complexity of molecular self-assembly in these cubic phases. In the homologous series of 4'-alkoxy-3'-nitrobiphenyl-4-carboxylic acids **14** (Figure 6) and also in other homologous series the $Im\bar{3}m$ phase appears between two $Ia\bar{3}d$ cubic phases with nearly identical lattice parameters and similar structure, that is, in both $Ia\bar{3}d$ phases the rod-like cores of the molecules form the networks and the alkyl chains form the continuum.^[74] A possible explanation for the presence of two similar $Ia\bar{3}d$ phases could be, that for short chains the influence of the rod-like core is large and the $Ia\bar{3}d$ phase of the short chain compounds, occurring adjacent to the smectic phases, has triangular layer sheets (Figure 9). With growing chain length, the influence of the molecular shape decreases and the $Ia\bar{3}d$ phase of the long chain compounds ($n = 22$ – 26 , occurring adjacent to the columnar phase) is, especially at higher temperature, probably more similar to a structure composed of branched columns (Figure 8a); the $Im\bar{3}m$ phase could therefore be an intermediate structure occurring at the transition between these two modes of $Ia\bar{3}d$ phases which is stable at a distinct rod/chain ratio, that is, at a certain degree of molecular flexibility.

The rod-like shape of the rigid segments in polycatenar compounds also influences the structure of the smectic and columnar phases formed by these molecules. In contrast to the columnar phases of disc-like molecules, for polycatenar mesogens ribbons of parallel aligned rod-like molecules form columns with a non-circular cross sectional shape (Figure 5b). If orientational order of the molecules in adjacent ribbons is long range, rectangular and oblique lattices are often found, which are replaced by hexagonal columnar phases upon further chain elongation or with rising temperature. In these

hexagonal columnar phases the ribbons of the rod layers are thought to lose their close contact and adopt a time- and space-averaged packing on a hexagonal lattice (Figure 5c).^[77,84]

Besides the significant insights into mesophase formation, the work on polycatenar molecules also provided new building blocks for molecular design of cubic and columnar mesogens, namely the di- and trialkoxy benzoates and the 3,4,5-tris-(*p*-*n*-alkoxybenzyloxy)benzoyloxy units (DOBOB) introduced by Malthete^[85] and Kok.^[86] Nowadays these units belong to the most often used building blocks for the design of mesogenic materials. Percec et al. have further extended this concept to even larger groups by dendritic branching of benzyl ether-based structures.^[87] Instead of attaching three or more linear alkyl chains also bulky groups as oligo(dimethylsiloxane) groups,^[88] perfluorinated chains,^[89,90] branched alkyl chains,^[91] and strongly folded flexible chains, such as oligo(ethylene oxide) or oligo(propylene oxide),^[92] can be used to change the phase structure from lamellar to bicontinuous cubic and columnar.

3.2. From Supramolecular Mesogens to Self-Assembled Polymolecular Aggregates

Self-assembly of mesogenic unit from smaller building blocks leads to supramolecular LC, which is well-known for hydrogen bonding in benzoic acids dimers, related complexes between benzoic acids and pyridines^[93,94] and the more recently introduced halogen bonding.^[95] The hydrogen bonding aggregates **11** (Figure 5) and **15** (Figure 11) are examples of polycatenar and disc-like mesogens based on intermolecular hydrogen bonding.^[96] In this case LC phase formation can be considered as a stepwise process, involving the formation of discrete anisometric (disc-like) entities, which then self-assemble in columns which arrange on a periodic 2D lattice. The hydrogen bondings are in this case predominately perpendicular to the column long axis. Disc-like molecules incorporating amide groups (for example **16**) form hydrogen

bonding along the long axis of the resulting column, in this way stabilizing these columns, often with formation of a helical superstructure owing to the mismatch of the distances provided by C=O...H-N hydrogen bonding and π -stacking between the aromatic cores.^[97-99]

Self-assembly of taper-shaped molecules with hydrogen bonding groups at the apex, like amides,^[100] diols,^[101,102] carbohydrates,^[103-107] and other polyalcohols^[94,108,109] provides large aggregates, formed by cooperative and dynamic hydrogen bonding networks between these groups (Figure 11–13 for compounds **17–26** as selected examples).^[110] In this case there is no preferred direction of the hydrogen bondings and self-assembly occurs simultaneously along the columns and perpendicular to the columns. Thus the molecules immediately form columnar aggregates by nanoscale segregation of polar and lipophilic units, that is, by *endo* recognition of the hydrogen-bonding polar groups and *exo*-recognition of the lipophilic chains, without the intermediate stage of disc-like supramolecules. As no specific disc-like shape is provided by any discrete supramolecular species, the mesophase type easily changes and mainly depends on the number and length of the alkyl chains, and therefore, these columnar phases typically occur in phase sequences smectic–bicontinuous cubic–columnar–micellar cubic (see the next Section) upon changing the alkyl chain volume. This behavior is retained if the hydrogen bonding groups at the apex are replaced by ionic groups (compounds **27–29** in Figure 14).^[111] Thus the self-assembly of these molecules is dominated by amphiphilicity and nano-segregation and the mesophase type is determined by the resulting interfaces, whereas the effects of molecular shape are reduced compared to disc-like mesogens. Therefore, these LC phases could be regarded as thermotropic analogues of the corresponding lyotropic LC phases in aqueous systems. However, until the middle of the 1990s, the micellar cubic phase with the largest interface curvature was still missing for thermotropic LCs.

3.3. Micellar Cubic Phases

3.3.1. Micellar Cubic Phases of Flexible Amphiphiles

The micellar cubic phase (Cub_I), formed by spheroidal aggregates, was first discovered for 3,4,5-trialkoxylbenzamides derived from *N*-methylglucamide (**31**) and was introduced as a novel mode of thermotropic liquid crystal self-assembly in solvent-free systems by Tschierske et al.^[106,112] Figure 12a shows the original texture photo presented in the report from 1996^[112] indicating a birefringent columnar phase with spherulitic texture developing in the contact region between the smectic phase (SmA) of the single chain glucamide **19** and the optically isotropic micellar cubic phase (Cub_I) of the three-chain glucamide **20**, in complete agreement with the increase of the interface curvature in the phase sequence SmA–Col_{hex}–Cub_I upon increasing the concentration of the three-chain compound **20**. This indicated a micellar structure of this cubic phase, which was additionally confirmed by XRD indicating a cubic *Pm* $\bar{3}$ *n* lattice^[113] and by conductivity measurements of related 1-amino-propane-2,3-diols **21**.^[101,113] Electric conductivity is based here on proton conductivity by the hydrogen-

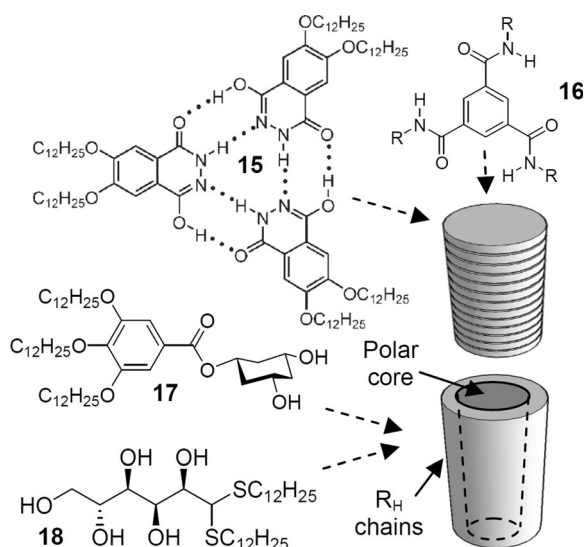


Figure 11. Hydrogen bonding in columnar LC phases.

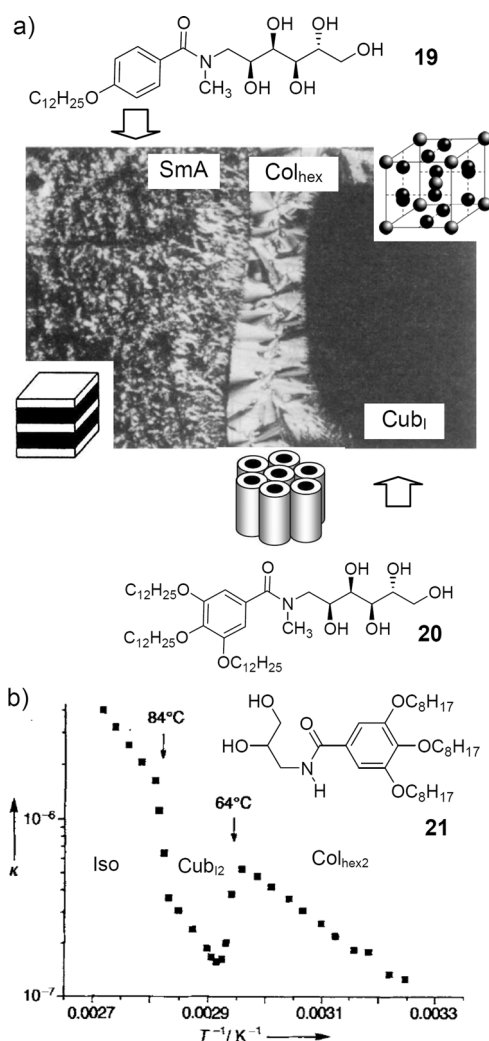


Figure 12. a) Contact region between the SmA phase of **19** and the micellar cubic phase (Cub_I) of **20** at $T=115^{\circ}\text{C}$ showing the development of a Col_{hex} phase^[112] between these two LC phases with different interface curvature and b) conductivity (κ) versus inverse temperature plot for the diol **21**.^[113] a) Reproduced from Ref. [112] with permission of The Royal Society of Chemistry; b) reproduced from Ref. [113] copyright 1997, Wiley-VCH.

bonding networks,^[114] which drops by nearly an order of magnitude at the transition from infinite columnar aggregates in the Col_{hex} phase to the isolated spheroidic aggregates in the Cub_I phase (Figure 12b).^[113] This concept was later used by Kato et al. for switching of ion conductivity.^[115] Percec, Ungar et al. have found this type of cubic phases for series of dendritic molecules and further investigated the $Pm\bar{3}n$ cubic phase by XRD and electron density reconstruction.^[11]

In the series of compounds **22–26** shown in Figure 13, the phase sequence SmA–Cub_V–Col_{hex}–Cub_I even develops in two opposite directions, either by increasing the size of the lipophilic segments, leading to negative curvature (type 2 phases)^[106,112] or by increasing the polar hydrogen-bonding units, which leads to the normal type phases (positive curvature, type 1 phases).^[116–119] The SmA phase with zero curvature divides the two sets of morphological equivalent structures with opposite sign of the interface curvature and

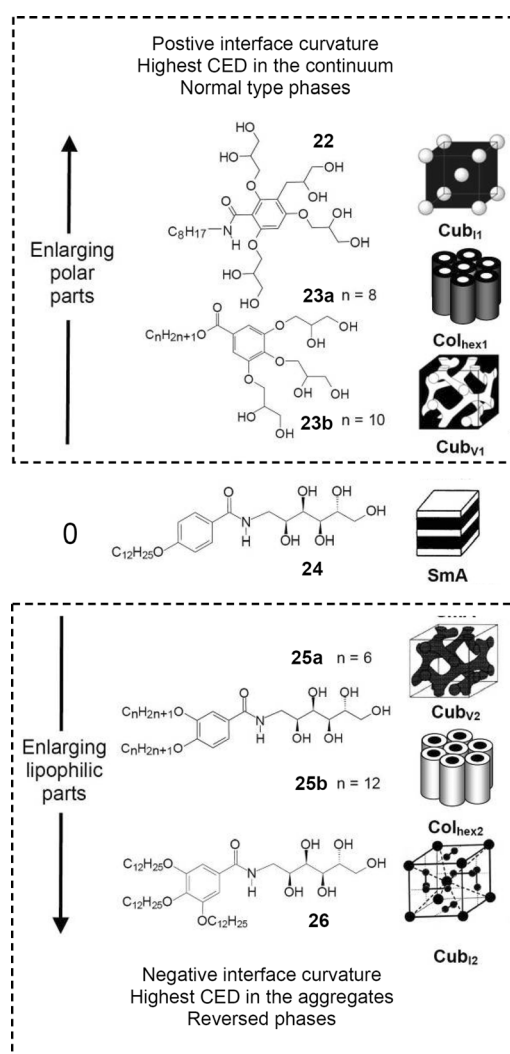


Figure 13. Phase sequence observed for solvent-free compounds **22–26** depending on the volume fraction of the incompatible molecular segments (polar parts: black, lipophilic parts: white) for **22**; a $Im\bar{3}m$ lattice is shown as a possible structure, but a full XRD analysis was not possible in this case.^[116] Reproduced with modifications from Ref. [270], The Royal Society of Chemistry.

reversed distribution of cohesive energy density (CED). This series illustrates the similarity of self-assembly in thermotropic and lyotropic LC systems, which are essentially based on the same fundamental principles of nanoscale segregation and curvature of interfaces.^[120]

Since their discovery^[112] the micellar cubic phases were found in numerous self-assembled thermotropic LC systems (Figure 14).^[11,71,87,115,120–135] In the series of LC carbohydrates, for example, they were intensively investigated by Goodby et al.^[107] Most extensive investigations with a broad range of structural variations have been carried out by Percec et al. for dendritic molecules based on benzylether type dendritic units (for example **32**), which was recently extensively reviewed.^[87] Remarkably, the vast majority of these micellar cubic phases have the space group $Pm\bar{3}n$ composed of 8 micelles per unit cell.^[11,113,136] Possible reasons for the dominance of this

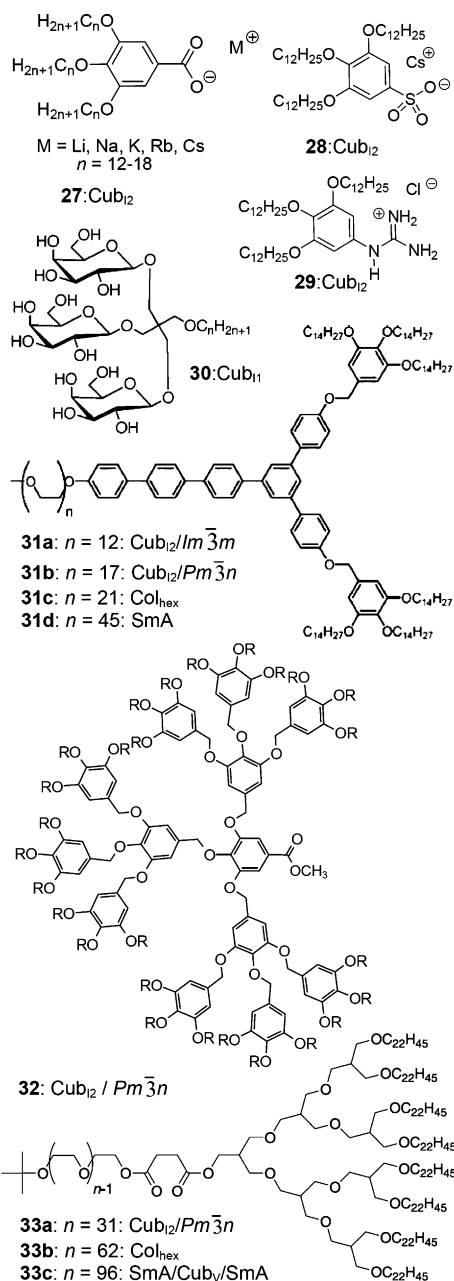


Figure 14. Examples of mesogens forming micellar cubic phases (Cub₁ = normal type; Cub₂ = reversed type).^[87, 107, 125a,c, 132–135]

relatively complicated packing over the simpler $Fm\bar{3}m$ and $Im\bar{3}m$ lattices will be discussed in Section 4.1.

3.3.2. Micellar Phases of Rod-like Molecules

In contrast to the taper-shaped and dendritic amphiphiles, the degree of interface curvature achievable with rod-like molecules is more limited, which is due to the longitudinal extension of the rod-like cores, and therefore the formation of micellar cubic phases is much less likely for these rigid compounds.^[137] Coil-rod-coil molecules with oligo(ethylene oxide) or oligo(propylene oxide) terminal chains (Figure 15), and related compounds with branched or dendritic chains^[92, 138] form square or hexagonal mesh phases, replacing

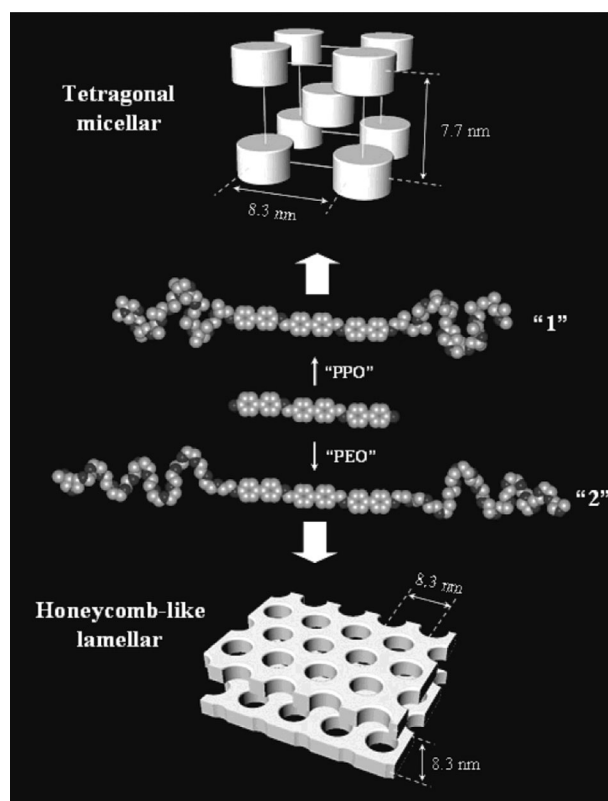


Figure 15. Transition from mesh layers to a tetragonal packing of discs upon increasing the terminal chain size of coil-rod-coil molecules.^[138b] Reprinted with permission from Ref. [138b], copyright 2005, American Chemical Society.

the non-distorted lamellar (smectic) phases. These mesh layers show a direct transition to distinct types of 3D packing of disc-like aggregates with hexagonal, body-centered tetragonal or monoclinic 3D lattice, replacing the micellar cubic phases composed of spheroidic aggregates and formed by flexible or conical molecules (Figure 15).

The sexithiophene-based hexacatenar compound **12** (see Figure 5)^[139] has flexible ethylene spacers between the relatively rigid and nearly rod-like sexithiophene core and the two branched end groups. The flexible spacers provide sufficient flexibility to allow the formation of spherical micellar aggregates, leading to a micellar cubic phase with $Pm\bar{3}n$ space group. It appears that this is the first example of a polycatenar compound forming a micellar cubic phase (Cub_i) instead of the usually observed bicontinuous cubic (Cub_v) and columnar phases (Col).

3.3.3. Cubic Phases of Disc-like Molecules

Most disc-like molecules apparently disfavor the formation of bicontinuous cubic phases at the smectic–columnar transition, and isotropic liquid and nematic phases were found instead.^[140,141] There are only few disc-like molecules forming cubic phases, and in many cases there is no knowledge about their structure.^[71a,142–144] Formation of bicontinuous cubic phases was recently observed by Aida et al. for disc-like triphenylenes with a periphery of imidazolium salt groups at

the ends of the six alkyl chains (Compound **64a** in Figure 31 a in Section 7.1);^[178] most of them are $\text{Cub}_V/\text{Ia}\bar{3}d$ phases and in one case the rare $\text{Cub}_V/\text{Pn}\bar{3}m$ phase was observed.

More recently Ohta et al. reported several series of phthalocyanines with different types of cubic phases (for example **34**).^[145] Often the thermal phase sequence $\text{Col}_{\text{hex}}-\text{Cub}_V/\text{Pn}\bar{3}m-\text{Cub}_V/\text{Pm}\bar{3}n-\text{Col}_{\text{squ}}-\text{Iso}$ is observed (arrows in Figure 16).^[146] The unusual features of this sequence are the

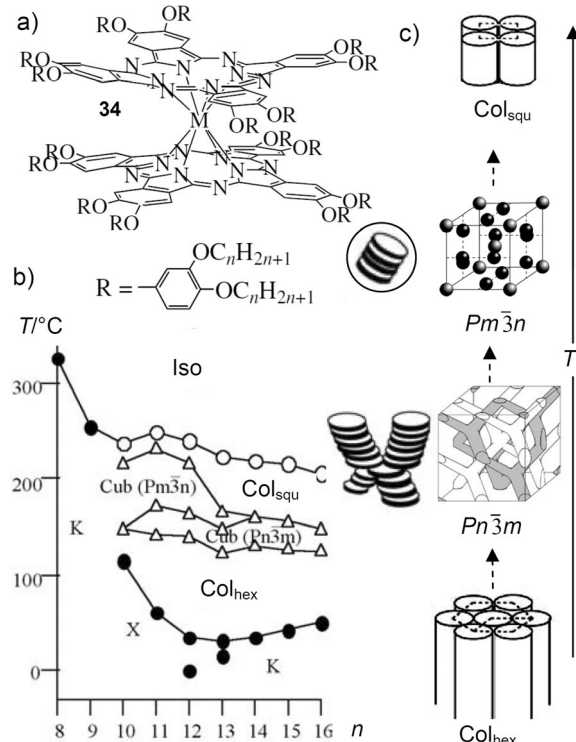


Figure 16. a) Phthalocyanines showing bicontinuous cubic $\text{Pn}\bar{3}m$ and micellar cubic $\text{Pm}\bar{3}n$ phases; b, c) chain-length-dependent mesophase sequence of **34** ($M = \text{Lu}$; Col_{squ} = columnar phase with square lattice);^[146a] b) Reproduced with modification and permission from Ref. [146a], copyright 2010 World Scientific Publishing Company.

appearance of cubic phases between two columnar phases, a hexagonal and a square, the direct transition between two distinct cubic phase types, a bicontinuous ($\text{Pn}\bar{3}m$) and a micellar ($\text{Pm}\bar{3}n$) without intermediate columnar phase, and the formation of the rarely observed bicontinuous cubic phases with $\text{Pn}\bar{3}m$ space group for nearly all investigated compounds (Figure 8b). Thus it appears that disc-like molecules have a higher ability than rod-like molecules to form this lattice. Obviously the formation of nodes with a valence of $\nu = 4$, as required in the tetrahedral branchings in the $\text{Pn}\bar{3}m$ phase, is favored by sliding of the disc-like units as shown in Figure 16c, whereas rod-like molecules can more easily form lower valence nodes ($\nu = 3$ in the gyroid). The micellar cubic $\text{Pm}\bar{3}n$ phases of compounds **34** are presumably formed by short rotationally disordered rod segments. Micellar cubic phases with a $\text{Pm}\bar{3}n$ lattice were also observed for other disc-like molecules and supramolecular architectures, such as hydrogen-bonded G-quartet supramolecules with sodium salts,^[147] flat triphenylenes, and conic cyclotrivenatrylenes with peripheries of dendritic groups.^[148,149]

3.4. Star Mesogens and Spherical Mesogens

Until around 1995, the common opinion was that mesogenic properties could only be achieved with molecules incorporating either a sufficiently large (rod- or disc-like) anisometric unit (classical shape anisometric mesogens), or alternatively if polar groups with strong intermolecular attractive forces, such as hydrogen bonding and ionic groups were involved in amphiphilic mesogens. Therefore, it was surprising at that time to find that also flexible molecules having neither a specific shape nor containing any ionic or hydrogen bonding site could show LC phases. Columnar phases were for example found for molecules with linear connected 3,4-dialkoxybenzoyl groups (compound **43** in Figure 18)^[150,151] and star-shaped pentaerythritol tetrabenzoates (**35–38**)^[36] shown in Figure 17 and Tables 1 and 2.^[152] The pentaerythritol tetrabenzoates **35a–e** (Figure 17) with star-like shape were the first examples of non-anisometric and “non-amphiphilic” low-molecular-weight molecules forming the whole sequence of LC phases from smectic via bicontinuous

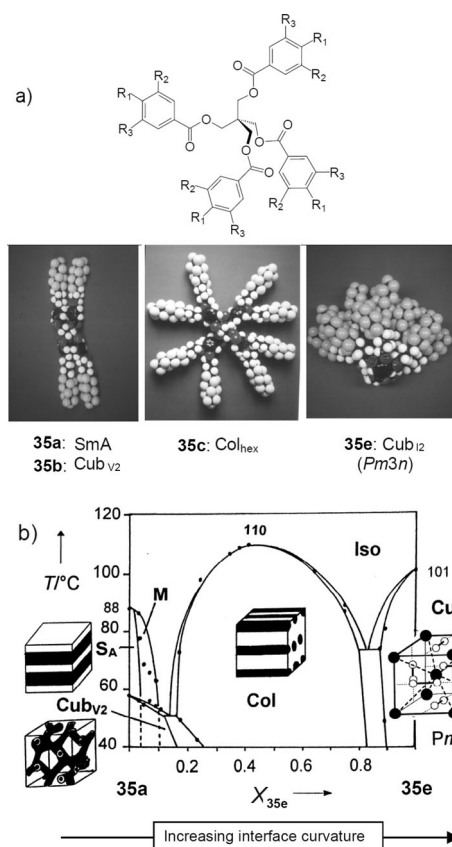


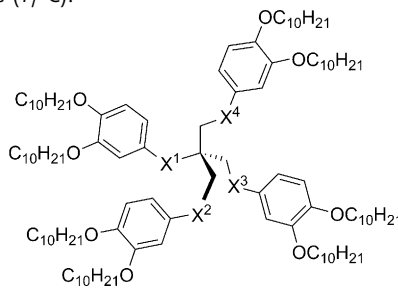
Figure 17. Modes of self-assembly of the tetrahedral molecules **35** depending on the volume ratio of the two incompatible units: a) self-assembly of the individual compounds depending on the number and degree of fluorination of the non-polar chains (**35a**: $R_1 = (\text{CH}_2)_4\text{C}_6\text{F}_{13}$, $R_2, R_3 = \text{H}$; **35b**: $R_1 = (\text{CH}_2)_6\text{C}_4\text{F}_9$, $R_2, R_3 = \text{H}$; **35c**: $R_1, R_2 = (\text{CH}_2)_4\text{C}_6\text{F}_{13}$, $R_3 = \text{H}$; **35e**: $R_1-R_3 = (\text{CH}_2)_4\text{C}_6\text{F}_{13}$) and b) phase diagram of a mixture of compounds **35a** and **35e** with different chain number, depending on composition and temperature.^[155] a) Reproduced with modifications from Ref. [120b] with permission of The Royal Society of Chemistry; b) reproduced from Ref. [155] copyright 2000, Wiley-VCH.

uous cubic and columnar^[153] to micellar cubic by changing the number, length, and degree of fluorination of the attached chains.^[154,155] Despite the tetrahedral central unit, providing a nearly isometric molecular shape, the molecules are sufficiently flexible to adopt any other shape. The actual average shape and the distribution of the distinct shapes of the molecules is selected during the self-assembly process driven by the optimization of the segregation of the polar central units from the lipophilic periphery, as shown in Figure 17a.

If the cross-sectional area of the molecule (A) is independent on the distance (r), that is, $A(r)$ is constant as in compound **35a** with a single chain at each benzene ring, then smectic phases are formed; if the cross-section area A increases linearly with the distance r , that is, $A(r) \propto r$, as in compounds **35c,d** with two chains at each ring, then the compound prefers to form a columnar phase and if there is a square relation $A(r) \propto r^2$ the micellar cubic phase is formed for compound **35e**.^[137,155]

For these pentaerythritol tetrabenzoates and related molecules LC self-assembly occurs exclusively by nanoscale segregation of the more polar benzoate units from the nonpolar chains, that is neither rigid anisometric units nor specific attractive forces as hydrogen bonding or ionic interactions are involved.^[156] The benzoate units form the aggregate cores and the fluid alkyl or R_F chains form the continuum around them, and the resulting columnar aggregates organize at constant distance on a hexagonal lattice. The degree of incompatibility, that is, the difference in cohesive energy density (CED)^[157] between the two blocks forming the amphiphile, determines the mesophase stability. For example, replacing the polar COO groups in compound **37** successively by the less polar CH_2O groups (**38a–d**) reduces the core polarity and thus decreases the CED difference between the core region and the aliphatic chains, leading to mesophase destabilization (Col_{hex} –Iso transition temperatures; see Table 1).^[158] On the other hand, increasing the CED difference by replacing COO by CONH (**36**) stabilizes the LC phases.

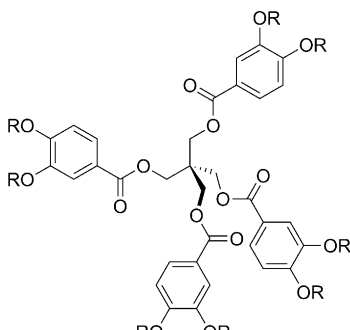
Table 1: Effect of modification of the core polarity on the phase transition temperatures ($T/^\circ\text{C}$).^[156]



| Comp. | X ¹ | X ² | X ³ | X ⁴ | Cr | Col _{hex} | Iso |
|------------|----------------------------------|-------------------|------------------|------------------|----|--------------------|--------|
| 36 | CONH | COO | OOC | OOC | ● | 47 | ● |
| 37 | COOCH ₂ | COO | OOC | OOC | ● | 54 | (● 47) |
| 38a | CH ₂ OCH ₂ | COO | OOC | OOC | ● | 7 | ● 32 |
| 38b | CH ₂ OCH ₂ | CH ₂ O | OOC | OOC | ● | 10 | ● 24 |
| 38c | CH ₂ OCH ₂ | CH ₂ O | OCH ₂ | OOC | ● | 11 | ● 23 |
| 38d | CH ₂ OCH ₂ | CH ₂ O | OCH ₂ | OCH ₂ | ● | 14 | ● 21 |

It should be noted that it is the difference in CED between the incompatible blocks that determines the stability of a mesophase with respect to the disordered isotropic liquid state and not the CEDs of the individual segments or the total of the CED of the whole molecules.^[154] Therefore, the CED difference between polar core and periphery could also be increased by reducing the CED of the chains by replacing R_H chains by R_F chains with lower CED. Therefore, introducing perfluorinated segments into alkyl chains in almost all cases leads to increased mesophase stability, as shown in Table 2 for the series of pentaerythritol tetrabenzoates **37**, **35c**, and **35d**. The fluorophobic effect is nowadays a well-established concept used for mesogen design,^[159,160] which has recently been reviewed in detail^[161,162] and therefore is not discussed herein.

Table 2: Effect of the degree of fluorination on the transition temperatures ($T/^\circ\text{C}$).^[154]



| Comp. | R | Cr | Col _{hex} | Iso |
|------------|--|----|--------------------|--------|
| 37 | C ₁₀ H ₂₁ | ● | 54 | (● 47) |
| 35c | C ₆ F ₉ (CH ₂) ₆ | ● | < 20 | ● 100 |
| 35d | C ₆ F ₁₃ (CH ₂) ₄ | ● | 88 | ● 131 |

Increasing the molecular size is an alternative way to increase the mesophase stability, which for example is achieved by increasing the number of interconnected benzoate units.^[36,120] Similarly, for dendritic molecules, increasing the generation number increases the mesophase stability as well as it shifts the LC phase type from Col_{hex} to Cub₁ as $A(r)$ changes from $A(r) \propto r$ to $A(r) \propto r^2$.^[87,11,163,164] These relationships between molecular size, CED difference, mesophase stability, and mesophase type are analogous to those observed for the stability of morphologies in binary block copolymer melts, where the order–disorder transition temperature (T_{o-d}) according to (3) depends on the Flory–Huggins interaction parameter χ_{A-B} between the two polymer blocks A and B.

$$T_{o-d} \approx \chi_{A-B} = NV(\delta_A - \delta_B)^2(RT)^{-1} \quad (3)$$

$$T_{cl} \approx \chi_{\text{core-chain}} = V_{\text{mol}}(\delta_{\text{core}} - \delta_{\text{chain}})^2(RT)^{-1} \quad (4)$$

The parameter χ_{A-B} depends on the CED difference between the polymer blocks, which can be calculated from the difference of the solubility parameters $\delta_A - \delta_B$ of the two segments,^[165] the number of repeat units N , and the average volume of the repeat units forming the polymer blocks V .

Considering the core units of mesogenic molecules as A and the peripheral chains as B, Equation (4) would be applicable to liquid crystalline molecules composed of two blocks with distinct cohesive energy density (binary block molecules) and it has indeed been used to estimate mesophase formation from interaction parameters.^[36b,165–168] However, caution is required, as LCs incorporating rigid segments are more complex systems where rigid/flexible incompatibility, molecular shape, and topology have a significant influence on mesophase type and mesophase stability.

Overall, investigation of the tetrahedral block molecules has contributed to the general understanding of mesophase formation in the framework of a uniform concept of soft matter self-assembly involving lyotropic systems, thermotropic LC phases of amphiphilic and anisometric molecules and morphologies formed by binary block copolymers and dendrimers, as outlined in recent reviews.^[60,66,112,169] Even self-assembly in solid crystals is nowadays discussed by considering nanoscale segregation effects and minimal surfaces.^[170]

In Figure 18, additional examples of star-shaped, dendritic, and other nearly spherical molecules are collated.^[35a,171]

Compound **44**, reported by Lattermann et al., can be regarded as a first example of flat three-star mesogens with C_3 -symmetry.^[172] Lehmann et al. extended the concept by further linear extension of the aromatic units attached to the trigonal center (compounds **45**)^[37] and a great number of other trigonal star molecules with columnar LC phases was synthesized meanwhile.^[47] LC dendrimers have also developed to a broad research field, which has been well reviewed.^[87,173]

3.5. Rod-like Units: Emergence of Tilt and Rugged Energy Landscapes

As shown in Section 3.1, the increase of the curvature of internal interfaces leads to a change of the phase type. However, rigid rod-like units disfavor a splayed organization and in this way disfavor formation of curved interfaces. Tilt of rigid units with respect to the normal to these interfaces is a powerful tool to increase their cross-sectional area and thus it can adjust the interfacial area to that provided by the other

molecular segments. This can also avoid or reduce the interface curvature. In smectic phases, these effects contribute to the often observed transition from nontilted SmA phases to uniformly tilted SmC phases by increasing the alkyl chain volume or upon reducing the temperature, when a denser packing of rod-like units takes place. Because tilt and interface curvature are in competition, bicontinuous cubic phases ($Ia\bar{3}d$) can occur at the SmA–SmC transition, as shown in the phase diagram in Figure 6 for compound **14** with $n = 15$.^[174] This competition between interface curvature and tilt of rigid units leads to rugged energy landscapes^[175] with several close minimum structures arising from the complex interactions between molecular shape, tilt of molecular segments, nanoscale segregation, and curvature.^[176,177]

In a similar manner in columnar phases, the tilt of rigid units with respect to the normal to the column long axes can release the frustration arising from the mismatch of interfacial areas and can thus avoid a transition to micellar cubic phases with stronger curvature. For disc-like molecules, the tilt of these units leads to an elliptical cross-sectional area of the columns, giving rise to transitions from hexagonal Col_{hex} phases to columnar phases with reduced symmetry (Col_{rec} , Col_{obl}).^[47] Also in col-

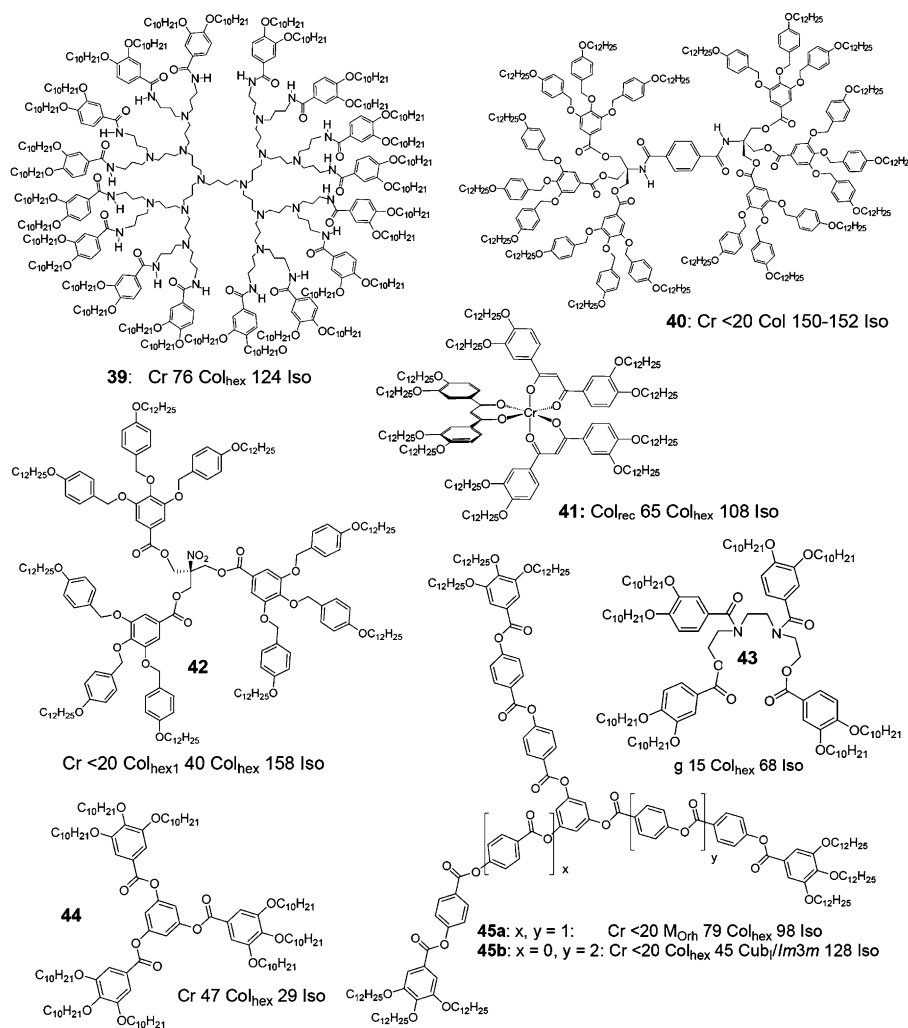


Figure 18. Examples of “non-anisometric” mesogens forming predeominately columnar LC phases ($T/^\circ\text{C}$).^[35a,37,151,163,171,172,180]

umnar phases of non-discotic molecules, as polycatenar^[178] star-shaped, and dendritic molecules rigid segment play an important role in their self-assembly. For example, replacing the flexible alkyl chains of the dendron **46**, forming a micellar cubic phase ($\text{Cub}_1/\text{Pm}\bar{3}\text{n}$) by more stiff semiperfluorinated chains removes the micellar cubic phase, which is replaced by a hexagonal columnar LC phase in the fluorinated dendron **47** (see Figure 19).^[179] This is opposite to the usually observed

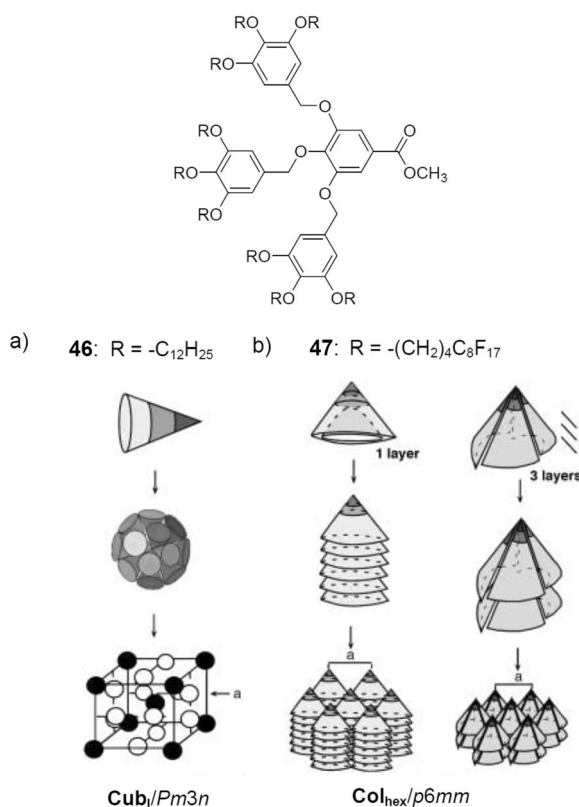


Figure 19. Self-assembly of dendrons a) **46** with alkyl chains and b) **47** with semiperfluorinated chains.^[179] Reproduced with permission,^[179] copyright 2003, Wiley-VCH.

trend, where increasing the chain volume by fluorination replaces columnar by micellar cubic phases.^[122,155] For compound **47**, the rigid rod-like R_F segments in the column stratum disfavor interface curvature, thus avoiding the increased curvature in the micellar aggregates and retaining the columnar organization. A similar effect was observed for the tetrahedral compounds **35a,b** (Figure 17a) where increasing the length of the fluorinated segment in the alkyl chain removes the bicontinuous cubic phase with curved interfaces and replaces this by a SmA phase without curvature.

Star mesogens such as **45a** provide another example for the mesophase modifying effects of rigid unit (Figure 18). These molecules with identical length of all arms form exclusively columnar phases, irrespectively of the rod-length,^[37] whereas micellar cubic phase are formed if the rod-length becomes different as in compound **45b**.^[180] Investigations have shown that in the columnar phase of **45a** the

molecules adopt an E-shaped conformation with parallel aligned aromatics, which are arranged with a tilt with respect to the normal of the column long axis.^[37] This tilted packing of the aromatics in the columns can reduce the mismatch of interfacial areas provided by the parallel organization of three aromatic rods with in total nine alkyl chains at their ends. In this case, the tilt retains a close packing of the aromatics, which stabilizes the columnar phase and inhibit the transition to the micellar cubic phases, because formation of spherical aggregate would distort the dense parallel organization of the rod-like aromatics. However, if the length of the three legs becomes different (compound **45b**), the mixing of rod-like cores with different length disturbs the parallel organization of the aromatics and thus reduces this additional stabilization of the columnar aggregates. In this case, formation of a micellar cubic phase is the preferred way to release the frustration owing to the mismatch of interfacial areas. Similar effects can be observed if rod-like aromatic units, like biphenyls, are introduced into dendritic molecules.^[87]

Along with the effects on interface curvature, the tilted arrangement of rod-like aromatic units also allows a denser packing of these units and above a certain packing density helical superstructures can arise in the columnar aggregates. Moreover, helical columns can register on a 3D lattice, and the denser packing could lead to enhanced charge carrier mobility along the columns.^[37,87,181]

4. Organizations of Spheroidic Aggregates

4.1. From $\text{Pm}\bar{3}\text{n}$ to $\text{Im}\bar{3}\text{m}$ Cubic and 3D Tetragonal Phases

As shown in Figure 7, mesophases can be described by the geometry of the supramolecular aggregates, ranging from layers to spheroids. The packing of the aggregate cores on a spatial lattice takes place with constant distance between them and minimized area of the resulting inter-aggregate interfaces. Whereas it is clear that the hexagonal honeycomb represents the minimum surface solution for the packing of columns with circular cross-section (Figure 7c), leading to a dominance of Col_{hex} phases, the problem of optimized packing of spheres in space is more complex. Only recently it has been shown that the Weaire–Phelan foam composed of two dodecahedra and six tetradehedra per unit cell (Figure 7d)^[182] is the optimized solution for the packing of soft (easily deformable) spheroids with minimized interfacial area, leading to the most common $\text{Pm}\bar{3}\text{n}$ cubic lattice (Figure 20e), whereas the $\text{Fm}\bar{3}\text{m}$ lattice (composed exclusively of dodecahedra) provides the most dense packing for hard spheres (Figure 20a).^[183] The foam composed of tetradehedra, which was previously assumed to be the minimal interfacial area solution for foams (Kelvin's problem), allows a packing of spheres with minimized chain stretching and favors the $\text{Im}\bar{3}\text{m}$ lattice for spheres with medium softness (Figure 20b).^[137] There are at least two even more complex solutions for the spatial packing of spheres, both reported by Ungar et al. for the packing of spherical dendrimer aggregates.^[137] The tetragonal $\text{P4}_2/\text{mnm}$ lattice^[132,184–186] has in total 30 spheroids at five nonequivalent crystallographic positions

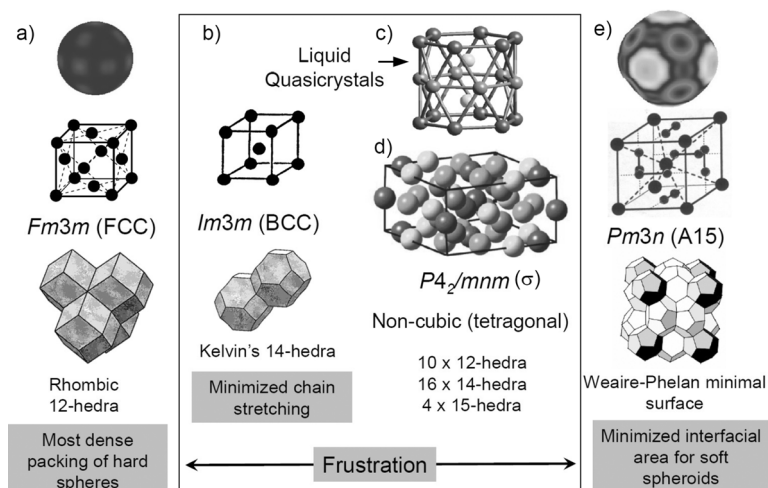


Figure 20. Self-assembly of spherical aggregates and the resulting Voronoi polyhedra forming minimal surfaces between the aggregates, depending on the softness of the spheres; inspired by Refs. [137, 183]. Reproduced from Ref. [120d] copyright 2012, Wiley-VCH.

(Figure 20d). The second is a quasiperiodic packing with 12-fold symmetry, which is discussed in the next Section.^[187]

The relatively complicated $Pm\bar{3}n$ lattice, allowing only a low packing density for hard spheres (hard sphere packing fraction: 0.524, which is the same as in the simple cubic packing) is largely dominating among the micellar cubic arrangements, whereas the simpler $Im\bar{3}m$ lattice with a much denser packing (hard sphere packing fraction: 0.680) is rare.^[137] It is remarkable that a similar abundance is found among the transition-metal alloys, which also can be considered as arrangements of soft spheres owing to the presence of partly filled d- and f-orbitals, related to the soft corona formed by the alkyl chains of the supramolecular spheres.^[188] These soft transition metals and the dendrimers avoid interstices larger than tetrahedral, leading to the tetrahedral closed packed structures (TCP, Frank–Kasper phases),^[189] for example, $Pm\bar{3}n$ (A15 phases) and $P4_2/mnm$ (σ phases). Larger interstices require a significant chain stretching to reach the center of the interstices, which is energetically costly.^[190] Indeed, the closest-packing modes of hard spheres in the face-centered $Fm\bar{3}m$ lattice and the 3D hexagonal packing (HPC, both with hard sphere packing fractions: 0.7405) were never observed in thermotropic cubic LC phases of organic compounds (but see Section 5.2 for gold nanoparticles). Aside from these general considerations, there is presently no rule for the precise prediction of a distinct type of micellar cubic phase from the molecular structure.^[12, 87, 132, 134, 180, 191–196] The broadest systematic study regarding the phase sequence $Pm\bar{3}n$ – $Im\bar{3}m$ was performed with alkali-metal 3,4,5-trialkoxybenzoates **27** (Figure 14), where small alkali-metal ions (Li, Na) and short alkyl chains give the temperature dependent phase sequence Col_{hex} – $Cub_I/Im\bar{3}m$ – Iso .^[132] Increasing the sphere size either by increasing the alkali metal ion size or by elongation of the alkyl chains is favorable for replacing the $Im\bar{3}m$ phase by the $Pm\bar{3}n$ phase. With increasing temperature, the phase sequence of these compounds is Col_{hex} – $Cub_I/Pm\bar{3}n$ – $Cub_I/Im\bar{3}m$ – Iso , that is, the

$Cub_I/Pm\bar{3}n$ phase is the cubic phase occurring adjacent to the columnar phase.^[132]

Considering the dominance of the $Pm\bar{3}n$ lattice among the micellar cubic arrangements, it should also be noted that the $Pm\bar{3}n$ lattice is not restricted to the packing of spheroids (Figure 21a); in fact, to achieve dense packing a distortion of the shape is required for the micelles located on the faces of the unit cell (in the tetradecahedra).^[87, 136] Therefore, this lattice also allows a dense periodic packing of short rod-like molecules, as for example two-atomic gases in crystalline phases (γ -O₂, β -F₂, and N₂).^[197] This structure composed of short rods was also proposed by Fontell et al.^[198] for micellar cubic phases of lyotropic systems.^[199] We have considered this structure as an alternative model for the $Pm\bar{3}n$ thermotropic micellar cubic phases of small conical amphiphiles.^[113] In this model (Figure 21 b), eight short rods, representing segments

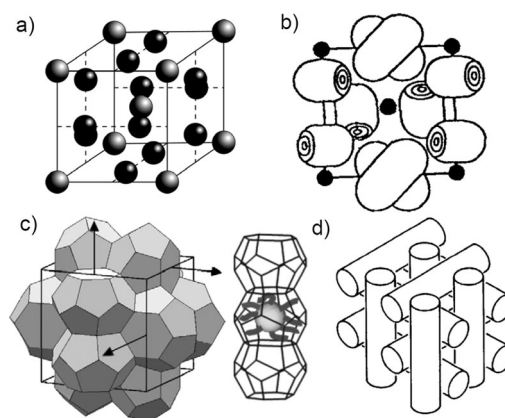


Figure 21. Different models of the $Pm\bar{3}n$ type micellar cubic phases: a) packing by two sets of different spheres; b) packing of eight identical rods with different rotational disorder; c) Weaire–Phelan foam with oblate micelles in the tetradecahedra and arrows indicating the potential growth direction of pinched columns; d) lattice of columns.^[136, 191]

of the infinite rod-like aggregates of the adjacent hexagonal columnar phases, are located in the center, at the corners, and pair-wise on each face of the unit cell. Those located in the center and at the corners are isotropically disordered, whereas those on the faces are only rotationally disordered around their long axes. In another model it was suggested that the micelles on the faces could have an oblate shape.^[200] Such oblate micelles could fit better into the tetradecahedra located on the faces of the cubic unit cell and thus favor the $Cub_I/Pm\bar{3}n$ structure. In contrast, spherical micelles allow a better interdigitation of the alkyl chains of adjacent micelles, which is favorable for the $Im\bar{3}m$ lattice.^[190] These models are difficult to distinguish, as XRD gives only a time- and space-averaged picture and also the resolution of electron-density maps is limited, and therefore these packing modes should still be considered as possible alternatives,

especially for the $Pm\bar{3}n$ cubic phases formed by disc-like mesogens.^[145,147] Even a packing of undulated (pinched) columns parallel to the (1,1,1) directions could in principle be possible (Figure 21c,d).^[191,201,202] This structure is known for the packing in the cubic blue phase II, a highly chiral nematic phase composed of double-twist cylinders.^[203]

4.2. Liquid Quasicrystals

New non-cubic modes of sphere packings have been discovered by Ungar and Percec et al., among them a 3D tetragonal phase with $P4_2/mnm$ lattice, and first examples of liquid quasicrystals (LQC) with dodecagonal symmetry.^[187] To understand these mesophase structures the organization of the spheres can be represented as 2D nets packed on top of each other with the spheres located on the nodes of the net-layers (Figure 22). In the 3D packing of spheres considered

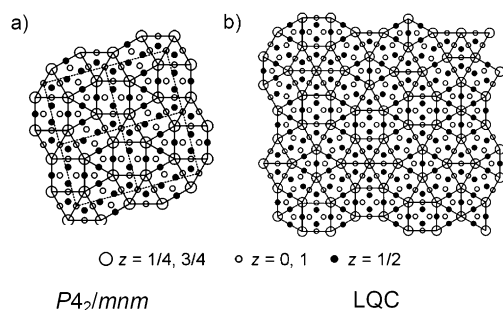


Figure 22. Packing of spheres a) in the tetragonal $P4_2/mnm$ phase and b) in the dodecagonal LQC; the sparingly populated nets (large cycles) are decorated with the spheres in the dense nets above and below (filled and open dots).^[187b] Reproduced from Ref. [187b] copyright 2011, Wiley-VCH.

here, differently populated nets alternate. One way to represent these structures in a simplified way is to view them as tilings of the sparsely populated layers (large cycles) with the spheres in adjacent dense layers (small dots) being considered as decorations of the basic tiling provided by the sparse layers.^[187]

Figure 22a shows the tiling of the $P4_2/mnm$ phase; the arrangement of the spheres in the sparsely populated layer can be described by a tiling pattern combining squares and equilateral triangles in the ratio 1:2. There are numerous additional possible tiling patterns formed by combinations of squares and equilateral triangles in different ratios.^[204] At a certain ratio of square to triangles corresponding to 1:2.31^[205,206] the long-range positional order (translational symmetry) of the spheres in this 2D net is lost while the orientational order of the triangles and squares is retained (Figure 22b), leading to a “crystallographic forbidden” dodecagonal symmetry. Shortly after Shechtman’s Nobel-Prize-honored discovery of quasicrystals,^[207] the first dodecagonal quasicrystal was reported in a metal alloy,^[208] whereas the LQC formed by the spherical aggregates of the dendron **48a** (Figure 23) represents the first soft quasicrystal.^[209,210]

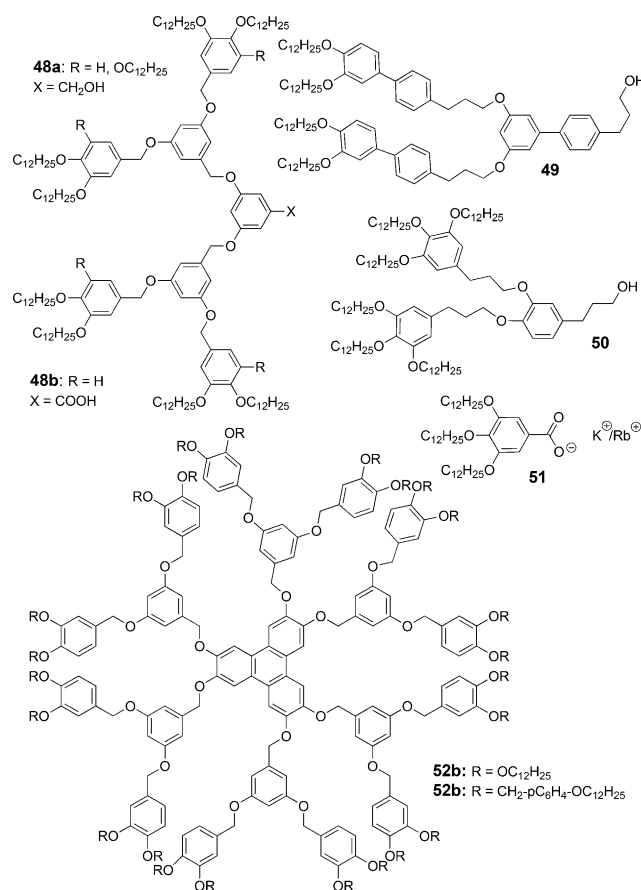


Figure 23. Examples of dendritic molecules forming LQC phases.^[187b]

In the meanwhile LQC phases with dodecagonal symmetry have been found for more than 20 dendritic compounds, and some representative examples are shown in Figure 23.^[187,194,211] Although there is presently no general rule for the design of LQC it appears that sufficiently strong cohesive forces at the apex of dendritic molecules (provided by OH, COOH, or alkali-metal carboxylates; see compounds **48–51**) are required to avoid expansion of the spheres or formation of other modes of self-assembly (see Section 6). Similarly, covalent connection of the dendrons by a multivalent central unit seems to be also successful (triphenylene **52**); moreover the 3,5-substitution pattern at the dendritic branching points appears to be advantageous for LQC formation, too.^[187b,211c]

Only recently, dodecagonal quasicrystals based on sphere packing were also found for block copolymers,^[212] in colloids,^[213] and for lyotropic systems. In the latter case the remaining mesoporous silica obtained by sol-gel process based on lyotropic LQC templating^[214] is a foam corresponding to the Voronoi tessellation of the quasicrystalline micellar packing. Dodecagonal quasicrystalline packing in only two dimensional sheets, that is, in single layers of spheres, was reported for nanoparticle monolayers.^[215] For star polymers, a quasiperiodic 2D packing of prismatic cells with square and triangular cross-sectional area in a ratio 1:2.31 was reported by Dotera et al.^[206]

5. Packing of Spherical Nano-objects in Liquid-Crystal Templates

5.1. Silsesquioxanes, Fullerene, and Metal Clusters

The self-assembly forces provided by dendritic, rod-like, and disc-like mesogenic or promesogenic units can also be used to organize large spherical molecules, such as fullerenes, silsesquioxanes, and polyoxometallates, or even larger nano-objects, periodically in space. Polyoxometallates and other metaloclusters have been integrated in lamellar phases,^[216,217] and lamellar and columnar arrangements have been reported for fullerenes^[218] and silsesquioxanes.^[219,220] Typically, these spherical objects tend to segregate into distinct domains within the lamellar or columnar aggregates formed by LC self-assembly of the mesogenic groups. This often leads to a short-range and in some cases also to an additional long-range correlation between these spherical units in the aggregates.

In particular, side-on attachment of rod-like mesogens to silsesquioxanes and other oligosiloxane-based scaffolds (for example compound **52**, Figure 24)^[221] or fullerenes^[218,222] was studied intensively. In most cases, nematic phases with cybotactic clusters composed of columnar aggregates were observed owing to the competition between the mesophase

stabilizing effect of molecular pre-organization and the disturbance of parallel alignment of the rod-like units by the bulky laterally attached moieties. At reduced temperature, columnar phases were found in some cases for supermolecules incorporating siloxane scaffolds (see Figure 24b). As a result of the incompatibility between the spheroidal scaffolds with the attached rod-like mesogenic units, the spherical moieties segregate and line up in columns, which are embedded in a nematic-like continuum of the rod-like units.^[223–225] This organization of columnar aggregates in a nematic continuum seems to be quite general, as it was also observed for hexagonal columnar LC phases of gold nanoparticles (discussed in the next Section) and for T-shaped facial amphiphiles (Section 8.5.2).

5.2. Liquid-Crystalline Gold Nanoparticles

LC self-assembly is also a powerful method for tailoring the spatial organization of nanoparticles;^[226] the focus is here on small (size around one to few nm) spherical gold nanoparticles (GNPs) for which an especially wide variety of different LC arrangements was recently found by several groups.^[196,227,228] Two types of GNPs were reported: single-shell and double-shell GNPs. Single-shell GNPs have a surface shell composed of a mixture of mesogenic thiols (ligands) and non-mesogenic *n*-alkanethiols (co-ligands); these particles are usually obtained by exchange reactions.^[229] In this case the ligand/co-ligand ratio and the length of the alkyl chain of the co-ligands have a strong effect on the mode of self-assembly. A specific feature of thiol-covered GNPs is that ligands and co-ligands can migrate along the gold surface and therefore the precise shape of the GNP-mesogen complex can change during self-assembly (see Figure 26a), which has a large influence on the modes of self-assembly and can also cause hysteresis effects if this reorganization is slow.

Double-shell GNPs are completely covered by COOH terminated *n*-alkane thiols, and in a following step amine terminated mesogenic ligands were attached by ionic self-assembly. In most cases dendritic and rod-like units were used as ligands, whereas disc-like and bent-core units were sparingly used.^[228,230,231]

The spherical GNP decorated with dendrons often form micellar cubic phases. However, the lattice types of these cubic phases are in most cases different from those observed for self-assembly of the dendrons themselves and also different from the closest hard-sphere packed structures commonly observed for non-modified monodisperse GNPs.^[232] Thus it seems that on the one hand the GNP surface is softened, that is, minimization of the interfaces becomes more important, but on the other hand the relatively large and hard gold nanoparticles shift the self-assembly of the dendrons towards the hard core-packing modes (Figure 20). For example, the rarely occurring $Im\bar{3}m$ phase was observed for single shell GNP with **53**,^[196] whereas the common soft sphere packing mode with $Pm\bar{3}n$ lattice has not yet been observed (Figure 25a). The simple-cubic phase with $Pm\bar{3}m$ lattice was found for double-shell GNP covered with dendrons **54** (Figure 25b).^[227] This kind of cubic lattice has previously

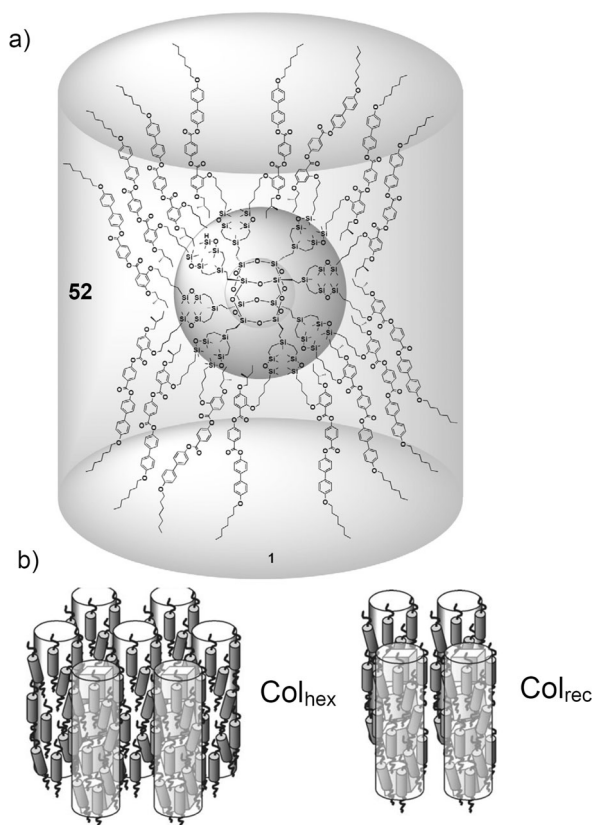


Figure 24. a) Supermolecular mesogen **52** with side-on attached rod-like mesogenic units at a spherical central silsesquioxane scaffolds; b) representation of the structures of the hexagonal and rectangular columnar phases formed by **52**. Reprinted from Ref. [223a], copyright 2008 Wiley-VCH.

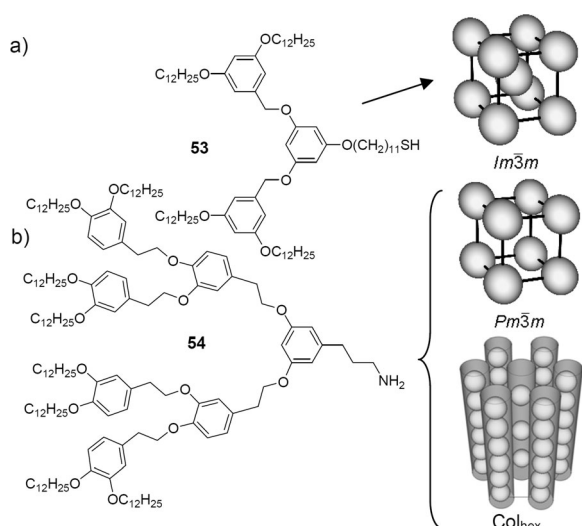


Figure 25. Examples of dendritic ligands and the modes of self-assembly of a) single-shell^[196] and b) double-shell GNP derived from these ligands.^[227] Reproduced with modifications and permission from Ref. [227], copyright 2012, American Chemical Society.

only been known for polonium as the only metal and for the packing of colloids with a cubic shape.^[233,234] It seems that also in this case the packing is dominated by the relatively hard core of the gold nanoparticle covered with the first layer of charged organic ligands, whereas the oppositely charged dendritic units attached to this surface mainly fill the space in the relatively large octahedral interstices of this lattice. Along with this cubic lattice, a packing in columnar aggregates on a hexagonal lattice was also observed (Figure 25 b). Remarkably, this hexagonal lattice is more complex than usual Col_{hex} phases, as it is formed by a mixture of dense and sparse GNP strings; the sparse strings are located on the hexagonal lattice and the dense GNP strings on the corners of the corresponding Voronoi honeycomb.^[227]

Rod-like thiols can be attached either end-on or side-on to GNPs. The end-on topology is known to stabilize lamellar organizations. Typically a short range ordering of the particles in the layers without long range correlation of their positions in adjacent layers is observed.^[235–237] For GNP decorated with *n*-alkanethiol and rod-like ligands carrying branched end-chains at the rod-like units **55** (ca. 1:1 ratio, in total ca. 80 ligands/particle), transitions from a short-range to a long-range order of the GNP were observed, which are connected with a transition from simple lamellar phases to more complex LC phases with 2D or 3D lattices.^[237] These transitions are mainly associated with a redistribution of the mesogenic ligands on the gold surface, changing the overall shape from spherical to cylindrical (Figure 26 b, from right to left). In the smectic phase, the alkyl chains of the co-ligands concentrate around the equator whereas the mesogens are collated at the poles, providing an overall rod-like shape and enabling an improved segregation of aromatic cores from the aliphatic chains (end-chains, aliphatic spacers and alkyl chains of the co-ligands). The chain length of the co-ligands has a significant effect on the mesophase structure, as long chains have a higher segregation tendency and also provide a stron-

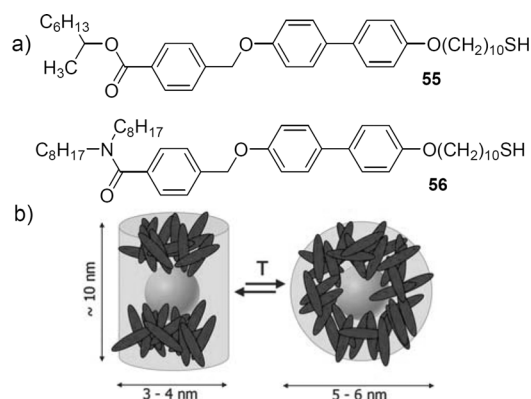


Figure 26. Rod-like mesogens used for terminal attachment to single-shell GNP and b) reorganization of these mesogens on the GNP surface.^[237] Reproduced from Ref. [237] with permission of The Royal Society of Chemistry.

ger steric frustration for layer formation, owing to the “aliphatic” expansion around the equator of the GNPs. For GNP with ligand **55**, strong steric distortion of the layers by long co-ligands leads to the disruption of the layers and formation of a body-centered orthorhombic 3D phase as the LC-GNP supermolecules line up in columns perpendicular to the layer planes.^[237a] In this $R\bar{3}m$ lattice, the staggered arrangement of the GNP in adjacent columns maximizes the mixing of the alkyl chains of the co-ligands around the GNP equator with the aliphatic ends of the mesogenic units and thus minimizes the steric distortion by these co-ligands. For GNP with ligand **56**, in an alternative mode a disruption of the layers can take place upon an increase in temperature in the other direction, along the layer planes, so that strings of GNP form columns developing parallel to the previous layers.^[237b]

A quite general and unusual feature of the LC phases of mesogen-coated gold nanoparticles is that the textures observed between crossed polarizers often do not correspond to the mesophase structure determined by XRD. These LC phases appear optically isotropic, only weakly birefringent,^[237] or with a nematic schlieren texture,^[238] although a well-developed lamellar, columnar, or 3D long-range order is indicated by XRD. This means that the non-birefringent nanoparticles provide the positional order and determine the phase structure, whereas the birefringent mesogenic units have no long range order or only orientational order. Nevertheless, the presence of these mesogens strongly affects the order of the NPs.

A series of distinct LC phase structures was also reported for hybri structures of gold-nanoparticles attached laterally to rod-like mesogens (Figure 27).^[238,239] Apart from hexagonal (Col_{hex}) and rectangular ($\text{Col}_{\text{rec}}/c2mm$) columnar phases, there are three distinct types of 3D structures. These are the simple 3D hexagonal packing of spheres ($P6/mmm$), the face-centered cubic packing of spheres ($Fm\bar{3}m$, FCC), and a rhombohedral phase ($R\bar{3}m$). Typically the textures are nematic-like, indicating a long-range orientational order of the rod-like mesogens. The aliphatic co-ligands are preferentially found at the poles of the GNP and the mesogens

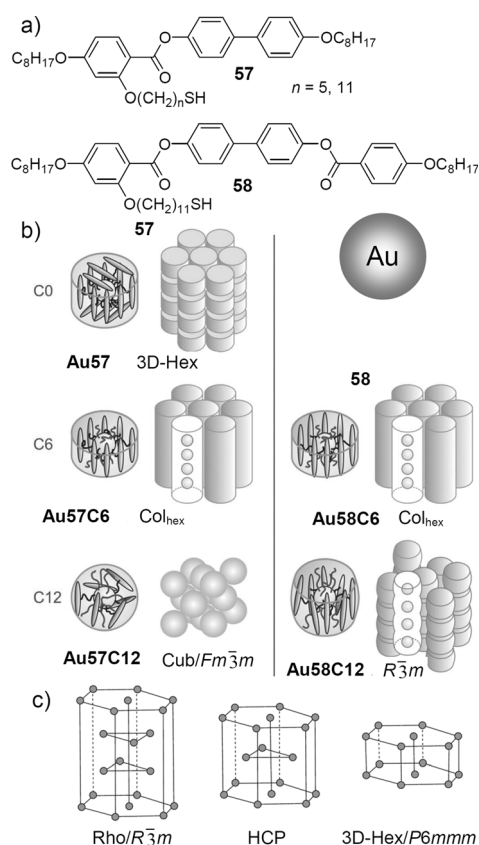


Figure 27. a,b) LC phases of GNP with laterally attached rod-like mesogens^[238] and c) 3D lattices based on hexagonal packing of the GNP (HCP=hexagonal closest packing). b) Reproduced with modifications from Ref. [238b] with permission of The Royal Society of Chemistry.

surround the equator; that is, their preferred position is reversed with respect to the GNP with terminally attached mesogens. In this way the lateral connection with the rod-like units favors the stacking of the GNPs in strings along columns. The mode of correlation between the columns, and hence the mesophase type depends mainly on the length of the rod-like mesogenic core, the ratio between ligand and alkyl co-ligand, and also on the length of the alkyl chain of the co-ligands. At intermediate ligand fraction, the strings of GNP form columns that are packed on a hexagonal 2D lattice with the mesogens surrounding these columns and being aligned parallel to the column axis, which is very similar to the Col_{hex} phase found for the silsesquioxane-based supermolecular mesogens **52** (Figure 24b). An additional periodicity of the GNP along the columns was observed for **Au57** with a complete coverage of the GNP by the rod-like ligands **57** (Figure 27). The longitudinal register of these columns without shift leads to a 3D hexagonal packing of spheres on a *P6/mmm* lattice. In **Au57C6** and **Au58C6** with additional C₆H₁₃SH (**C6**) co-ligands, usual hexagonal columnar phases without long-range correlation of the GNP along the columns were observed. **Au58C12** with longer co-ligands forms a rhombohedral 3D phase (*R $\bar{3}m$*) with a longitudinal shift of these columns by 1/3 of the intracolumnar periodicity

(Figure 27). Thus in this case, increasing the influence of the co-ligand changes the mode of column correlation.

Only the complex **Au57C12** shows a face centered cubic phase (*Fm $\bar{3}m$*). It is thought that this is due to the lower aspect ratio of the ligand **57** combined with the longer **C12** co-ligands leading to a loss of long range orientational order of the mesogens. As a result, the organization of the GNP in strings is lost and the spheres organize in the isotropic environment with the closest hard-sphere packing of the *Fm $\bar{3}m$* -lattice.^[238b] Although this phase might be only surface-induced, it completes the phase sequence of cubic phases formed by spherical objects shown in Figure 20. Overall, LC self-assembly is a powerful tool to organize nanoparticles into well-defined spatial arrays of interest for application as photonic materials and metamaterials.^[239,240]

6. Vesicular Liquid-Crystal Phases

Vesicular LC phases are a new kind of LC phase with cellular structure that is formed by the spatial organization of cylindrical, spherical, or polyhedral aggregates of curved single layers, bilayers, or double layers, that is, formed by hollow cylinders, spheres, or polyhedra. These are usually filled by the same material as found in the continuum surrounding these aggregates. Nevertheless, in special cases interior and continuum can also be different, as will be shown below. This type of mesophase, which can be considered as a special kind of columnar or cubic LC phases with core-shell morphology, was already in 1958 recognized by Luzzati and Skoulios for lyotropic hexagonal columnar phases formed by aqueous soaps. These Col_{hex} phases, having a lattice parameter much larger than usually expected for columnar phases, have been assigned as “complex hexagonal phases”^[241] and can be considered as vesicular columnar phases (Figure 28a).

Percec et al. observed a transition from simple hexagonal and micellar cubic phases to columnar and cubic phases with unusual large lattice parameters in thermotropic phase sequences of dendritic molecules.^[83] Such conical amphiphilic molecules usually form columnar or micellar cubic phases owing to the segregation of the polar apex from the lipophilic periphery (see Section 3.3 and Figure 28b, structure **A**). However, if the cone angle is reduced and therefore more molecules are required in the cross section of the columns or spheres, the aggregate diameter has to increase. With decreasing cone angle, the truncation of the apex becomes a problem, as the apex of real molecules cannot become infinitely sharp. This leads to free space in the centers of the aggregates that has to be filled. Relatively small spaces could be easily filled by fluctuations, whereas larger spaces obviously require the inversion of the orientation of some molecules which then provide their alkyl chains for space filling (Figure 28b, structures **B,C**). Increasing the number of inverted molecules leads to double layer type vesicular LC phases as observed for compound **59** (Figure 28c). Owing to the bilayer-like organization of the molecules, the spheroidal vesicular aggregates (ca. 100–1000 molecules) are much larger than those of related “micellar aggregates” (< 100 molecules); similar results were found for the columnar phases.^[83]

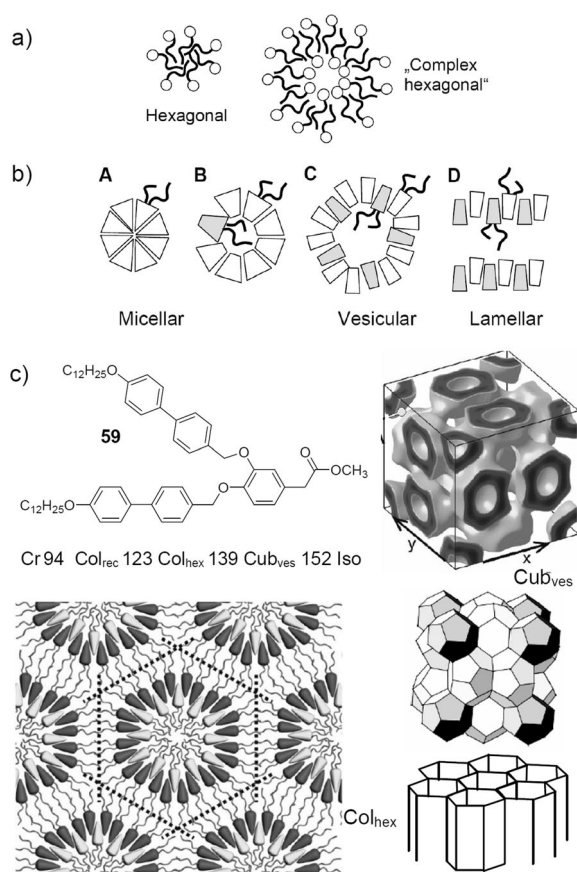


Figure 28. a) Hexagonal and “complex” hexagonal columnar phases of simple amphiphiles; b) transition from micellar to vesicular and double-layer lamellar phases by reducing the cone angle and increasing truncation of the apex of the amphiphilic molecules (the alkyl chains are only shown for some molecules); c) representative example of a taper-shaped molecule forming hexagonal columnar and vesicular cubic phases of the double-layer type; electron density map of the vesicular cubic phase and models of the hexagonal columnar and cubic phases ($T/^\circ\text{C}$).^[83] Parts adopted with permission from Ref. [83], copyright 2010, American Chemical Society.

Electron-density maps of these vesicular columnar and cubic phases indicate a reduced electron density around the minimal surfaces between the aggregates (Voronoi honeycombs and Voronoi polyhedra, respectively) and also in the centers of the cells.^[83] This suggests that the alkyl chains are organized around the minimal surfaces between the cylinders and polyhedra, as well as in their interior. The aromatic segments line the inside of the resulting polygonal/polyhedral cells and separate the alkyl chains inside and outside the cells. This provides an opposite sign of the curvature for the aromatic–aliphatic interfaces inside and outside the aggregates, which must be adjusted by chain folding, by intercalation of the chains at the outside, and by an unequal number of molecules forming the inner and outer layers of the cells. Owing to the giant size of the aggregates, the space in the interstices between them must be filled by significant deformation of the cylindrical or spherical aggregates.^[83] Therefore, they adopt to the shape of the polyhedra and polygons of the corresponding Voronoi cells (Figure 28c).

Alternatively, the cone-shaped molecules can form lamellar phases with a more or less intercalated double-layer structure by antiparallel packing (Figure 2b, structure **D**). Formation of these lamellae instead of usual columnar and micellar cubic aggregates is favored for molecules with a reduced taper angle, a relatively small polarity difference along the taper units (weakly polar apex), and by incorporation of smectogenic rod-like segments (1,4-benzene rings, 2,6-naphthalenes, 4,4'-biphenyl systems). However, the spontaneous curvature of these layers with formation of vesicular LC phases is surprising: considering the shape of the molecules and the ratio of the relative volumes of the incompatible segments, formation of these structures instead of simple double layer smectic phases would not be expected. It appears that some mismatch between the distinct interfacial areas, combined with packing constraints provided by the molecular shape prevents a strict antiparallel molecular packing, gives rise to layer distortion and favouring curvature. The precise mechanism of formation of this kind of vesicular LC phases is not yet clear.

Another type of vesicular columnar phases was reported by Lee et al. for bent aromatic molecules with a bulky branched lateral polyether chains at the apex on the convex side of the bent oligophenylene **60** (Figure 29a).^[242] In this case self-assembly takes place with the main axis of the oligophenylene cores being aligned perpendicular to the column axis, favoring hexagonal cylinders. The resulting voids in these cylinders are filled by turning the apex of some of the molecules inward, which distorts the hexagonal shape, but time- and space averaging retains a hexagonal lattice despite of the local distortion.

For thermotropic LC systems, this inversion of the orientation of some molecules appears to represent a general possibility for the filling of the space arising in aggregates with increased diameter (Figure 28b, structure **B**).^[83] This requires a reduced molecular amphiphilicity, and indeed it was shown for dendritic molecules that replacing the weakly polar ester groups at the apex by more polar and cohesive hydrogen bonding groups, like CH₂OH or COOH, leads to the formation of the usual micellar aggregates with small diameter or to a complete change of the mode of molecular organization.^[83,211c]

Besides these double-layer type vesicular LC phases there are also monolayer type vesicular phases. An illustrative example for formation of thermotropic monolayer type vesicular columnar and cubic LC phases is provided by rod-like imidazolium salts **62**, reported by Cheng et al. (Figure 30). These compounds have a short single alkyl chain at the ionic end (N-terminal chain) and three long alkyl chains at the non-ionic end (C-terminal chains).^[82] During self-assembly the short N-terminal chains form the cores, the aromatic segments form the shells around these cores and these core–shell columns are embedded in the continuum formed by the long flexible C-terminal chains. In this case, a self-sorting of short and long alkyl chains is induced by the incompatibility and segregation of the ionic ends of the rods, forming the inner surfaces of the aromatic shells, from the nonionic ends forming the outer surfaces. In this way, an antiparallel packing of these cores is avoided,

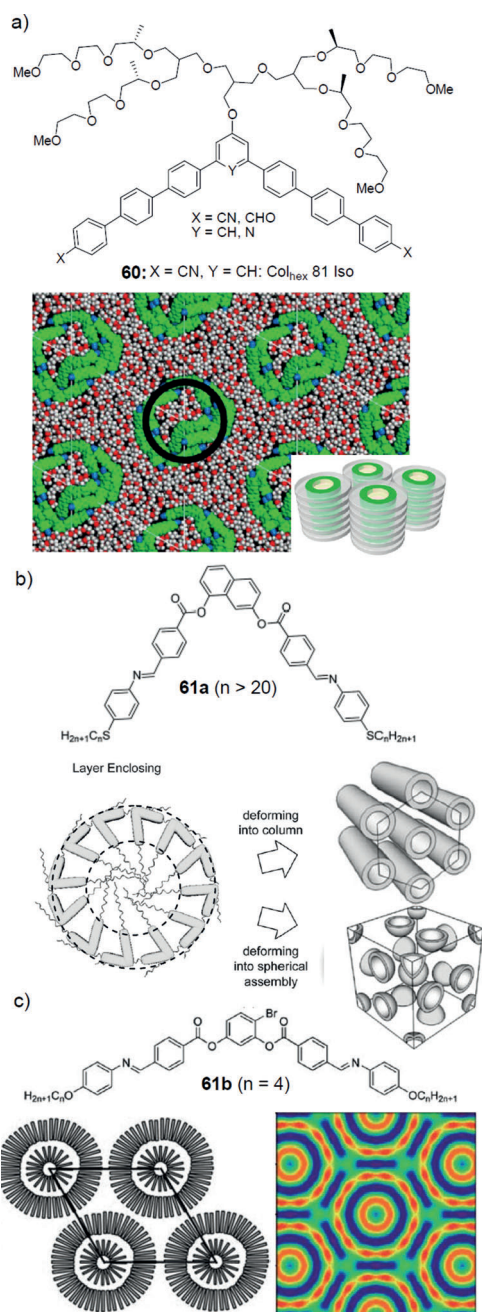


Figure 29. Vesicular LC phases formed by bent-core molecules: a) vesicular columns of compound **60** with snapshot after MD annealing;^[242] b) vesicular columnar and spheroidal cubic phases of compounds **61a**; and c) bilamellar cylinder structure formed by **61b**; the electron density map at the right shows the hexagonal deformation of the outer cylinders (red = high electron density, aromatic groups; blue = low electron density, alkyl chains).^[243, 244] a) Reproduced with permission from Ref. [242], copyright 2012, American Chemical Society; c) reproduced from Ref. [244] with permission of The Royal Society of Chemistry.

which would lead to a lamellar organization. In a similar manner, core-shell spheroids were also obtained for the vesicular $Pm\bar{3}n$ -type cubic phases formed by molecules with longer C-terminal or shorter N-terminal chains.^[82] Owing to the strong restriction of the space available for the N-terminal

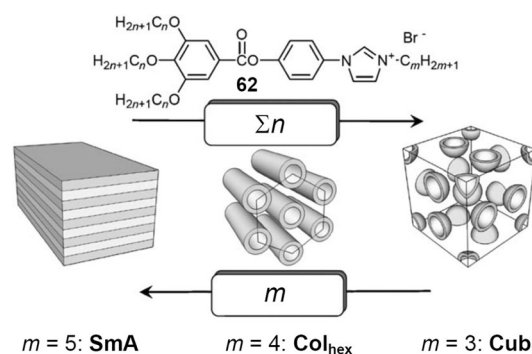


Figure 30. Self-assembly of polycatenar imidazolium salts **62** ($n = 14$) into vesicular columnar and cubic phases. Reproduced from Ref. [82], copyright 2012, Wiley-VCH.

chains inside the vesicular aggregates, only slight elongation of these chains is sufficient to give dramatic effects. In this way it was possible to achieve the phase sequence $SmA-Col_{hex}-Cub_I/Pm\bar{3}n$ for a series of only three directly neighboring homologues differing by only one single CH_2 unit from each other (Figure 30).^[82]

Recently, LC phases with monolayer vesicular structure were also reported by Watanabe et al. for giant Col_{hex} and $Cub/Pm\bar{3}n$ phases of bent aromatic molecules with terminally attached alkyl chains (bent-core mesogens; see also Section 10) based on 1,7-substituted naphthalene cores (**61a**; Figure 29b).^[243] For the soft crystalline Col_{hex} phase of the bromo-substituted bent-core molecule **61b**, a structure was even proposed, which is formed by cylinders composed of two concentrically enclosed layers of molecules, that is, combing cylinders having different degree of curvature (Figure 29c).^[244] It is thought that in these cases, the curvature of the layers is due to the nonsymmetric structure of the bent aromatic core (1,7-substitution of naphthalene in **61a** and 4-Br substituent at the resorcinol core in **61b**).^[243, 244]

Alternatively, monolayer-type vesicular LC phases are also favored if the molecular symmetry is reduced by chemically different chains (for example R_F/R_H) with different chain volumes attached at the opposite ends of the molecule (Section 7.2). The segregation of these incompatible chains, the smaller forming the interior of the vesicle-like aggregates and the larger forming the continuum, leads to a special type of vesicular phases having an interior which is different from the continuum.^[83] Here the chain incompatibility replaces the incompatibility of the distinct ends of the aromatic cores in the imidazolium salts **62**.

These examples show that for thermotropic LCs, besides the well-known micellar columnar and cubic LC phase, also vesicular LC structure can be formed, very similar to the self-assembly of amphiphiles in dilute aqueous systems;^[9] even multi-lamellar vesicles appear to be possible. Also new phase structures, resulting from the combination of different aggregates can be expected. The $Im\bar{3}m$ -type bicontinuous cubic phase with giant lattice parameters, found for the cubic phases of polycatenar compounds and dibenzoylhydrazines (see Figure 10, model C in Section 3.1), could probably be an example.^[58] If model C would be correct, it is composed of spherical vesicles located in the center and at the corners of

the $Im\bar{3}m$ unit cell, combined with a net of branched columns which separate these vesicles. These nets can probably compensate the different packing density of the chains inside and outside the vesicles.^[80] Overall, it seems that vesicular LC phases could pave the road to numerous new and highly complex modes of self-assembly in LC phases and other soft matter systems.

7. Polyphilic Liquid Crystals

As soon as amphiphilicity and nanoscale segregation were recognized as the major basis of periodic order in LC phases, the question arose as to whether combination of more than only two incompatible units in polyphilic mesogens could lead to even more complex LC phase structures,^[120] similar to those found for the morphologies of triblock copolymers.^[62,245,246]

7.1. Rod-like and Disc-like Polyphilic Liquid Crystals

Combination of two different and incompatible chains or groups at opposite ends of rod-like segments (for example, combinations of R_H , R_F oligosiloxanes, polyether chains, ionic groups) often leads to a transition from monolayer to double-layer and bilayer smectic phases, which are caused by the segregation of the distinct and incompatible chains into different layers.^[247–250] However, as there is always a difference in size between the distinct chains, there is also a tendency towards curvature and layer modulation. This steric effect is in competition with the effects of segregation, that is, to remove interface curvature, the incompatible chains at both ends are forced to mix, which could restore single-layer structures. This was discussed in more detail in a recent review for LC with fluorinated chains.^[161]

Examples of polyphilic disc-like molecules are collated in Figure 31 a–c. Depending on the ratio and the distribution of incompatible units around a disc-like core, different phase structures, including 2D super-lattices, lamello-columnar phases, core-shell columns and multi-column structures can be observed for polyphilic disc-like mesogens (Figure 32). Superlattice formation is a typical feature of disc-like molecules with one or two (adjacent) alkyl chains substituted by incompatible chains or groups (for example compounds **63a** and **63b**). If nanoscale segregation is strong enough that separation of these units takes place, this leads to well-defined columnar domains incorporating these units, and these columns are arranged on a 2D lattice, which is much larger than the original lattice formed by the columns of the disc-like units (Figure 32b).^[123,251–256]

Janus-type disc-like molecules, composed of two incompatible half-discs with similar size, such as a hydrocarbon substituted and a fluorocarbon substituted half (for example, compound **65**), have a strong tendency to form distinct layers for each of the chain types. Between these layers, the disc-like cores are still organized in columns and retain a 2D periodic lattice, which is however distorted, leading to lamello-columnar phases with rectangular $p2mg$ lattice (Fig-

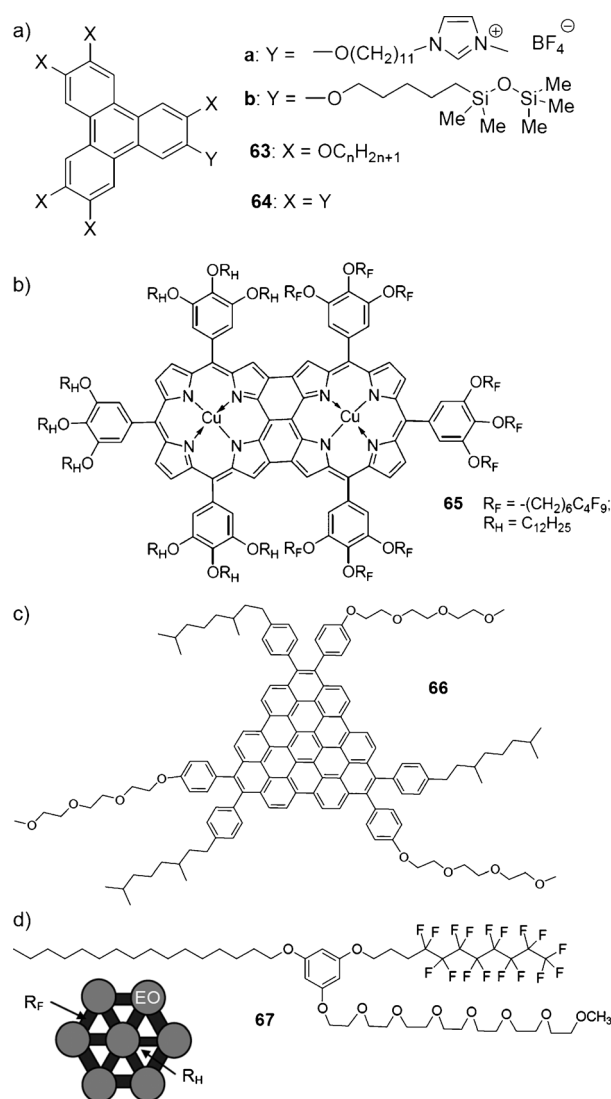


Figure 31. Selected examples of disc-like polyphiles a) with one incompatible chain (**63**), with a periphery of segmented chains (**64**);^[78,251,256,257,259] b) Janus-type molecule **65**; c) molecule with alternating chains (**66**), and d) star-tripophile **67** and model showing its lyotropic self-assembly.^[260]

ure 32c).^[257] A lamello-columnar phase with $p2mg$ lattice was also found for star-shaped molecules derived from compounds related to compound **45** (Figure 18), where the R_H chains at one arm were replaced by R_F chains.^[37,258]

For disc-like molecules with strictly alternating chains (for example, compound **66**), there is the possibility of segregation of these chains into separate columns, leading to columnar phases composed of three distinct types of columns (Figure 32d).^[259] Only recently, such a structure was observed for the star polyphile **67** (Figure 31d). In the lyotropic Col_{hex} phase of this compound, obtained after mixing with water, all three different chains are separated, leading to a three-compartment structure composed of hexagonally packed polar channels involving the EO chains and the water molecules (EO, gray) embedded in a hydrophobic matrix which is split into lipophilic (R_H , white) and fluorophilic (R_F ,

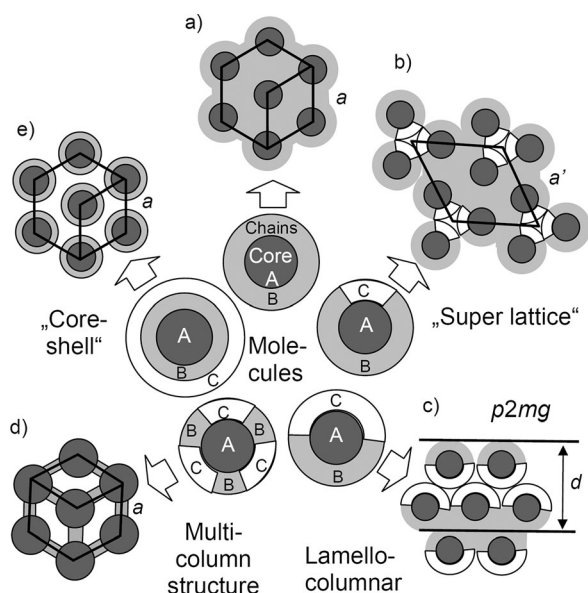


Figure 32. Modes of self-assembly as found for LC phases of triphilic disc-like molecules (cuts at right angle through the columns).

black) prismatic domains.^[260] This compound could be considered as a low-molecular-weight analogue of ternary star copolymers, and indeed a similar morphology has previously been reported for the related polymers.^[246,261] Self-assembly of **67** only occurs in water, as it enhances the CED of the oligo(ethylene oxide) chains by providing hydrogen bonding.

Disc-like molecules that are fully substituted by identical chains composed of aliphatic spacers and incompatible end groups (for example compounds **64a** and **64b**), have a tendency to form core-shell columns where the aromatic cores are arranged in the column cores, the alkylene spacers form the shell around these columns, and the terminal units form the continuum in which the core-shell columns are organized (Figure 32e).^[77,78,123,250,251]

7.2. Dendritic Janus Polyphiles

Selected examples of flexible Janus-type molecules with different size of the two halves are shown in Figure 33a. The hexasubstituted benzanilide **69**, combining one half decorated with bulky perfluorinated chains and the other half with alkyl chains, forms a hexagonal columnar LC phase. In the columns, the smaller alkyl chains form the centers of the columns, the aromatic groups are arranged in cylindrical shells surrounding the aliphatic columns, while the much bulkier fluorinated chains are located in the fluorinated continuum around the core-shell columns (Figure 33c; B = R_H, C = R_F).^[262] In this core-shell structure, the aromatic cores form the shell instead of the core part that is observed for usual core-shell organizations (Figure 33b). This phase could alternatively be regarded as a special type of monolayer-type vesicular columnar LC phases where the interior of the cylinders is different from the continuum surrounding them (see Section 6). Compound **68**^[263] is an example for a Janus-type dendrimer, in this case

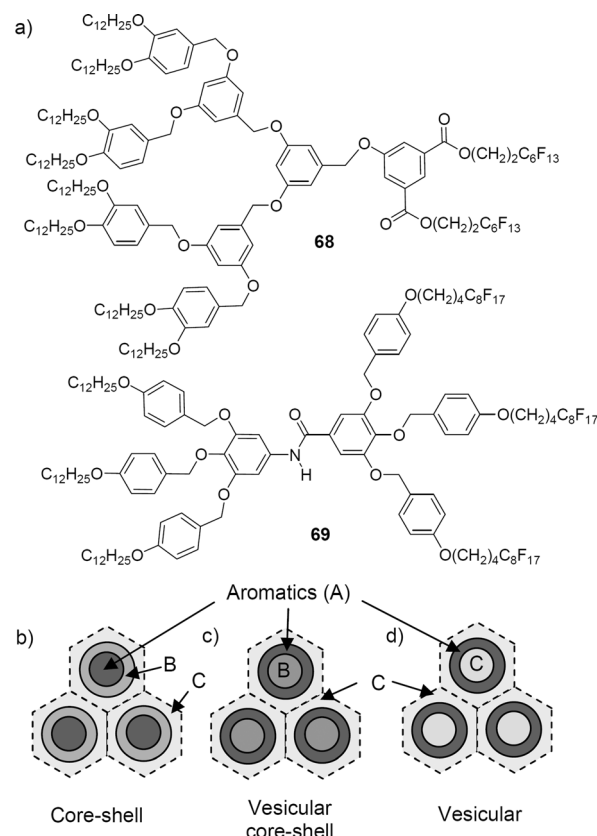


Figure 33. a) Examples of Janus-type molecules^[262,263] and b)–d) different core-shell columnar phases; b) usual core-shell structure with aromatic units in the core; and c), d) vesicular LC phases with aromatic shells. In (c), the content of the inner columns is different from the continuum, and in (d) it is the same (cuts perpendicular to the columns).

the two R_F chains represent the smaller units compared to the eight alkyl chains.^[264] Such compounds form LC phases in which the R_F chains self-assemble into columns or spheroidal domains which then arrange in different types of complex 2D or 3D ordered LC phases.^[265]

8. Complex Compartmentalization Patterns of T- and X-Shaped Polyphiles

The effects of bulky lateral substituents in a lateral position of rod-like molecules have been investigated by Weissflog et al.^[266] and others.^[267,268] In most cases these substituents lead to a loss of long-range positional order, and smectic phases were replaced by nematic phases or LC properties were lost completely. However, positionally ordered LC phases can be retained if lateral and terminal chains are incompatible.^[268,269] This paves the way to the combination of shape anisotropy and polyphilicity in a competitive manner, which turned out to produce completely new LC phase structures with enhanced complexity if terminal and lateral chains at a rod-like core are incompatible and one of them provides sufficient cohesive energy density, either by forming hydrogen bondings or by being an ionic group. T-

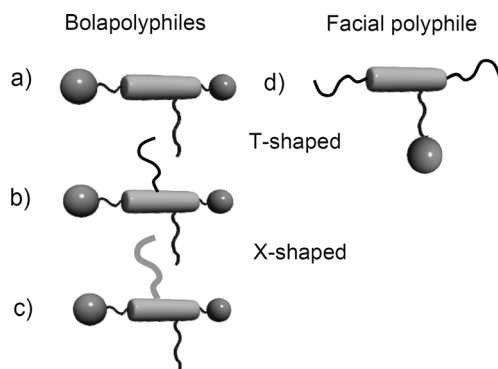


Figure 34. Polyphilic T- and X-shaped bolapolyphiles and facial polyphiles.

shaped polyphiles with only one lateral chain and X-shaped polyphiles with two lateral chains can be distinguished, as shown in Figure 34.^[161,270–272]

T-shaped polyphiles are composed of three incompatible units and thus represent triphiles in most cases. For X-shaped polyphiles, the two lateral chains could either be identical or very similar (triphilic molecules, Figure 34b) or different (tetraphilic molecules, Figure 34c). There are two distinct groups of T-shaped polyphilic mesogens. In one group the lateral unit is a polar moiety, whereas the terminal chains are lipophilic, such polyphiles are known as “facial polyphiles” (see Figure 34d).^[269,273] The reversal of the position of polar and lipophilic moieties leads to rod-like polyphiles with two polar end groups and one or two lipophilic side groups, designed as “bolapolyphiles” (Figure 34a–c). The term “bola” indicates that a hydrophobic unit is functionalized with hydrophilic groups at both ends.^[274] These new types of mesogenic compounds and their complex LC phases have been discovered in my group at Halle University,^[275,276] that is, at the same institute where about 100 years earlier D. Vorländer has developed the fundamental concepts of LC design. The huge number of new LC phases formed by these compounds was investigated during the last decade in close collaboration with the group of G. Ungar at the University of Sheffield.

8.1. T-Shaped Bolapolyphiles

Typical rod-like building blocks for the design of T-shaped bolapolyphiles are oligo(1,4-phenylenes),^[113,275–277] oligo(2,5-thiophenes),^[278–283] or oligo(1,4-phenylene ethylenes).^[284,285] In most cases, glycerol units were used as polar terminal groups; polar groups

incorporating amides^[286,287] or single OH groups were occasionally also used.^[288] For the lateral chains, a broad variety of different groups is available, including linear and branched alkyl chains (R_H),^[275] oligo(dimethyl siloxanes), carbosilanes,^[286] and numerous other bulky lipophilic groups.^[289] Often semiperfluorinated chains (R_F) were used,^[161,276,290–292] which have increased incompatibility with the polar groups and the aromatic units, providing considerably enhanced phase stabilities.^[161] These chains also have a significantly larger volume compared with alkyl chains of the same length, thus having a stronger effect on the mesophase type. In molecules with R_F chains, the perfluorinated segments are usually decoupled from the aromatic core units by flexible alkyl spacers. This facilitates the synthesis and reduces the melting points, leading to broader mesomorphic temperature ranges. Moreover, the incompatibility between R_F and R_H segments or between R_F and R_H chains can be used as an additional source of intramolecular incompatibility (see Section 8.6).

8.1.1. Liquid Crystals Composed of Polygonal Honeycombs

Bolaamphiphiles without lateral chain form monolayer smectic phases (SmA) with high transition temperatures. In these smectic phases, the rod-like units and the glycerol groups are organized in alternating layers (Figure 35a).^[108,293,294] Relatively short lateral chains segregate into distinct domains with only short range correlation, indicated by a diffuse small-angle scattering in the XRD patterns. This phase, assigned as SmA⁺, is composed of random mesh layers with holes filled by the flexible lateral

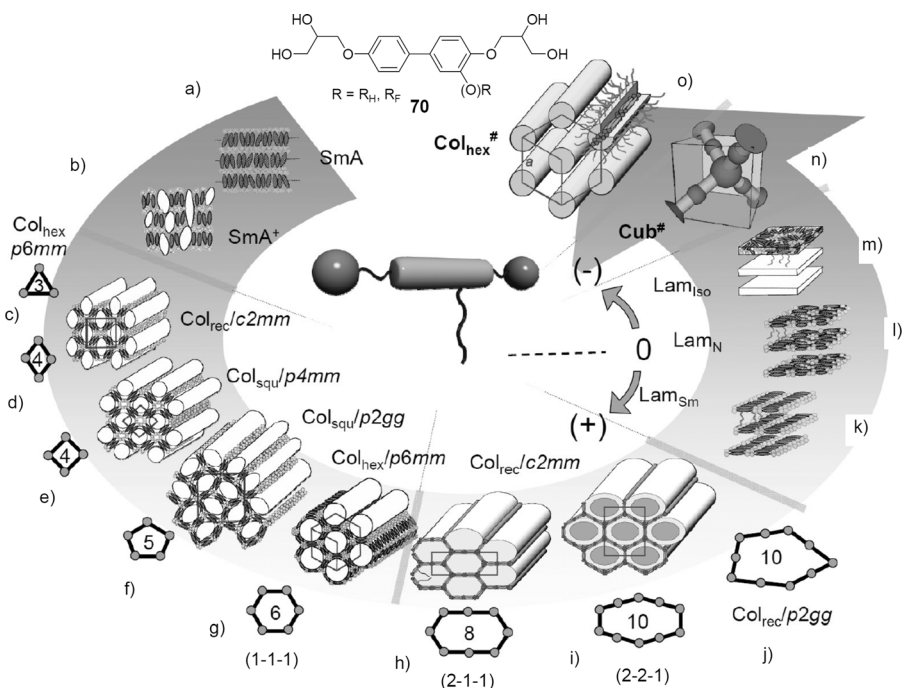


Figure 35. Sequence of LC phases formed by self-assembly of the T-shaped bolapolyphiles **70** as observed on increasing the size of the lateral chain (counter-clockwise); for structures c) and o) molecules with further extended aromatic cores are required.^[272] Reproduced from Ref. [272], <http://rsfs.royalsocietypublishing.org/>.

chains (Figure 35b).^[276] On further increasing the chain length, the domains fuse to infinite columns, which develop parallel to the layer planes and register on a long range periodic 2D lattice. During formation of the 2D lattice, the layers become broken, yielding honeycombs. The honeycomb occurring adjacent to the SmA^+ phase often has a rhombic shape of the cells, leading to a centered rectangular lattice with $c2mm$ plane group ($\text{Col}_{\text{rec}}/c2mm$; Figure 35d).^[276] On further chain elongation, a series of different honeycombs with different cross-sectional shape of the cylinders is formed (Figure 35e–j).

In all these LC phases, the π -conjugated rod-like cores of the T-shaped molecules are arranged perpendicular to the column long axes, forming cell walls connected at the seams by the hydrogen-bonding glycerol groups. The resulting honeycomb cells of polygonal cross-section and infinite length are filled with the lateral chains. Depending on the ratio of the volume of the chains to the length of the rod-like core, cells ranging from rhombic or triangular via square and pentagonal to hexagonal and so on were obtained (Figure 35d–g).^[272, 275, 276, 289]

These LC phases with 2D periodicity can be considered as a special kind of columnar phase. In contrast to the columnar phases formed by disc-like, polycatenar, dendritic, and star-shaped molecules, where the more rigid aromatic cores form the individual columns, which are then arranged on the 2D lattice in the continuum of the fluid alkyl chains (see Figures 1 and 5c) the structure of the honeycomb phases is reversed (see Figure 35c–g). In this case, the rigid aromatic cores form a continuous framework of cylinders fused to a polygonal honeycomb around the fluid columns of the alkyl chains, which are arranged on a 2D lattice. Therefore, the space available inside the prismatic cells is strictly limited and slight changes of the size of the lateral chains or the length of the aromatic cores have a strong impact on the mesophase symmetry and morphology. The general trend is to undergo a transition of the cross-sectional shape of the polygonal cylinders from smaller to larger polygons with increasing size of the lateral chain; that is, by moving anticlockwise in Figure 35. Extension of the rod-like cores at constant volume of the lateral chain has the opposite effect, as shown in Figure 36. Because longer rods provide more space inside the

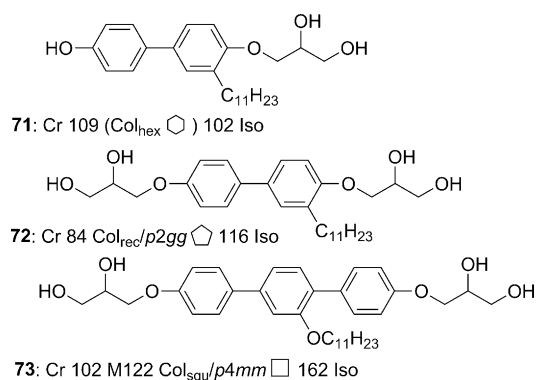


Figure 36. Effect of core length on the mesophase types of T-shaped bolapolyphiles and their transition temperatures ($T/^\circ\text{C}$).^[288, 276, 297]

cylinders the number of walls in the cross section of the cylinders must be reduced by moving clockwise in Figure 35. Although the molecules in these honeycombs are interconnected by relatively strong hydrogen bonding to infinite honeycombs, there is still a high degree of dynamics with the molecules adapting different conformations rapidly rotating and exchanging their positions. Thus, these are true LC phases with viscosities comparable with those of other columnar LC phases formed by usual disc-like or polycatenar molecules.

The hydrogen bonds between the glycerol groups have cooperative character, which favors large polymeric aggregates over smaller dimers, trimers, and so on. Therefore, the hydrogen bonds form networks along the columns, which connect the bolaamphiphilic cores not only to single nets but also fuse these nets to infinite honeycombs. These hydrogen bonds also have a high degree of dynamics,^[295] and thus store a significant amount of entropy. This provides an additional entropy reservoir^[296] besides that provided by the fluid lateral chains inside the cylinder cells, thus favoring LC self-assembly. The hydrogen bonding networks form polar columns with a high tendency to segregate from the lipophilic segments. Structural variations that increase the CED difference between these columns and their lipophilic surrounding stabilize the honeycomb LC phases; the most important are the increase of the number of hydrogen bonds and increasing the lipophilic character of the lateral chains. Also elongation of the rod-like cores stabilizes the LC phases owing to increased rigid-flexible incompatibility and increased attractive π – π and dispersion interactions along the cylinder walls.

Projected on an Euclidian plane, these structures can be considered as 2D nets,^[298] with the hydrogen bonds located on the nodes and the aromatic cores interconnecting these nodes to the 2D net (see Figure 37). Alternatively, these nets can be

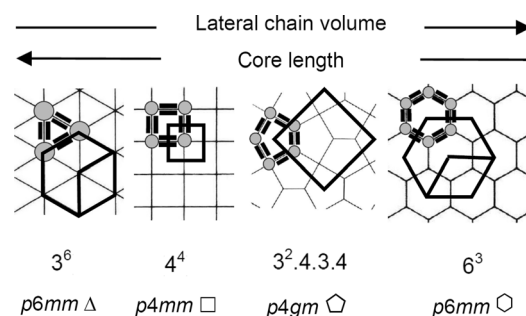


Figure 37. Tiling patterns formed by self-assembly of T-shaped bolapolyphiles, their tiling-notations (Laves-tiling, top line) and plane groups with highest symmetries (bottom line).

described as periodic tiling patterns by polygonal tiles^[299] with distinct 2D topologies v^n , where n indicates the number of vertices of the polygonal tile and v their valence.^[270] For example, the symbol 3².4.3.4 of the pentagon tiling indicates a sequence of two three-fold, one four-fold, one three-fold, and one four-fold vertex around each pentagon.^[299] The easy formation of honeycombs with a pentagonal cylinder cross-section is an especially interesting and very unusual feature of these liquid-crystalline honeycombs. Although regular penta-

gons cannot tile an Euclidian plane periodically, in the fluid LC state the pentagonal cylinders can easily deform into non-regular shapes for which numerous different monohedral tiling patterns (all tiles have the same size and shape) exist.^[299] The most symmetric monohedral edge-to-edge tiling has a $p4gm$ square lattice. This lattice represents a herring-bone like packing of pairs of pentagonal cylinders (Figure 37). Often however the pentagonal cylinders are more distorted, which leads to a rectangular $p2gg$ lattice.^[270,276,300]

Simulations using coarse grained methods and dissipative particle dynamics have successfully been used to reproduce the experimentally observed development of the polygonal honeycomb phases ranging from rhombic/triangular to hexagonal.^[301,302] An especially interesting aspect of Monte Carlo simulations is that the phase structures can be considered as mainly entropy driven, that is, the observed mesophases are determined by maximizing the entropy.^[303,304]

8.1.2. Giant Honeycomb Phases

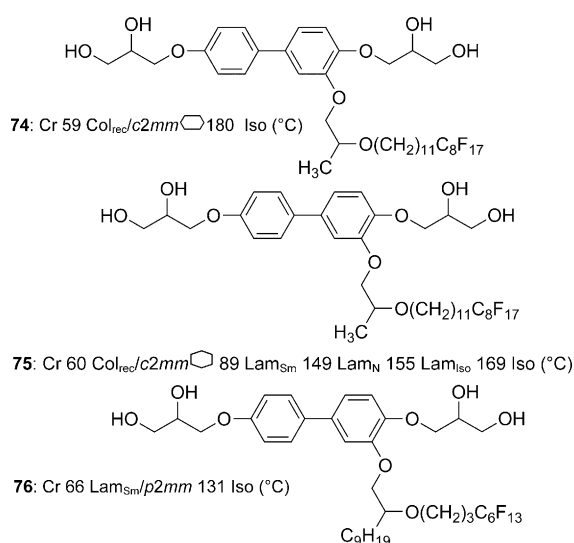
Further extension of the lateral chains beyond the hexagonal honeycombs requires the formation of cylinders with a number of sides larger than six (Figure 35h–j). If these cylinders would have a regular cross-sectional shape, a periodic edge-to-edge tiling would be impossible. However, again the fluidity in the self-assembled LC systems allows them to adjust their cross-sectional shape in such a way that they can adopt to a periodic edge-to-edge tiling on a rectangular 2D lattice.^[270,276,289] In these giant cylinder phases, some or all cylinder walls have double lengths, being formed by two end-to-end connected molecules instead of just one.^[14,305] In most cases, expansion of hexagonal cylinders takes place along one of the diagonals, which leads to (2-1-1) hexagons with 8 molecules in the circumference (Figure 35i; compound **74**). These elongated cylinders allow the chains to easily reach the middle of the cylinders and provide an improved parallel alignment for relatively long and linear lateral chains.^[14,276,286,289] If the lateral chains are even larger and the chain flexibility is increased, (2-2-1) hexagons with 10

molecules in the circumference can then be formed (Figure 35i, compound **75**), resulting from the expansion of the (1-1-1) hexagons perpendicular to two opposite sides.^[14,305] Giant pentagonal cylinders, where each side contains two end-to-end molecules (see Figure 35j) are another mode of organization of ten molecules in the circumference.^[276] Remarkably, simulations failed to give uniform giant honeycomb phases,^[301–303] and therefore these structures could be considered as being more complex than those of the simple honeycombs.

Another special feature of giant honeycombs formed by molecules with lateral alkyl chains having a perfluorinated end groups is a nano-segregation inside the cylinders. This intracellular segregation leads to honeycombs with “core-shell-in-cylinder structure”, that is, the interior of the cylinders is divided into a R_F -rich core and a hydrocarbon-rich shell (see Figure 35i).

8.1.3. Laminated Liquid-Crystal Phases

Increasing the temperature or further enlargement of the lateral chain volume causes the giant cylinders of the LC honeycombs to burst; the side walls are removed leaving layers (Figure 35k–m). In these layers, the polar rod-like bolaamphiphilic cores (rod-like cores plus polar groups) are separated by the layers formed by the disordered lateral chains. Unlike the usual smectic phases, in the Lam_N and Lam_{Sm} phases the π -conjugated rod-like cores are oriented parallel to the layer plane.^[270,276,286,288–291,305,306] In the layers, these cores can adopt in-plane isotropic, nematic-like, and smectic-like order, respectively, giving the three-dimensional Lam_{Iso} , Lam_N , and Lam_{Sm} phases. In the Lam_{Sm} (Figure 35k) and Lam_N phases (Figure 35l) there is orientational correlation of the aromatic cores in adjacent layers, leading to biaxial smectic phases, whereas the Lam_{Iso} phase (Figure 35m) is optically uniaxial and can be regarded as a special kind of SmA phase without preferred direction of the aromatic cores.^[306] The absence of a long-range positional correlation of the in-plane periodicity of the layers in the Lam_{Sm} phase indicates an only weak positional coupling of these layers by the layers of the fluid chains. However, for bolapolyphiles with a branched lateral chain, consisting of an alkyl and a perfluoroalkyl branch (for example compound **76**), the positional coupling between the layers becomes stronger and in this case the occurrence of positional correlation between adjacent layers leads to a long-range 2D lattice with $p2mm$ plane group symmetry normal to the layer planes.^[292] As it will be shown in Section 8.3 (Figure 40c), the R_F segments can form distinct columns within the non-polar sublayers of the lateral chains, and these columns provide a stronger coupling between adjacent layers, allowing long-range positional correlation. All these “laminated” isotropic, nematic, and smectic phases are of significant interest for condensed matter physics in general, as they offer the possibility to investigate phase transitions in quasi 2D systems.^[307]



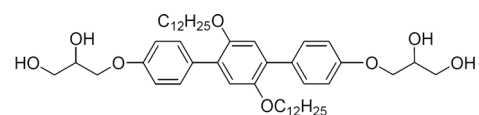
8.1.4. Hexagonal Honeycombs and Lamellar Phases Formed by Rod-like Polymers with Lateral Chains

Lam phases and honeycomb structures are also formed by π -conjugated LC polymers with lateral chains, as used for organic semiconductors.^[48,308] For polymers with a certain lateral chain density, lamellar LC phases are formed in which the aromatic backbones are organized in layers and parallel to the layer planes. These layers are segregated from layers comprising the lateral aliphatic chains, similar to the Lam_N phases.^[309–312] If the rod-like polymer backbone is formed by a regular sequence of different building blocks, noncorrelated (Lam_{Sm}) and correlated Lam_{Sm} phases (Col_{rec} phases) were observed.^[310,313] Reduction of the number or length of lateral chains leads to hexagonal honeycombs with walls formed by the rod-like polymer backbones.^[309,314] In these honeycombs the polymer backbones are arranged parallel to the column long axis and not perpendicular as in the honeycombs of the polyphiles. As the orientation of the aromatic cores is parallel to the cylinder long axis, there is no restriction to the size of the cylinder walls and the diameter of the hexagonal cells can be changed continuously as required by the lateral chain size. Because hexagonal cylinders maximize the volume to cylinder-surface ratio, no cylinders with other polygonal shapes than hexagonal were observed. Upon increasing the alkyl chain volume, the size of the hexagonal cells adjusts to the lateral chain volume before a direct transition to the layer structure takes place.

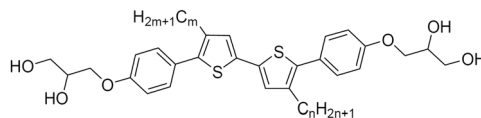
8.2. X-Shaped Polyphiles with Two Similar Lateral Chains: Single-Wall Honeycomb Phases

Fixing two or more instead of only one lateral chain to bolapolyphiles could provide other molecular shapes than just the T-shape. Two chains can be fixed at opposite sides of the same ring of the rod-like core which provides X-shaped molecules with a fixed orientation of the two chains (for example, compound **77**).^[315] If the chains are fixed to different rings of the aromatic core, as in compounds **79** and **80**, their orientation with respect to each other is not fixed and can change during self-assembly from the X-shaped to a Π -shaped conformation (both chains at the same side).^[279,280] The additional chain has a significant effect on the structure of the honeycomb framework. T-shaped compounds with only one lateral chain give rise to LC honeycomb phases where the cross-section of the honeycomb walls contains two rods arranged side-by-side, that is, the honeycombs have double walls (Figure 38a).^[270]

However, attaching two lateral chains to opposite sides of the aromatic core in the X-shaped polyphiles generates polygonal honeycombs with walls that are only one molecule thick (Figure 38b).^[279,280,315] The reason is that for the X-shaped molecules the back-to-back alignment of the rod-like units in the walls is distorted by the additional chain.^[270] As a consequence of the thinner walls the stability of the LC phases is reduced (compare compounds **78** and **79** in Figure 38) and effectively more space is left available for the lateral chains inside the cells, which influences the shape



77: Cr 86 ($\text{Col}_{\text{sq}}/\text{p}4\text{mm}$ 64) Iso



| Comp. | <i>m</i> | <i>n</i> | Phase transitions ($T/^\circ\text{C}$) |
|-----------|----------|----------|---|
| 78 | 12 | 0 | Cr 155 $\text{Col}_{\text{sq}}/\text{p}4\text{mm}$ 166 Iso |
| 79 | 6 | 6 | Cr <20 $\text{Col}_{\text{hex}}/\text{p}6\text{mm}$ Δ 85 Iso |

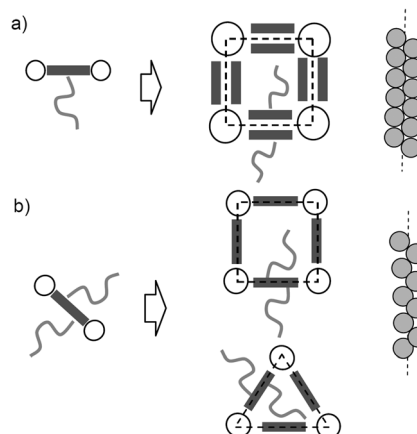
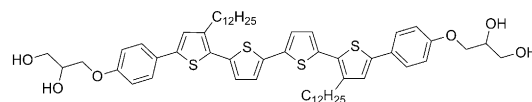


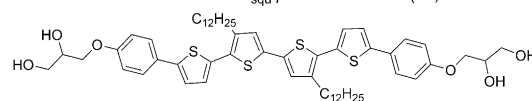
Figure 38. Comparison of selected X-shaped (**77**, **79**) and T-shaped (**78**) bolapolyphiles: a) double-wall square cylinders of T-shaped bolapolyphiles; and b) single-wall cylinders as formed by X-shaped polyphiles.^[279,315]

of the honeycomb cells. For example, the dithiophene **78**, with a single lateral dodecyl chain, forms a square honeycomb ($\text{Col}_{\text{sq}}/\text{p}4\text{mm}$), whereas compound **79**, having two short hexyl chains with the same or a slightly larger total size, has a smaller triangular honeycomb instead ($\text{Col}_{\text{hex}}/\text{p}6\text{mm}$ Δ phase; see Figure 38).^[279]

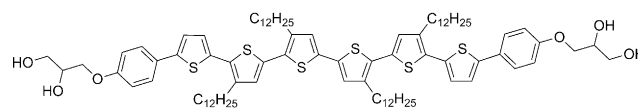
A square columnar phase is also formed by the tetrathio-phenylene **80a**,^[280] whereas the isomeric compound **80b** with a changed position of the lateral chains forms a nematic



80a: Cr 130 $\text{Col}_{\text{sq}}/\text{p}4\text{mm}$ 151 Iso ($^\circ\text{C}$)



80b: Cr 138 ($\text{Col}_{\text{sq}}/\text{p}4\text{mm}$ 125 N_{Cy}) 151 Iso ($^\circ\text{C}$)

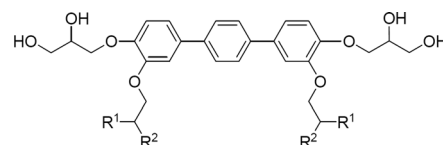


81: Cr 109 Col_{hex} Δ 148 Iso ($^\circ\text{C}$)

phases beside the $\text{Col}_{\text{sq}}/p4mm$ phase.^[282] A cybotactic structure composed of small square honeycomb clusters (N_{Cyt}) is proposed for this nematic phase. This nematic phase with negative birefringence is related to the columnar nematic phases of disc-like molecules (N_{Col}), but it has an inverted structure, the aromatic units form the continuum instead of the column cores and the alkyl chains form the columns instead of the continuum. It is considered as a disordered phase occurring at the discontinuous $\text{Col}_{\text{sq}}/p4mm$ -to- $\text{Col}_{\text{hex}}/p6mm$ transition. At reduced temperature, this transition takes place in a more ordered way via a $p4gm$ square columnar phase composed of a mixture of square and triangular cylinders with a ratio 1:2 (see Section 8.5.1 for a more detailed discussion of this phase). For this ordered mode of transition, numerous additional complex tiling patterns composed of triangular and square cylinders with other ratios could be expected,^[204] eventually leading to 2D quasicrystalline arrangements if the square to triangle ratio approaches the value 1:2.31.^[206] Bolaamphiphiles with sufficiently long rod-like cores, as for example the sexithiophene **81**, retain the capability of forming polygonal honeycombs, although even four lateral chains were attached in this case.^[283]

8.3. Bolaamphiphiles with Branched Lateral Chains: Longitudinal Rod-Bundle Phases and Crossed-Column Phases

Combining a *p*-terphenyl-based bolaamphiphilic core with two branched chains with at least one branch in each chain being fluorinated (for example compounds **82** and **83**) increases the volume of the lateral chains beyond the limits of the Lam phases. For these compounds, the infinite layers of the Lam phases break up into laterally isolated columns of rod bundles.^[316,317] Along the bundles the molecules are aligned parallel to the column long axis and these bundles are rotationally disordered with respect to their long axes and pack on a hexagonal lattice (Figure 39a,b). This creates a columnar LC phase in which rod-like aromatics are arranged parallel to the column long axis, which are assigned as a longitudinal rod-bundle phase (Figure 39a).^[317] This orientation of the aromatic cores contrasts the organization of the rigid segments in the columnar phases of disc-like and polycatenar compounds^[178] and also in the honeycomb cylinder phases of other T-shaped and X-shaped polyphiles,^[270] where the aromatic groups are always organized perpendicular or slightly tilted to the column long axis. The orientation of the π -conjugated units is also parallel to the column long axis only in the columnar phases formed by main-chain polymers (see Section 8.1.4). In this sense the strings of bolaamphiphiles in the longitudinal bundle phases could be regarded as bundles of supramolecular hydrogen-bonded main-chain polymers. The formation of these rod bundles requires the side-by-side organization of the rods with the lateral chains pointing outwards; that is, the preferred conformation should in this case be the Π -shaped. In the rod bundles, the aromatic cores and the polar glycerol groups are segregated, leading to a periodicity along the columns. These modulated columns can lock into register with



| Comp. | R ¹ | Phase transitions (T/°C) |
|------------|--|---|
| 82a | R ¹ = R ² = (CH ₂) ₃ C ₄ F ₉ | Cr 83 M 97 Col _{hex} 161 Iso |
| 82b | R ¹ = R ² = (CH ₂) ₃ C ₁₀ F ₂₁ | Cr 122 Col _{hex} 175 Iso |
| 83 | R ¹ = C ₁₁ H ₃₃ ; R ² = (CH ₂) ₃ C ₈ F ₁₇ | Cr 76 R ³ m 125 Col _{hex} 156 Iso |

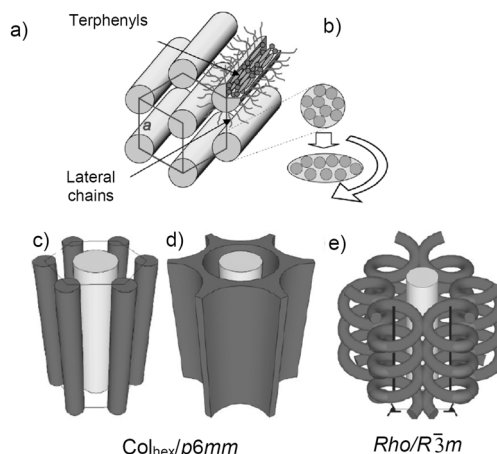


Figure 39. Bolaamphiphiles with two branched lateral chains forming longitudinal rod-bundle phases: a) Organization in the rod-bundle phases; b) the local cross-section of the columns is thought to be elliptical, but circular when averaged over time and space; c)–e) structures resulting from the segregation of the R_F chains; dark gray = R_F -rich regions; light gray = columns of the rod-bundles.^[317] Reprinted with permission from Ref. [317], copyright 2011 American Chemical Society.

each other with defined longitudinal shift by a third of the periodicity on a rhombohedral ($R\bar{3}m$) lattice.^[317]

In the rod-bundle-type LC phases, the R_F chains can partly segregate from the R_H segments and form regions with enhanced R_F concentration. These regions have a different shape depending on the size and distribution of the R_F segments (Figure 39c–e). For compounds with R_F segments at each chain end, the segregation of R_H and R_F chains takes place only in the plane of the hexagonal lattice, leading to R_F -rich columns located at the vertices of the Voronoi honeycomb (compound **82a**, Figure 39c) which fuse to a fluorinated honeycomb if the R_F segments are elongated (compound **82b**, Figure 39d). For compounds such as **83** with only one fluorinated branch in each lateral group, R_F/R_H segregation along the *c* axis, that is, parallel to the column long axis, provides the locking of the modulated columns into register, which leads to the $R\bar{3}m$ lattice with a helical structure of the R_F -rich regions (Figure 39e).^[317]

Even more complex LC phases were found for the biphenyl derivative **84** (Figure 40) with only one branched lateral chain combining a R_F chain with a carbosilane chain.^[318] In this case, the column register takes place without longitudinal shift, leading to a $P6/mmm$ lattice (Figure 40a). On decreasing the temperature, a transition to a Lam phase takes place via a 3D orthorhombic intermediate phase

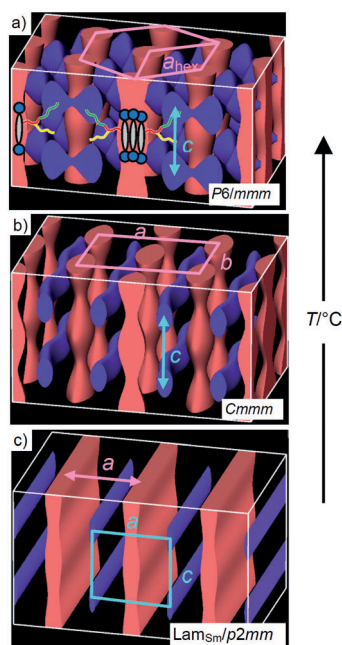
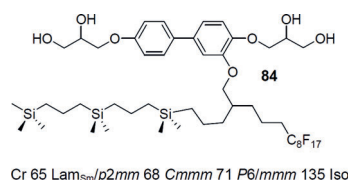


Figure 40. Organization of compound **84** as illustrated by experimental electron density maps (red = low density = bolamphiphilic moieties, blue = high density = richest in R_F chains); the space between is filled by the carbosilanes ($T/^\circ\text{C}$).^[318] Reproduced from Ref. [318], copyright 2011, Wiley-VCH.

(Cmmm) for which the R_F chains (blue) form R_F rich columns laying perpendicular to the main columns of the rod-bundles (Figure 40b). This organization of crossed columns is a new mode of organization of columnar aggregates. On further cooling, the rod-bundle columns fuse to form infinite sheets, leading to a $\text{Lam}_{\text{Sm}}/p2mm$ phase (Figure 40c).^[318] This is the same kind of correlated Lam_{Sm} phase as observed for compound **76** (Section 8.1.3) having a branched chain composed of R_F and R_H branches.^[292]

As shown in Figure 35, the Lam phases with zero interface curvature divide the columnar phases formed by the T-shaped polyphiles into two inverted structures with opposite sign of the curvature of the interface between the regions comprising the rod-like cores and the regions formed by the flexible chains. This is associated with a complete reorganization of the rod-like moieties with respect to the column long axes, which takes place in two steps; in the first step the polygonal cylinders burst with formation of layers (Lam phases). In the second step, the layers of these Lam phases split into infinite ribbons, giving rise to the longitudinal rod-bundle phases.^[317] This is analogous to the change from normal type to reversed type columnar phase as the volume of lipophilic chains of simple amphiphilic mesogens increases (see Figure 13). Bicontinuous cubic phases are often observed between lamellar and columnar phases.^[9] Preliminary results indeed

indicated the presence of such phases formed by branched axial rod bundles (Figure 35n).^[319,320]

8.4. Polyphiles with Bent Cores: Hexagonal Honeycombs with Hexagonal and Trigonal Lattices

A 120° bend in the aromatic core of the bolapolyphiles with a lipophilic lateral chain in the bay position at the concave side of the bent core (anchor-shaped compounds **85**)^[321] promotes the formation of hexagonal honeycombs and excludes other cylinder shapes. There are two different types of hexagons, either with 3 or with 6 molecules in the circumference (Figure 41a–c). Reducing the volume of the lateral chains leads to a change from larger 6-hexagons to smaller 3-hexagons (compounds **85a** and **85b**). In a similar way, reducing the length of the bent aromatic backbone (by removing the acetylene units) at constant chain volume leads to a change from smaller 3-hexagons to larger 6-hexagons. It should be noted that in the 3-hexagon honeycomb, only every second edge accommodates a hydrogen-bonding channel (Figure 41b); therefore it has the plane group $p3m1$ without a center of inversion, and thus this is a rare trigonal columnar

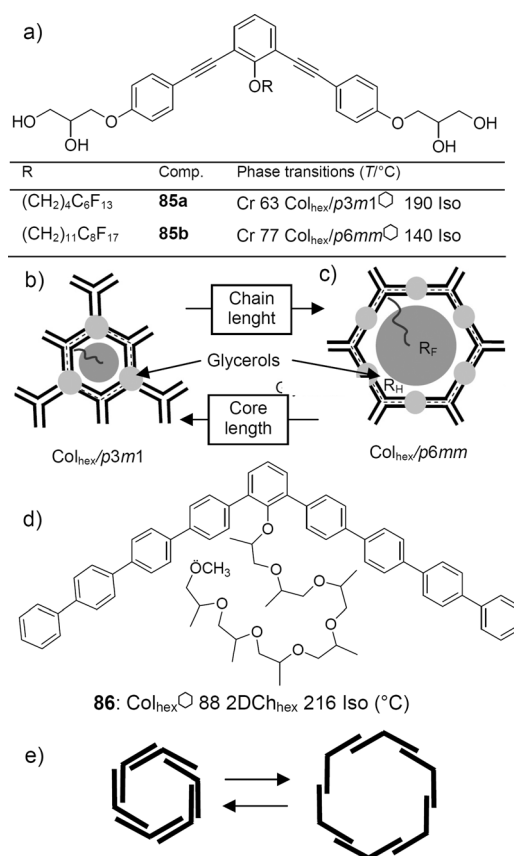


Figure 41. a) Anchor-shaped bolapolyphiles **85** and b,c) their hexagonal honeycomb phases; b) 3-molecule hexagons with $p3m1$ symmetry; and c) 6-molecule hexagons with $p6mm$ symmetry (dark gray = fluorinated cores, small light gray dots = glycerols);^[321] d) bent oligophenylene with a bulky polar group in the bay position (**86**); $2\text{D-Ch}_{\text{hex}}$ = hexagonal mesh layers; and e) change of the size of the hexagonal cylinders by sliding ($T/^\circ\text{C}$).^[322]

liquid crystalline phase with non-centrosymmetric structure.^[321] In the 6-hexagon honeycomb, the channels with the hydrogen-bonding glycerol groups are located in the middle of the cylinder walls instead of being at the edges as in the honeycombs formed by T- and X-shaped bolaamphiphiles with linear cores (Figure 41 c).

Anchor-shaped facial amphiphiles **86** without distinct end groups at the aromatic cores can slide over each other (Figure 41 d,e).^[322a] In this way the space available inside the hexagonal cylinders can easily adopt to that required by the lateral chains, although the hexagonal shape of the cylinders is retained. However, as these cylinders are not stabilized by hydrogen-bonding networks at the edges, these cylinders can easily break into smaller segments, which laterally fuse to hexagonal mesh layers (2D- Ch_{hex} phase). Bent molecules having the flexible group at the convex side of the bent aromatic core form vesicular columns, as discussed in Section 6 (Figure 29 a).^[242]

8.5. T-Shaped Facial Polyphiles

8.5.1. Liquid-Crystal Polygonal Honeycombs

Similar to the T-shaped bolapolyphiles discussed in the previous sections, the T-shaped facial polyphiles^[323–332] **87–89** also form polygonal honeycomb phases with cells, in this case ranging from triangular to pentagonal.^[300, 324, 326, 327, 329, 331] Because the positions of the different groups in the molecules are exchanged compared to those in the T-shaped bolapolyphiles, the honeycomb LC structures formed by these polyphiles are also reversed with respect to the position of polar and lipophilic chains. In these polygonal honeycombs, the lipophilic alkyl chains form the columns interconnecting the walls at the edges and the polar groups fill the interior of the resulting honeycomb cells. Because the alkyl chains at the ends of the rod-like cores of the facial polyphiles provide a much smaller CED difference to the aromatic cores compared to the hydrogen bonding groups in the bolapolyphiles, their segregation tendency is smaller and therefore these chains have to be considerably longer than the relatively short glycerol groups of the T-shaped bolapolyphiles. Therefore, much more space is available inside the cylinders which has to be filled by much larger lateral chains, and therefore honeycombs comprising triangular and square cylinders are dominating, whereas the larger pentagonal honeycombs are rare and hexagonal honeycombs or giant cylinder honeycombs have not yet been found.^[324, 326, 327, 329] The typical phase sequence observed upon increasing the length of the lateral chain (n) at constant alkyl chain length is $\text{SmA}^+/\text{Col}_{\text{hex}}/p6mm\Delta$ (triangles)– $\text{Col}_{\text{rec}}/p2gg\text{trapez}$ (trapezoids)– $\text{Col}_{\text{sq}}/p4gm\Delta/\square$ (squares + triangles)– $\text{Col}_{\text{sq}}/p4mm\square$ (squares)– $\text{Col}_{\text{sq}}/p4gmpentagon$ (pentagons). The same sequence is observed as the length of the terminal alkyl chains (m) is reduced at constant volume of the lateral chain; compounds **87** and **88** in Figure 42 form a large part of this sequence.^[329]

In the series of facial amphiphiles the triangular cylinder phase (Figure 42 a) is typically observed as the LC phase with the smallest possible cylinders. The next phase, the trapezoidal cylinder phase (Figure 42 b), is a new special mode of

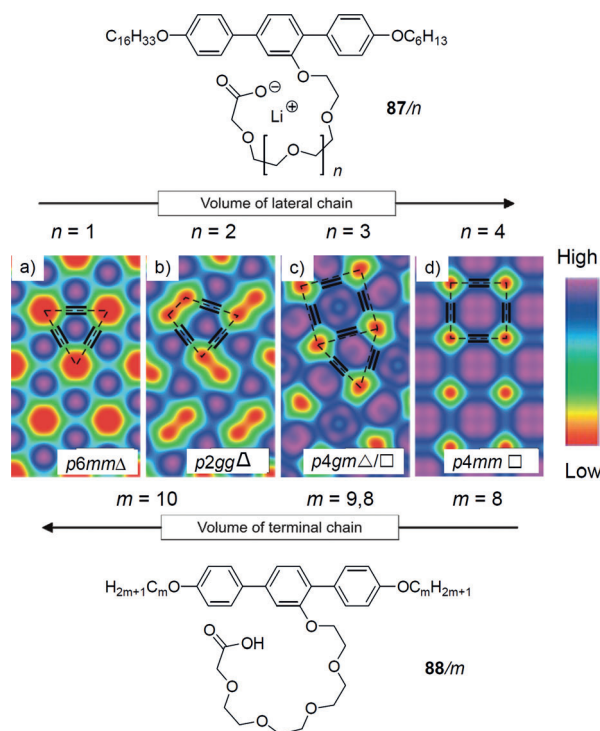


Figure 42. Sequence of polygonal honeycomb phases as observed for T-shaped facial polyphiles depending on the lateral chain length n (series **87/n**) and the terminal chain length m (series **88/m**); a–d) 2D electron density maps (view along the column axis); dark lines indicate the positions of the rod-like segments.^[329] Reprinted with permission from Ref. [329], copyright 2008 American Chemical Society.

organization observed only for facial polyphiles.^[329] This structure can be regarded as a slightly distorted triangular cylinder phase where the circular alkyl columns are deformed elliptically, thus adding a fourth short wall to the triangular cylinders (red regions in Figure 42 b). This deformation is attributed to the alkyl chains tending to become more stretched and pack parallel to each other at reduced temperatures. Furthermore, trapezoidal cylinders provide more space for the lateral chains than triangular ones do; thus this phase appears on reducing temperature or by increasing the side-chain size between the honeycombs composed of triangular cylinders and the $p4gm$ phase composed of a mixture of triangular and square cylinders (see below). The trapezoidal honeycomb phase is distinct from all other honeycomb phases in that one of the cylinder walls is composed of alkyl chains,^[329] which is another way to increase complexity of LC self-assembly.

The $\text{Col}_{\text{sq}}/p4gm\Delta/\square$ phase is another exceptional LC honeycomb phase as it is composed of two different types of cylinders, triangular and square in the ratio 2:1 (snub square tiling).^[300, 327] From a topological point of view this tiling is the dual of the tiling by pentagons. These two different phase structures with $p4gm$ lattice were achieved by reversing the volume fractions of lateral and end-chains of facial polyphiles, as shown for compounds **88** and **89** in Figure 43 a,b. In the tessellations of the two different LC honeycombs with $p4gm$ lattice ($\text{Col}_{\text{sq}}/p4gmpentagon$ and $\text{Col}_{\text{sq}}/p4gm\Delta/\square$) the nodes and tiles are exchanged (full and dotted lines in Figure 43 c).

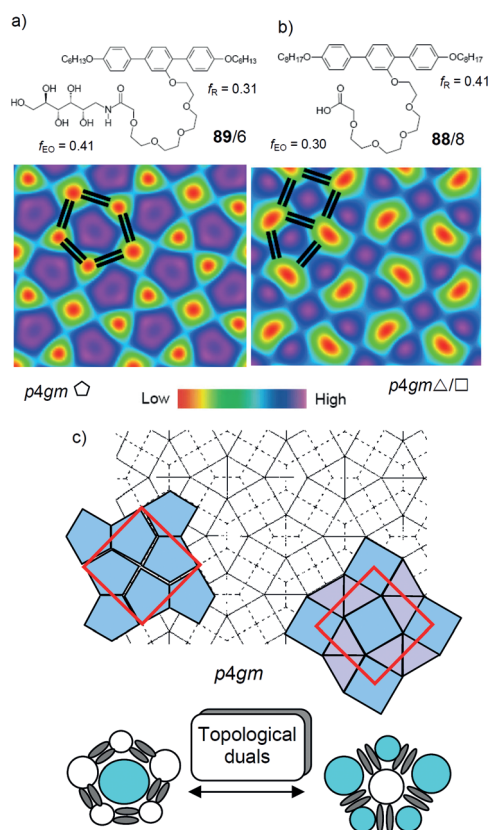


Figure 43. Topological duality of LC phases formed by two different T-shaped facial polyphiles depending on the volume fraction of the terminal alkyl chains (f_R) and polar lateral chains (f_{EO}); a) and b) show the experimental electron density maps for the two different honeycomb phases with $p4gm$ symmetry (blue/purple = highest electron density = polar lateral groups, red/yellow = lowest electron density = terminal alkyl chains; the positions of the rod-like cores are indicated by black lines). In (c), the Laves tiling composed of pentagonal tiles (left) is superimposed on the dual Archimedean tiling composed of squares and triangles (right).^[300] Reproduced with modification from Ref. [272], <http://rsfs.royalsocietypublishing.org/>.

In the resulting tessellation there are exclusively five-fold vertices exactly at the positions of the pentagonal tiles in the dual, and the triangles and squares develop from the three-fold and four-fold vertices, respectively. The pentagonal tiling is composed of identical tiles (Laves tiling), whereas the tiling composed of squares and triangles has identical nodes (Archimedean tiling).^[300] In principle, topological duals can be constructed for any periodic edge-to-edge tiling, except for the 4^4 -tiling by squares, which is its own dual.^[299] The hexagonal honeycomb structure, for example, has its topological dual in the tiling by equilateral triangles in the triangular honeycomb phase.^[324]

8.5.2. Non-honeycomb Hexagonal Columnar Phases

For facial polyphiles with relatively short terminal alkyl chains (compounds **89**/ m with $m = 4-6$; see Figure 43 a), a transition from the pentagonal LC honeycomb phase ($Col_{squ}/p4gmpentagon$) to hexagonal columnar phases takes place upon rising the temperature (Figure 44 h,i). In this type of Col_{hex} phases, the segregation of the aromatic cores from the alkyl chains is strongly reduced and the aromatic cores have no fixed positions around the polar columns formed by the lateral chains (Figure 44 i). Therefore, the hexagonal organization is not based on a polygonal honeycomb; rather it is due to the optimized packing of the polar columns in a continuum formed by the aromatic cores and the alkyl chains. In this continuum, the rod-like cores retain an alignment nearly perpendicular to the column long axis, as indicated by the negative birefringence of this mesophase ($Col_{hex}^{(-)}$ phase). This is probably due to the presence of a kind of small clusters with local honeycomb organization and only short-range correlation.^[327]

In some cases, upon increasing the temperature the sign of the birefringence becomes positive ($Col_{hex}^{(+)}$ phase, Figure 44 k). At the $Col_{hex}^{(-)}$ to $Col_{hex}^{(+)}$ transition, a continuous change of the orientation of the terphenyl groups from tangential to an orientation parallel to the columns takes place with zero birefringence if the maximum of the director distribution function corresponds to the magic angle (54.7°) with respect to the column long axis. It thus seems that upon heating, the cybotactic clusters decrease in size and the excluded volume effect becomes dominating, giving rise to an average alignment of the terphenyl groups closer to parallel to the column axis, leading to positive birefringence ($Col_{hex}^{(+)}$ phase).^[327] This special kind of hexagonal columnar phases is related to the Col_{hex} phases formed by side-on polypeds based

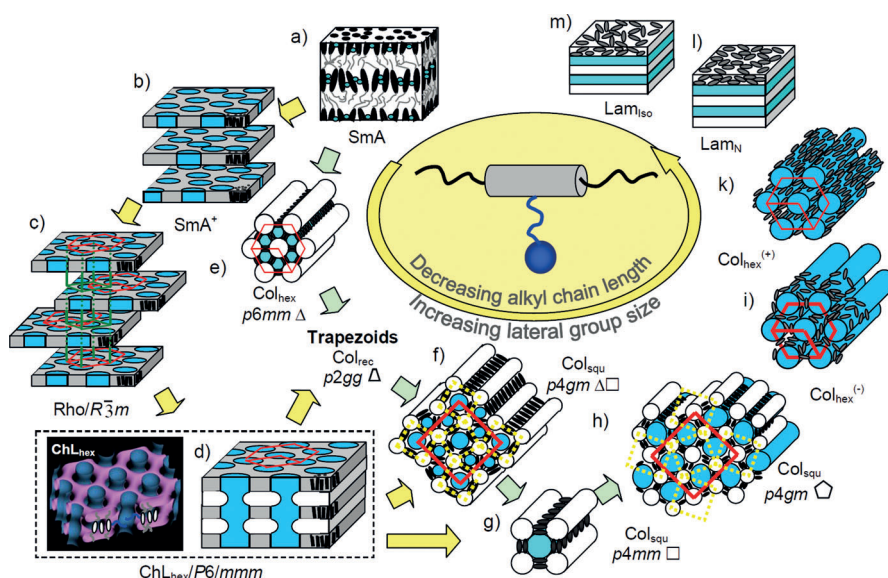


Figure 44. Sequence of LC phases formed by T-shaped facial polyphiles; structures (l) and (m) were only observed after addition of protic solvents; in (d) also the 3D electron density map of the ChL_{hex} phase is shown (blue = polar channels, purple = alkyl chains); for representations of the $R\bar{3}m$ and $P6/mmm$ lattices, see also Figure 27 c.^[270,327]

on laterally attached oligosiloxane scaffolds (Figure 24),^[221b] hybrid structures of gold nanoparticles attached laterally to rod-like mesogens (Figure 27),^[238] and “columnar nematic” phases of side-on polymers.^[333] In all these LC phases, incompatibility between lateral groups and the rod-like mesogenic units leads to formation of columns that are embedded in a continuum composed of orientationally ordered rod-like units.

8.5.3. Complex 3D Phases and Hierarchical Liquid-Crystal Phases

Another specific feature of the T-shaped facial polyphiles is a competition of the honeycombs incorporating triangular to square cylinders with alternative modes of self-assembly, leading to mesophases with 3D periodicity.^[327] The SmA^+ phases of the facial polyphiles have aliphatic and aromatic layers, and these layers are interrupted by domains containing the polar lateral groups, which are mainly located between the aromatic cores (Figure 44a,b). At reduced temperature, these domains can adopt a long range positional order on a hexagonal lattice in the layers, which leads to a correlation of the layers in an ABC fashion, giving rise to a 3D rhombohedral lattice ($R\bar{3}m$; Figure 44c).^[330] In this lattice, the polar domains of adjacent layers are staggered. However, if the length of the polar lateral chains is increased further, or the length of the terminal alkyl chains is reduced, then polar domains of adjacent layers can fuse to infinite columns that penetrate the layers at right angle and organize on a hexagonal lattice. This mesophase with a simple hexagonal 3D lattice ($P6/mmm$) consists of alternating mesh layers of aromatic cores and aliphatic chains penetrated at right angle by columns (blue) containing the polar lateral groups, and it is therefore assigned as a hexagonal-channelled layer phase (ChL_{hex} phase; Figure 44d). This mesophase is unique as it combines two distinct types of LC organization, smectic and columnar, in one common phase structure.^[327,330]

In contrast to the polygonal honeycombs, the aromatic cores are aligned parallel to the polar columns in the ChL_{hex} phases, and therefore this structure provides no restriction for the lateral expansion of these columns. This is advantageous for the self-assembly of molecules having highly polar lateral chains that are strongly incompatible with the aromatic cores (for example alkali-metal carboxylates, carbohydrates), thus storing relatively high interfacial energies. Increasing the column diameter by transition from honeycombs to channelled layer phases can minimize the total of the interfacial areas between the incompatible nanophases and favor the ChL_{hex} phase.

Because in triangular and trapezoid cylinders the diameter of the polar columns is most strongly limited, honeycomb phases incorporating such cylinders are easily replaced by the ChL_{hex} phase, whereas square or pentagonal cylinders, providing larger cross-sectional areas, are retained.^[324,327,330]

A series of different LC phases was found for binary systems of the facial polyphile **90** with COOH-terminated oligo(ethylene oxide) side chains in combination with dendritic oligoamines (DAB dendrimers), forming supramolecular ionic dendrimers (Figure 45).^[331] With increasing dendrimer concentration, the volume of the lateral group is

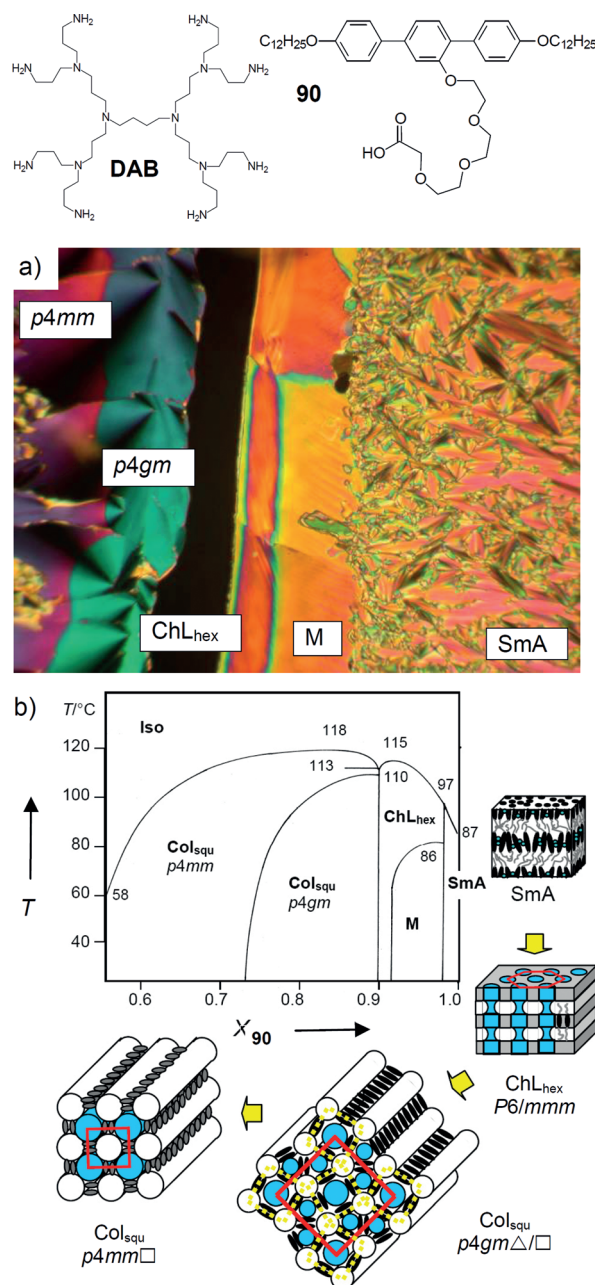


Figure 45. a) Textures of the LC phases occurring in the contact region of the system **90** + **DAB** (**DAB** G2, crossed polarizers, the dark area is the homeotropically aligned ChL_{hex} phase) and b) binary phase diagram.^[331] Reproduced with modifications from Ref. [331] with permission of The Royal Society of Chemistry.

increased and simultaneously the CED of the lateral groups becomes weaker because the concentration of ion pairs decreases by increasing dilution by excess **DAB**. As a result of these two effects, a large section of the phase sequence of facial polyphiles, ranging from a SmA^+ phase for the pure polyphile via ChL_{hex} and $\text{Col}_{\text{sq}}/p4gm/\Delta/\square$ to the $\text{Col}_{\text{sq}}/p4mm/\square$ square cylinder phase for the highest dendrimer concentration, was observed for this binary system by increasing the dendrimer concentration.^[331]

The structure of the ChL_{hex} phase is in some respect reversed to the rod-bundle phases of some bolapolyphiles (Figure 39). In both cases, the rod-like cores are aligned parallel to the columns and provide a periodicity parallel to the column long axis owing to the segregation of the end-groups; in the longitudinal rod-bundle phase the periodicity occurs inside the columns whereas in the ChL_{hex} phases it is outside. The periodicity inside the columns favors staggering with formation of a $R3m$ lattice, whereas the periodicity outside the columns inhibits a staggering, leading to the $P6/mmm$ lattice.

Other examples of structures combining layers and columns were found for polythiophenes with laterally attached disc-like triphenylene units^[334] and for comb-coil diblock copolymers consisting of an amorphous polystyrene (PS) coil-like block and a smectic supramolecular comb-like LC block based on poly(4-vinylpyridine) (P4VP) where the pyridines are hydrogen bonded with 3-pentadecylphenol (PDP).^[335] In the hierarchical structures of these LC-comb-coil polymers, the LC lamellae, formed by the supramolecular comb-like blocks, are penetrated at right angles by the PS columns (Figure 46a) or form columns in the PS matrix (Figure 46b). The first structure is similar to the ChL_{hex} phase;

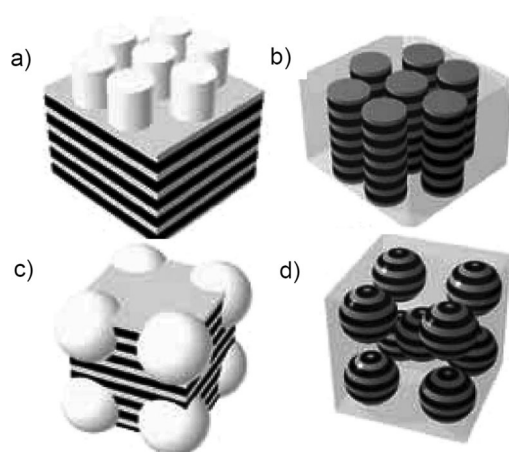


Figure 46. Hierarchical structures formed by LC-PS diblock copolymers depending on the block length: a) CYL-in-lam, b) lam-in-CYL; c) SPH-in-lam; d) lam-in-SPH (CYL = cylinder, SPH = spherical aggregates, lam = lamellae).^[335] Reprinted with permission from Ref. [335], copyright 2006 American Chemical Society.

the latter is related to the longitudinal rod-bundle phases (Figure 39). For these polymers, related hierarchical structures have also been reported for gyroid networks of branched columns and spherical aggregates (Figure 46c,d).^[335]

8.6. X-Shaped Bolapolyphiles with Different Arms: Liquid Crystals with Complex Compartmentalization Patterns

X-shaped bolapolyphiles with two different and incompatible groups at opposite sides of the rod-like core are quaternary block molecules and provide an opportunity to

create liquid crystalline honeycombs with cells of different composition. If projected on a Euclidian plane, such structures can be described as tessellations by two or more differently colored tiles (multicolor tilings).^[285]

8.6.1. Trigonal and Hexagonal Two-Color Tiling Patterns

Compound **91** (Figure 47a), combining a fluorinated chain (R_F -chain) and a carbosilane chain (R_{Si}) at opposite sides of an oligo(*p*-phenylene ethynylene) core, forms two $\text{Col}_{\text{hex}}\Delta$ phases with a triangular honeycomb structure and separated by a second-order phase transition with critical behavior upon approaching the transition temperature. The $\text{Col}_{\text{hex}}\Delta/\Delta$ phase at low temperature is a periodic two-color tiling composed of two types of triangular cylinders with ratio

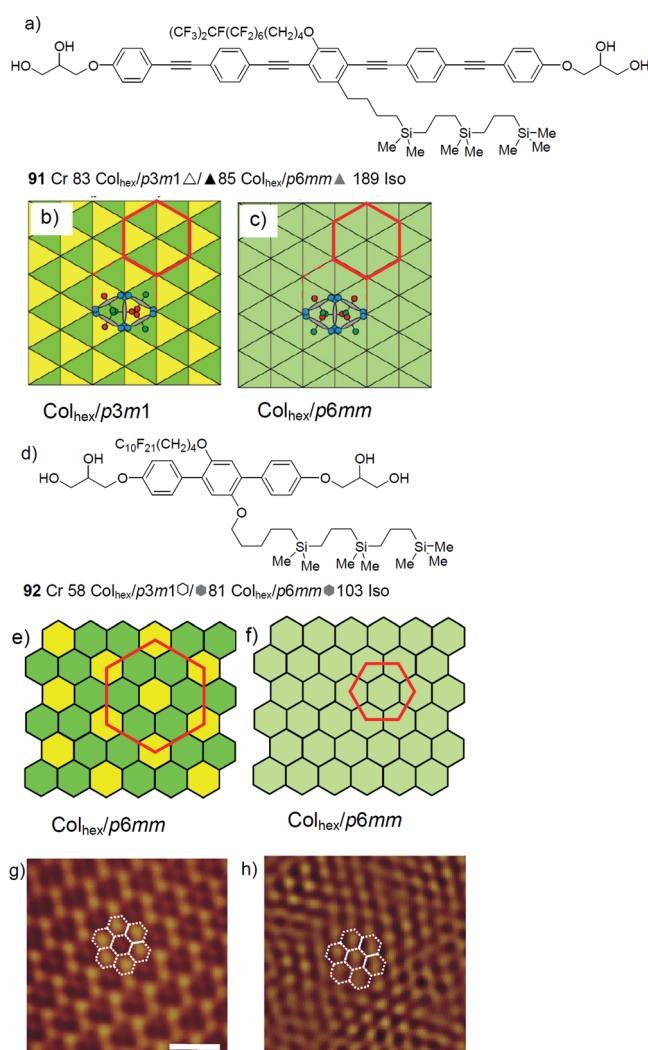


Figure 47. X-shaped bolapolyphiles with two incompatible lateral chains a) forming triangular honeycomb phases with models show in b,c), and d) forming hexagonal honeycombs with the models shown in (e,f). (green = excess of R_F -chains; yellow = R_{Si} -chains; light green R_F and R_{Si} mixed on space and time average) ($T/^\circ\text{C}$); g,h) show AFM phase images of the structures (e), (f), respectively;^[285] b,c) Reproduced from Ref. [272], <http://rsfs.royalsocietypublishing.org/>; g,h) Reprinted from Ref. [285] with permission from AAAS.

1:1; one type is filled with the R_F -chains, the other with the R_{Si} -chains (Figure 47b). The long-range periodic packing of these two types of cylinders reduces the symmetry of the Col_{hex} phase to trigonal ($p3m1$). At higher temperature, the correlation of the triangular cylinders forming the honeycomb is also long range, but the correlation of the “colors” of the honeycomb cells becomes only short range, so that the $p3m1$ lattice is only local and on a larger scale it is averaged to $p6mm$ ($Col_{hex}/p6mm\Delta$ phase; Figure 47c).^[285]

Compound **92** with a shorter terphenyl rod-like core also has two Col_{hex} phases, formed by cylinders, but with a hexagonal cross-sectional area (Col_{hex} hexagon phases; Figure 47d–h). In this case a complete segregation of the R_F chains from the R_{Si} chains is impossible, as formation of cylinders incorporating mixed chains cannot be avoided in a hexagonal honeycomb. In this case, the low-temperature Col_{hex} hexagon phase is a two color tiling with a $p6mm$ superlattice with three cylinders per unit cell (Figure 47e,g);^[285] the main columns on the hexagonal superlattice contain only R_{Si} chains and these are surrounded by hexagonal cylinders filled with a mixture of R_{Si} and R_F chains. Similar to the case of the triangular tiling, there is a second-order phase transition to a high-temperature phase with only short-range correlation of the positions of the colors, leading to a loss of the larger $p6mm$ superlattice, and only the smaller $p6mm$ lattice of the fundamental hexagonal honeycomb (one cylinder per unit cell) is retained (Figure 47f,h).^[285] The transition between short-range and long-range segregated structures is considered to be closely related the Curie transition in frustrated antiferromagnets on a Kagome lattice.^[285]

8.6.2. Liquid Crystals with Complex Multicolor Tiling Patterns

The complexity of LC phase structures can be further increased by introducing geometric frustration.^[336] In the case of the oligo(phenylene ethynylene) **93** shown in Figure 48, the size of the R_F chain was further increased, compared to compound **91**, so that an organization in a tiling pattern formed exclusively by triangular cylinders is no more possible

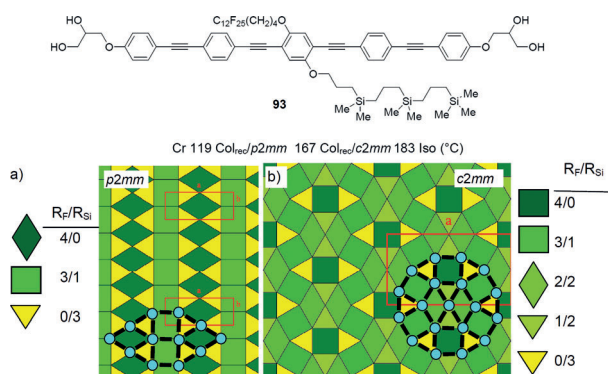


Figure 48. a) Three-color tiling and b) five-color tiling of the LC phases formed by the quaternary X-shaped polyphile **93** (dark green = R_F -chains; yellow = R_{Si} -chains; different green/yellow scales = mixed cells with different mixing ratios as indicated beside the models; black rods = rod-like cores, blue dots = glycerols).^[285] Reproduced with modifications from Ref. [13]; <http://rsfs.royalsocietypublishing.org/>.

and thus square cylinders are also formed. Because of the large difference in area between equilateral triangles and squares, the system experiences a frustration, the triangular cylinders being too small and square cylinders being too large. Further to this purely steric frustration, this compound must simultaneously relieve the frustration owing to the incompatibility of the side chains and their tendency to segregate into distinct cylinders, and all this has to fit into a periodic tiling pattern. The two LC phases formed by this compound, shown in Figure 48, are separated by a first-order phase transition at which the phase structure completely changes.

In the low-temperature phase with plane group symmetry $p2mm$ (Figure 48a), three distinct types of cylinders are combined, namely triangular, rhombic, and square shaped, each having a different composition. The triangular cylinders are filled only with the R_{Si} chains, the rhombic with the R_F -chains, whereas the vertical lines of square cylinders contain a 3:1 mixture of R_F and R_{Si} . The latter is because the molecules located between adjacent square cylinders have only the option to give their R_{Si} chains into one of the adjacent R_F filled square cylinders.^[285] The important point is that the mixing of different chains leads to a number of distinct compartments that is larger than the number of distinct chains available.

Upon increasing the temperature, the lateral chains expand and also the miscibility of the incompatible lateral chains increases. This increases the number of square cylinders slightly and leads to a phase transition to a $Col_{red}/c2mm$ phase with a larger lattice and an even more complex tiling pattern composed of in total 18 cylinders per unit cell. In this LC honeycomb, five distinct types of cylinders are found: triangular cylinders filled exclusively with R_{Si} chains, square cylinders filled with the R_F chains, and three additional types of cylinders with different shape (triangular/quadrangular) in which the R_F and R_{Si} chains are mixed in distinct proportions (3:1, 2:2, and 1:2; Figure 48b). This provides a LC structure composed of even five types of cells, which are different in shape and content, although there are only two types of distinct chains. If the honeycomb frame, which is composed of aromatic walls and hydrogen bonding columns at the edges, is also considered, there are in total seven distinct compartments. This impressively shows that with properly designed polyphilic molecules, new LC phases with unprecedented structural complexity can be created by combination of conflicting constraints which are interconnected to regulatory networks.

8.6.3. Liquid-Crystalline Honeycombs Involving Small and Large Cylinders

In the honeycombs formed by compound **93**, polygonal cylinders with similar size were combined (triangles, rhombohedra, and squares), but it is also possible to combine cylinders of very different size and shape, as for example triangles and hexagons in the Kagome pattern of compound **94**. The large hexagonal cells are filled with R_F chains and the small triangular cells are filled with the relatively short alkyl chains (Figure 49a).^[284]

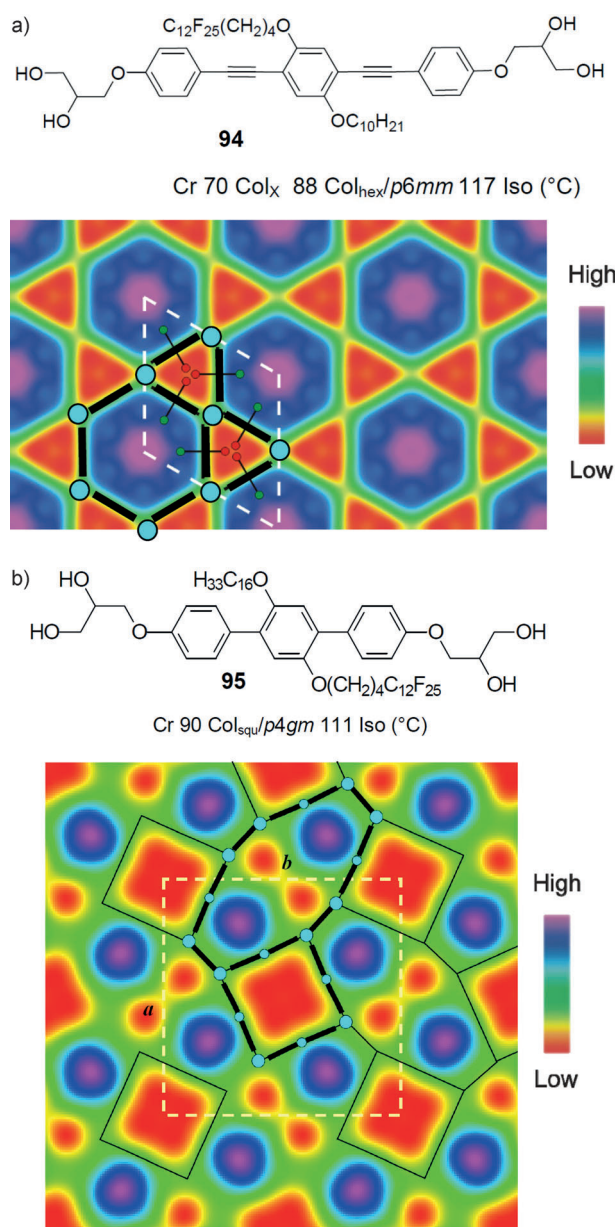


Figure 49. Experimental electron density maps of complex LC phases formed by the quaternary X-shaped polyphiphiles: a) Kagome of **94**, b) giant octagon-square tiling of **95**^[284,13] (black rods = rod-like cores, blue dots = glycerols).^[13] a) Reproduced from Ref. [284], copyright 2008, Wiley-VCH; b) reproduced with modifications from Ref. [13] copyright 2012, Nature Publishing Group.

Another even more complex example is provided by the octagon square tiling found for the *p*-terphenyl **95** and shown in Figure 49b, bottom. This honeycomb phase is also formed by two types of cylinders, in this case by square and octagonal cylinders in a 1:1 ratio.^[13] The alkyl chains are enclosed within square-shaped cylinders with eight molecules in the circumference with each side containing two bolapolyphiles in line (giant 8-squares). The second type of cylinders has a cross-section with the shape of elongated polygons with 12 molecules linked end-to-end along the circumference. This polygon is considered as a giant 12-octagon with two types of

alternating sides, four formed by two end-connected molecules, and four formed by only one. Because 4 of the 12 molecules forming the octagons lie on the boundary between two octagons their alkyl chains must be incorporated into the fluorinated giant octagons. These alkyl chains segregate from the R_F chains inside the octagonal cylinders and divide the R_F domains into two R_F -rich pentagonal columns, separated by two R_H -rich columns (Figure 49b). Thus, the structure simultaneously combines intercellular with intracellular segregation. Notably, the intracellular segregation in the giant 12-octagons differs from the usually observed simple core-shell structures. It divides the giant octagons into prismatic cells, which are separated by interfaces but not by any cylinder wall. This provides a further step towards increasing the complexity of liquid crystal and soft matter self-assembly.^[337] These examples indicate the enormous potential of the concept of competitive polyphilicity for creating a huge variety of new LC phases with increased complexity.

9. Tiling Patterns in Other Self-Assembled Systems

9.1. Compartmentalization in Block Copolymer Morphologies

The level of complexity achieved with the LC morphologies of polyphilic mesogens is unprecedented in other synthetic soft self-assembled systems. Although there are complex morphologies found for linear and star-shaped triblock copolymers,^[245,246] the number of distinct compartments is in all cases limited to a maximum corresponding to the number of incompatible units combined in the polymer, as different polymer chains cannot easily mix.

A wide variety of polymer morphologies representing Archimedean tiling patterns, which are very similar to those described in Sections 8.1.1 and 8.5.1 for LC honeycombs (Figure 35c–g), has been reported for flexible star-shaped triblock copolymers composed of three distinct polymer chains, in this case on an one or two orders of magnitude larger length scale (Figure 50).^[62,245,246,338,339] The $3^2.4.3.4$ tiling composed of square and triangular prismatic columns was also reported in 2005^[339] shortly after the discovery of this morphology in the LC phases of T-shaped polyphiles (Figure 43).^[300] The dual tiling by pentagons was known even earlier in LC systems formed by bolapolyphiles.^[276]

However, owing to the significantly higher viscosity of these polymers, the formation of the self-assembled structures is slow and requires casting from dilute solutions, followed by drying and annealing before the morphologies can be frozen and studied in the glassy state. In contrast, the complex LC structures are formed immediately in fast reversible phase transitions from the isotropic liquid state or from other LC phases on cooling with minimal hysteresis. An approach to structures with further increased complexity would be possible by hierarchical self-assembly combining the complex self-assembly of polyphilic LC with polymer self-assembly. Examples of hierarchical structures combining relatively simple LC and polymer morphologies are shown in Figure 46. The combination of the complex LC structures

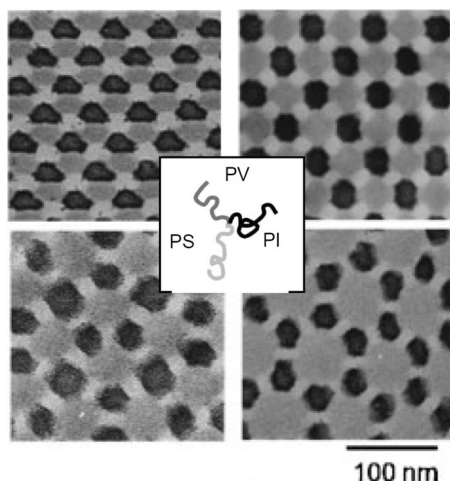


Figure 50. Star-shaped triblock copolymer composed of polystyrene (PS, light gray), polyisoprene (PI, black), and poly(2-vinylpyridine) (PV, gray) and representative morphologies (TEM pictures).^[338] Reprinted with permission from Ref. [338], Mcmillan Publishers Ltd.: Polymer Journal, copyright 2008.

described in Section 8 on a smaller length scale with the morphologies of multiblock copolymers on a larger length scale could provide a route to hierarchical structures with further enhanced complexity.^[335]

9.2. Self-Assembled Nets on Solid Surfaces and Channels in Solid-State Structures

Parallel to the developments in the field of LC honeycombs, periodic tiling patterns were found in self-assembled monolayer (SAM) on surfaces.^[340] Surface-supported triangular, rhombic, square, or hexagonal tiling motifs have been achieved in the recent years by hydrogen bonding^[341] or metal–ligand interactions at the nodes^[342] and van der Waals interactions between interdigitated alkyl chains.^[343,344] In contrast to the fluid self-assembled LC systems, the tiling of flat planes by pentagons is extremely rare for these 2D nets and other solid-state structures, and it never occurs without gaps, as the angles (and eventually also the side lengths) cannot easily be adjusted to the extent required for the organization in a periodic edge-to-edge tiling. Linear chains of self-assembled pentagons have been found for the organization of water molecules in channels on Cu(110) surfaces.^[345] The same type of chains of pentagons has been observed beside other motifs in self-assembled metal–organic networks of 1,3,5-trispyridylbenzene with copper atoms on Au(111) surfaces (Figure 51a,b),^[346] a similar structure was observed for the pentagonal macrocycle **97** on Au(111) (Figure 51c).^[347]

The most dense packing (packing density = 0.921) of regular pentagons in a plane is the packing in an antiparallel type of linear chain structure with *p2mg* symmetry (Figure 51d), which was recently observed for the crystalline packing of a cyclic amide with pentagonal shape.^[348] At only slightly lower packing density, the pentagons would adopt

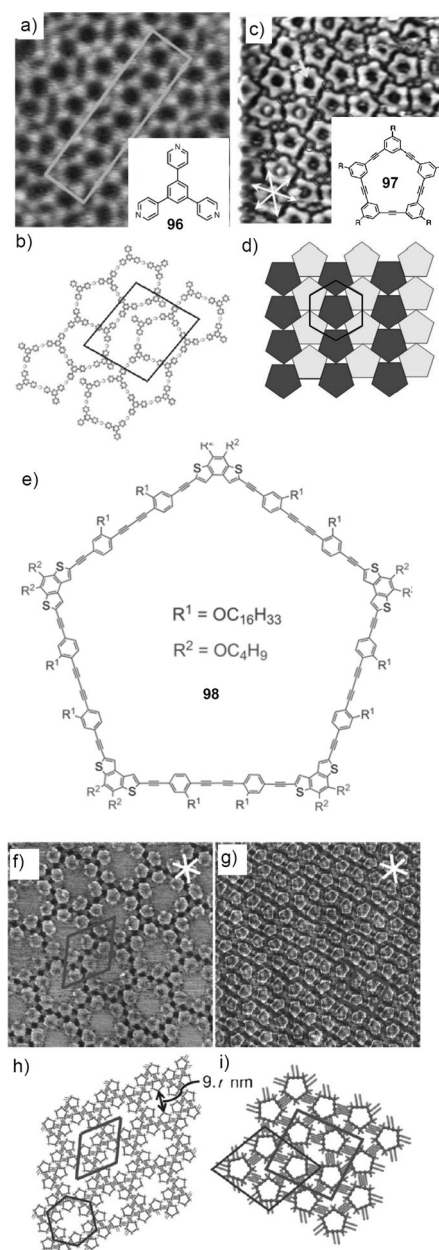


Figure 51. 2D lattices formed by pentagons: a,b) chains formed by 1,3,5-trispyridylbenzene **96** with Cu;^[346] c) surface coverage formed by the macrocycle **97** (R = H) on Au(111) 1-octanoic acid surface;^[347] d) most dense pentagon packing in crystal structures;^[348] e–i) tiling patterns of **98** at the HOPG-TCB interface (HOPG = highly pyrolytic graphite; TCB = 1,2,4-trichlorobenzene).^[350] a,b) Reproduced with permission from Ref. [346], copyright 2011, American Chemical Society; c) reproduced from Ref. [347] with permission of The Royal Society of Chemistry; d) reproduced from Ref. [348] copyright 2011, Wiley-VCH; and e–i) reproduced with permission from Ref. [350], copyright 2011, American Chemical Society.

rotational disorder and organize on a hexagonal 2D lattice, indicated by the hexagon in Figure 51d.^[348] For this reason, attempts to produce pentagonal tilings in columnar LC phases of pentagonal molecules have failed to date.^[349] Nevertheless, as shown in Figure 51e–i, interesting surface-stabilized periodic 2D packing motifs were observed for macrocycles **98**

with appreciable size and pronounced pentagonal shape, which self-assembled at the HOPG surface (Figure 51 e–i).^[350] These motifs are again based on a packing of ribbons of pentagons and do not represent tiling patterns without gaps.

Although attempts to produce periodic edge-to-edge pentagon tilings (without gaps) have failed to date on solid surfaces, the topological dual, the semiregular tiling by squares and triangles, was realized very recently.^[351] The softness and high valency of lanthanide nodes, combined with *p*-oligophenylene dicarbonitrile linkers, allows the formation of this tiling with the previously elusive five-vertex coordination motif.

The Kagome packing motif, formed by hexagons and triangles, was recently found for purely organic nets by solution depositions of hexaalkyl dehydrobenzo[12]annulenes **99**,^[344] where the aromatic groups form the nodes and the interdigitated alkyl chains form the net (Figure 52 a,b). The Kagome motif was also observed for hydrogen bonded^[352] and metal–organic nets on solid surfaces.^[353] The Kagome formed by self-assembly of **99** can accommodate different guest molecules in the distinct cells.^[354,355] As shown in Figure 52 c,d, the triphenylenes (TRI) fill the triangles and the coronenes (COR), surrounded by a shell of six isophthalic

acid molecules (ISA) that fill the larger hexagons.^[354] This structure could be considered as a 2D analogue of the “two-color Kagome honeycomb” shown in Figure 49 a. The triphenylenes (TRI) replace the alkyl chains in the triangular cells, with the coronenes (COR) and isophthalic acids (ISA) replacing the semiperfluorinated chains in the hexagonal cells. Even the often observed core–shell structure of the hexagonal cells with a fluorinated core surrounded by the alkyl spacers is resembled in this surface pattern by the coronenes surrounded with a ring of six ISA units.^[356]

DNA nanotechnology^[357] and programmed peptide self-assembly^[358] provide additional approaches to polygonal nets and cellular structures. Among solid-state structures with polygonal (mostly hexagonal and square) channels, metal–organic frameworks (MOFs)^[359] and more recently also covalent organic frameworks (COFs) have received significant attention.^[360] Going to larger sizes, rod-like nanoparticles having sticky ends and lateral tethers, similar to the T-shaped polyphiles, received significant interest. The self-assembly of such particles has been simulated by Glotzer et al., and these simulations indeed predicted Lam-like layers as well as square and pentagonal honeycomb structures.^[361] Figure 53

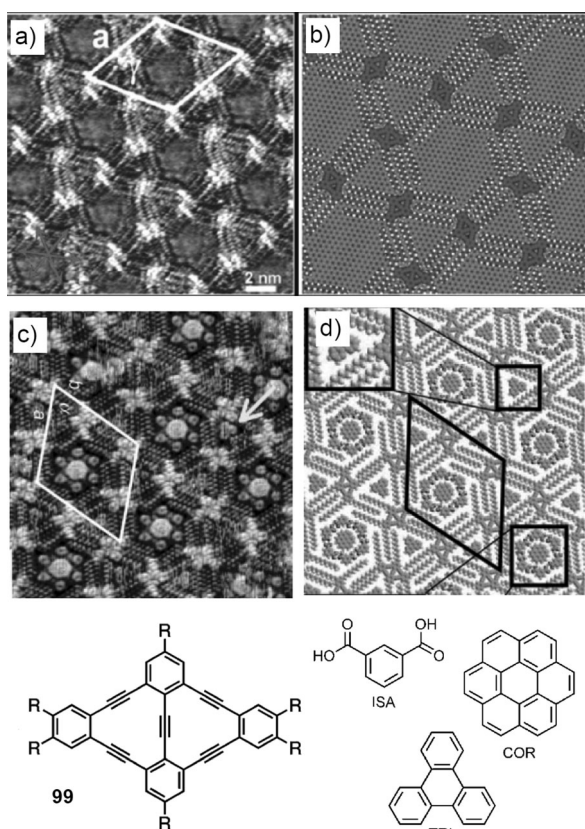


Figure 52. Kagome motifs by self-assembly on solid surfaces: a,b) Self-assembled Kagome net of compound **99** on HOPG surfaces;^[344a] c,d) “two-color Kagome” formed by a mixture of compound **99** with ISA, COR, and TRI; STM pictures at the left and packing models at the right.^[354] a,b) reproduced with permission from Ref. [344a], copyright 2009, American Chemical Society; c,d) reproduced from Ref. [354], copyright 2009, Wiley-VCH.

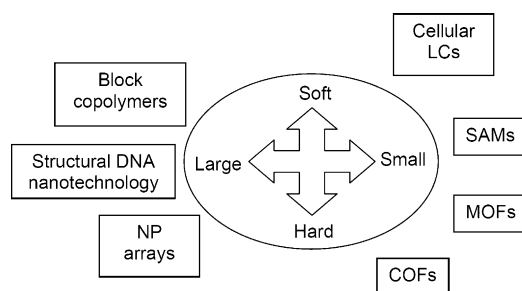


Figure 53. Current bottom-up approaches leading to periodic 2D and 3D arrays with cellular structure.

gives an overview over important current methods for producing 2D tiling patterns, channels, and cellular structures by molecular self-assembly.

10. Bent-Core Liquid Crystals: Chirality and Polar Order

10.1. Ferroelectric and Antiferroelectric Liquid Crystals

Although smectic and nematic phases are the simplest modes of LC self-assembly, their complexity can also be increased by a relatively simple change of the molecular structure by introducing a bend into rod-like molecules (bent-core mesogens; for examples see Figure 54).^[362–364] This gives rise to a restriction of the molecular rotation around the long axis, leading to a parallel alignment of the bend directions in the layers, and thus the polar moments along this direction (Figure 55 b).^[214] In this way, polar order can arise parallel to the layers of the smectic phases (SmAP and SmCP phases) as a new emergent property; this was first reported 1996 by Takezoe, Watanabe, and co-workers from TIT Tokyo.^[365]

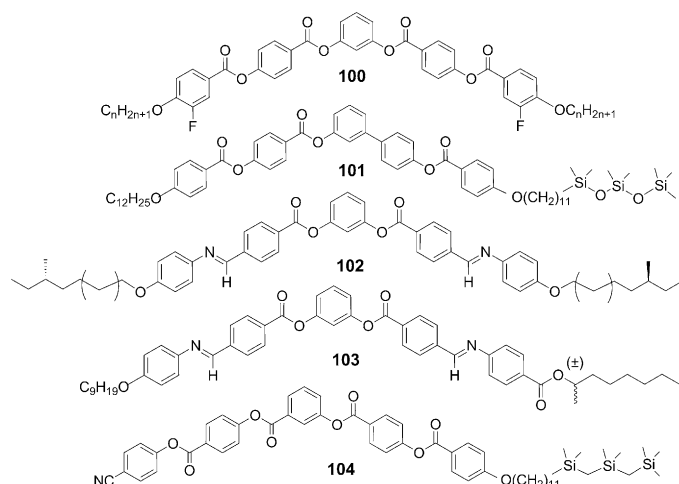


Figure 54. Examples of ferroelectric switching bent-core mesogens (100–103: SmCP_F, 104: SmAP_F).^[366, 369, 371, 374]

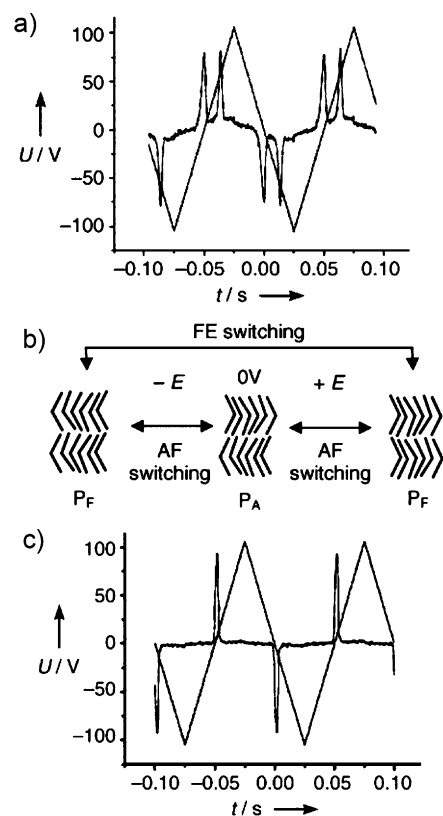


Figure 55. Polar packing of bent-core molecules in layers and their typical polarization current curves under an applied triangular wave voltage: a) antiferroelectric switching; c) ferroelectric switching; b) molecular packing and reorganization of the molecules during the distinct switching processes. Reproduced with modifications from Ref. [381b], copyright 2006, Wiley-VCH.

The polar order can be identified by switching experiments under an electric triangular-wave field by the appearance of one or two polarization current peaks. If there are two peaks per half period of the applied triangular-wave voltage,

the switching is tri-stable (antiferroelectric, AF). In this case the field-induced polar states (P_F) are instable and the system relaxes to the apolar ground state after switching off the applied field (Figure 55a,b). In the ground state, the polar direction of the molecules in adjacent layers is opposite (P_A). It is assumed that this apolar state with opposite direction of the molecular bend directions is favored by the dynamics in LC systems. As shown in Figure 55b, in this non-polar antiferroelectric state (P_A) the molecular ends in adjacent layers are aligned parallel at the interlayer interfaces, which is favorable for interlayer fluctuations, whereas in the polar states (P_F) they are not parallel, which inhibits these fluctuations, leading to an entropic penalty.^[366] If these interlayer fluctuations could be reduced, the influence of entropy is also reduced and the synpolar P_F state is less destabilized, leading to (an in most cases surface stabilized) bistable (ferroelectric, FE) switching, that is, a direct switching between the polar P_F states with opposite polar direction, but without relaxation at 0 V. This is indicated by the presence of only one current peak per half period of the applied triangular-wave voltage (Figure 55b,c). This transition from AF switching to FE switching can be achieved by molecular design (see Figure 54 for examples), namely by engineering of the interfaces between the layers by introducing bulky oligosiloxanes (101),^[366] carbosilanes (104),^[367] and other groups^[368] to one of the chain-ends or by branching of the terminal alkyl chains (102, 103).^[369, 370] Other possibilities involve the attachment of fluorine atoms to the periphery of the bent-core units (100),^[371] and several other structural variations.^[362]

It is obvious that the fluidity of these LC ferroelectrics^[372, 373] provides advantageous additional options for the application of these materials compared to solid state inorganic or organic ferroelectrics. However, this fluidity also allows an easier escape from macroscopic polar order by a splay of the polarization direction. This distorts the organization in flat layers, leading to numerous different types of undulated (wavy deformed) and modulated (fragmented) layer structures (leading to LC phases with 2D periodicity) occurring at different length scales; also non-periodic and helical structures could be observed. On the other hand, surface effects can stabilize the polar structures. Combined with layer distortion owing to steric effects, this polarization splay^[374] gives rise to a huge number of different LC phases.^[375] It is outside the scope of this review to discuss these complex relations in more detail.^[362]

10.2. Chirality and Symmetry-Breaking

In the polar smectic phases, the molecules could be tilted (SmCP_A, SmCP_F) or non-tilted (SmAP_A, SmAP_F, Figure 56b) with respect to the layer normal. In fact, the majority of bent-core LC phases are tilted phases with relatively large tilt angles of around 30–40°. This combination of tilt and polar order in the layers reduces their symmetry to C_2 , that is, these layers are inherently chiral although the molecules are achiral. As shown in Figure 56a, the spatial combination of tilt direction, polar direction, and layer normal define either a right-handed or a left-handed chiral system.^[376] Similar to

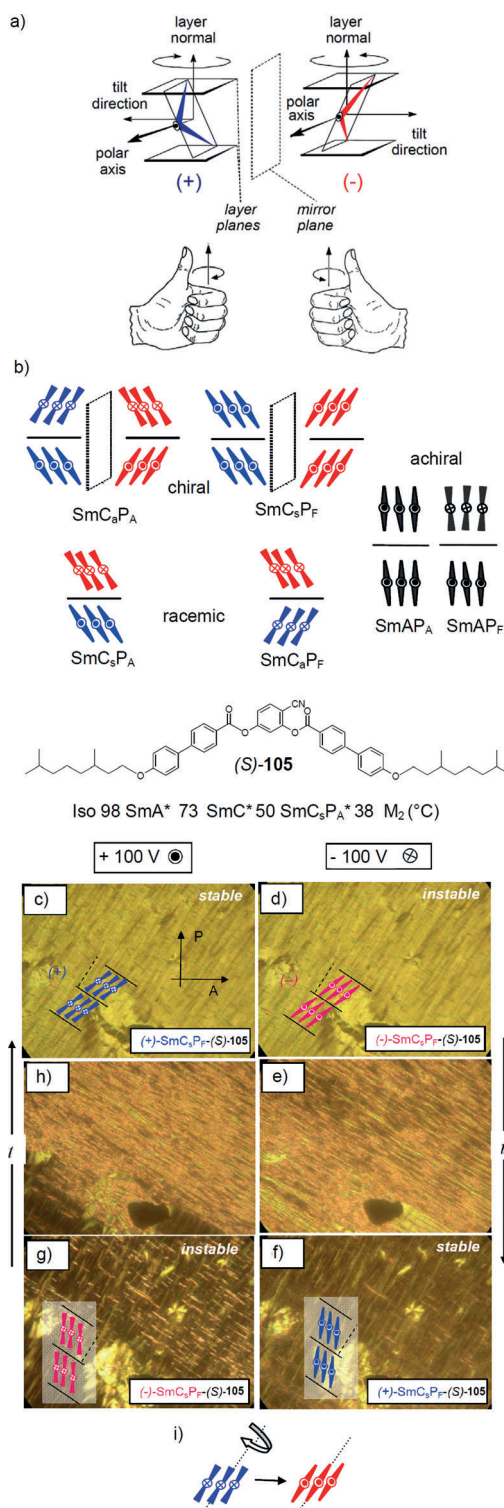


Figure 56. Self-assembly, chirality, and switching in the LC phases of bent-core mesogens: a) Layer chirality arising from the combination of tilt and polar order; b) the four possible structures resulting from the combination of chiral layers (red, blue); at the right the two non-tilted and therefore achiral phase types are shown; the view is along the polar axis, dots indicate the view on the apex, crosses indicate the view from the back; color indicates the chirality sense.^[362b, 376] c–h) field-induced switching of the layer chirality of compound (S)-**105** (phase transitions on cooling, M_2 =unknown mesophase) at $T=43^\circ\text{C}$, in ITO cells with parallel rubbing direction between crossed polarizers; the orientation of the molecules in the distinct states is shown in the models; the orientation of polarizer and analyzer are shown in (c); i) shows the field induced reorganization of the molecules around the long axis. For more explanations, see the text.^[382] Reproduced with modifications from Ref. [362b] and Ref. [382] with permission of The Royal Society of Chemistry.

the molecular chirality- which is determined by the spatial organization of achiral atoms in a molecule, the combination of tilt and polar order provides chirality for achiral molecules on a supramolecular level. This provides a new source of suprastructural chirality,^[376] which is distinct from the usually observed helical modes.^[377,378] The chirality sense is reversed by either reversing the polar direction or by reversing the tilt direction of the molecules in the layers.

As the bulk smectic phases are formed by quasi infinite stacks of these chiral layers, different phase structures can arise. In these bulk phases the polar correlation between adjacent layers can be either “ferroelectric” (P_F) or “antiferroelectric” (P_A), and the tilt correlation can be either synclinal (C_s) or anticlinal (C_a), leading to the four structures SmC_sP_A , SmC_aP_F , SmC_sP_A , and SmC_aP_F (Figure 56b). In the SmC_sP_A and SmC_aP_F structures, alternating layers with opposite chirality sense are combined, and therefore these structures are achiral. In the SmC_aP_A and SmC_sP_F structures, layers with identical chirality are combined; these are uniformly chiral and for each of them there are two enantiomorphic states (Figure 56b). As the polar and chiral LC phases are fluid and can be switched with external electric fields, this provides the unique possibility of electric-field-induced chirality flipping.^[362,376] Inversion of the layer chirality is possible if this switching occurs by a collective rotation around the long molecular axis, which reverses only the polar direction without changing the tilt direction (Figure 56 f).^[379–381]

Figure 56c–i illustrates this switching of layer chirality for compound (*S*)-**105**.^[382] This chiral compound was used in enantiomerically pure form to identify the flipping of chirality by changing the diastereomeric relationship between the fixed molecular chirality and the floppy suprastructural chirality.^[362, 376] The ground state has an achiral SmC_sP_A structure, but under an applied DC voltage of +100 V a uniformly chiral SmC_sP_F state is induced, which appears bright between crossed polarizers (Figure 56c). This field-induced SmC_sP_F state has uniform (+)-layer chirality, and together with the (*S*)-molecular chirality it is the diastereomeric state (+)-SmC_sP_F-(*S*)-**105**. Reversing the field direction (−100 V) switches the molecules around their long axes, which reverses the layer chirality to (−)-SmC_sP_B, but it does not change the tilt direction and therefore the new switched state (Figure 56d) cannot be distinguished optically from the initial state (Figure 56c). However, the resulting new diastereomeric structure (−)-SmC_sP_F-(*S*)-**105** is not the global energy minimum. Therefore, it is unstable and slowly relaxes (Figure 56d–f) to the more stable diastereomer (+)-SmC_sP_F-(*S*)-**105** by slow reorganization of the molecules with reversal of the tilt director (note that the polar direction, which is fixed

by the applied field, does not change). Through the tilt reversal, the direction of the optic axis changes such that it now nearly coincides with the direction of the polarizer, resulting in a texture appearing nearly dark (Figure 56 f). If the field direction is

reversed again by applying a positive voltage (+100 V), the molecules flip around the molecular long axis. The optical axis is not affected, and the texture thus remains dark (Figure 56g), but the layer chirality is changed to $(-)$ -SmC_sP_F, giving the $(-)$ -SmC_sP_F-(S)-105 state. Again being in a metastable diastereomeric state, the system slowly transforms to the stable and birefringent $(+)$ -SmC_sP_F-(S)-105 state, the same as at the beginning of this cycle, by slow reorganization with reversal of the tilt director (Figure 56c,g,h). This experiment confirms the chirality flipping under an applied electric field. In an analogous way the switching between the achiral racemic forms and homogeneously chiral structures is also possible. This experiment also provides evidence for the coupling between the fixed molecular chirality and the field-dependent superstructural chirality, leading to energetically distinct diastereomeric states.

As chirality is created by the spatial order of achiral molecules, the formation of chiral superstructures as helical filaments (Figure 57d)^[374,383] is often observed. An especially

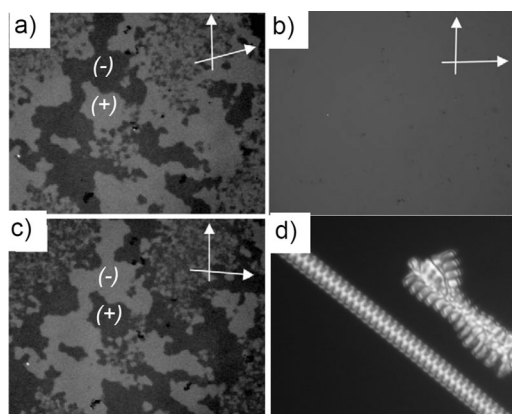


Figure 57. Examples of chiral superstructures in the LC phase of bent-core mesogens: a)–c) chiral domains of an optically isotropic “dark conglomerate” phase observable after uncrossing the polarizers by a small angle in either a) one or c) the other direction; dark and bright domains represent areas with opposite chirality; d) helical filaments occurring during the growths of the texture of a birefringent LC phase.^[388] a)–c) Reproduced with modifications from Ref. [388] with permission of The Royal Society of Chemistry.

interesting and often-observed feature is spontaneous symmetry-breaking by formation of conglomerates of chiral domains with opposite handedness (Figure 57a–c).^[181,362b,c,384–386] These LC phases, assigned as dark-conglomerate phases (DC-phases), have strongly deformed layer structures (sponge phases) and therefore appear optically isotropic or only weakly birefringent. Thus, in these fluid systems the spontaneous separation of the enantiomeric domains can be observed under a polarizing microscope by a slight deviation of the polarizers out of the 90° orientation either in one or the other direction. This spontaneous chiral domain formation can be considered as an LC analogue of Pasteur’s historical experiment with tartaric acid salts^[387] and thus shows that spontaneous symmetry-breaking is not restricted to crystalline solid-state materials, but is also possible in ordered, but fluid, liquid-crystalline systems.

The order in the polar LC phases of bent-core mesogens obviously allows a collective behavior of the molecules over larger distances. This might be the result of the fixation and pre-organization of the individual molecules in densely packed polar layers, allowing a coupling between suprastructural chirality (layer chirality) and helical conformers,^[389] leading to macroscopic chiral segregation. The higher the order in the LC phase is, the stronger the effects are. The B4 phase is the phase of this type with highest order.^[362,363,390,391] In this so-called “helical filament phase” the aromatic cores adopt a crystalline packing in helical filaments which are organized between the disordered alkyl chains. It can even be swollen by achiral nematic LC solvents to a high content (>98%) without reduction of chirality.^[391] However, there are also several examples of tilted polar smectic phases with fluid layers (SmCP_{A/F}),^[366,392] forming the so-called dark conglomerate phases (Figure 57a–c). Chiral domains have even been observed under special conditions in SmC phases (SmCP_R)^[393] and cybotactic nematic phases (N_{CybC})^[394] of bent-core mesogens.^[364,395] Recently, LC dimesogens composed of two rod-like units and connected by an odd-numbered (that is, bent) spacer were reported to show indications of chirality owing to a twist of the molecules.^[396] With decreasing packing density of the aromatic cores, that is, in the sequence B4 > SmCP_{A/F} > SmCP_R > N_{CybC}, the coupling between layer chirality and molecular conformational chirality becomes weaker and other effects, such as negative-bend elastic constants (k_{33})^[397] and surface effects^[398] in particular become increasingly important for occurrence and stabilization of chiral segregation. This spontaneous achiral symmetry-breaking occurring on a supramolecular level in fluid systems is one of the most fascinating feature of bent-core LC systems, which has stimulated research for chirality phenomena in other LC phases formed by rod-like molecules (SmB and E phases),^[399] in columnar,^[400] and in cubic phases.^[401] Overall, research on bent-core LC has contributed significantly to understanding of the emergence of chirality in fluid nanoscale structures.^[377]

11. Summary and Conclusions

LC self-assembly has developed into a scientific area with many facets since its discovery 125 years ago.^[7] This review attempts to sketch the way that this development has gone since then and focuses on some of the recent developments under the aspect of increasing the complexity of soft matter self-assembly. The unique dynamics in the ordered liquid-crystal state provides a random force on the systems degrees of freedom which plays a critical role for the emergence of order in these soft self-assembled systems.^[304] Owing to this dynamic nature, LCs can easily adopt to the global minima on rugged energy landscapes, providing the ability of self-healing and adaption. Their ability to select the lowest energy state can even be used to get best solutions for fundamental mathematical problems under complex boundary conditions; examples are complex 2D tiling patterns and 3D cellular structures.

In LC structures the distinct molecular parameters are interconnected to regulatory networks and by increasing the number of conflicting constraints higher levels of structural complexity of their self-assembled structures could be achieved,^[402] as shown for the series ranging from binary bolaamphiphiles by T-shaped bolatriphiles to X-shaped bolatetraphiles in Section 8 and the transition from a linear to a bent molecular shape mentioned in Section 10. Another constraint is provided by molecular chirality, which was not covered herein.^[403]

As the structures become more complex, new phenomena are emerging that make the LC structures indispensable in numerous areas. For example, the LC state provides an important method for the self-assembly of functional molecules into ordered structures in an bottom-up approach,^[404a] as widely used for organic solar cells,^[404b] organic semiconductors^[48] and for the spatial ordering of nano-objects into complex periodic arrays for metamaterials and other nanotechnological applications.^[226,239,405–407] It is also well-documented that LC states are essential in many parts of living organisms.^[408] Examples are the cell membranes representing vesicular structures formed by single layers of smectic bilayer phases;^[409] transition of these membranes to bicontinuous cubic structures^[410,411] are important for several membrane processes (cell division, gene transfer), and the formation of a hexagonal columnar phase allows the dense packing of DNA in the nuclei.^[412] Life itself might be considered as the presently most complex known mode of soft self-assembly and it appears that LC self-assembly has contributed to its emergence.^[402,413–415] Whereas molecular biology and biochemistry try to understand life in a top-down approach by analyzing biological self-assembly and self-organization down to the molecular level, LC science is complimentary and uses the opposite approach. In a bottom-up approach it contributes to the fundamental understanding of molecular self-assembly of simple molecules to soft matter structures with ever-growing complexity, that is, “...the evolution of matter from particles to thoughts...”.^[1]

Overall, liquid crystals have developed to a fascinating and prosperous field, reaching out into different areas of actual science by providing basic knowledge of the fundamental rules governing self-assembly from simple to complex modes.

Acknowledgements

The author thanks all of the students, postdocs, and collaborators who worked with him in the recent decades. The work of our own included here was supported by the Deutsche Forschungsgemeinschaft by several grants, in recent years by FOR 1145, by the Fonds der Chemischen Industrie, the ESF EUROCORES program SONS (Project SCALES), and the Cluster of Excellence “Nanostructured Materials” of the government of Saxonia-Anhalt.

Received: January 31, 2013

- [1] J. M. Lehn, *Angew. Chem.* **2013**, *125*, 2906; *Angew. Chem. Int. Ed.* **2013**, *52*, 2836; see also: J. M. Lehn, *C. R. Chim.* **2011**, *14*, 348.
- [2] “Self-assembly” is used herein for passive, equilibrium self-organization as defined in Ref. [1], in contrast to “self-organization”, which is reserved for active, out-of-equilibrium self-organization: J. D. Halley, S. A. Winkler, *Complexity* **2008**, *14*, 10.
- [3] a) G. M. Whitesides, B. Grzybowski, *Science* **2002**, *295*, 2418; b) J. M. Lehn, *Science* **2002**, *295*, 2400; c) O. Ikkala, G. ten Brinke, *Science* **2002**, *295*, 2407; S. C. Glotzer, M. J. Solomon, *Nat. Mater.* **2007**, *6*, 557; K. Ariga, J. P. Hill, M. V. Lee, A. Vinu, R. Charvet, S. Acharya, *Sci. Technol. Adv. Mater.* **2008**, *9*, 014109; X. C. Jiang, Q. H. Zeng, C. Y. Chen, A. B. Yu, *J. Mater. Chem.* **2011**, *21*, 16797.
- [4] L. M. Greig, D. Philp, *Chem. Soc. Rev.* **2001**, *30*, 287; V. E. Campbell, J. R. Nitschke, *Synlett* **2008**, *20*, 3077; P. A. Gale, *Philos. Trans. R. Soc. London Ser. A* **2000**, *358*, 431; B. A. Grzybowski, C. E. Wilmer, J. Kim, K. P. Browne, K. J. M. Bishop, *Soft Matter Rev.* **2009**, *5*, 1110.
- [5] P. J. Collings, M. Hird in *Introduction to Liquid Crystals Chemistry and Physics*, Taylor & Francis, London, **1997**; J. W. Goodby, *Liq. Cryst.* **2011**, *38*, 1363; D. Pauluth, K. Tarumi, *J. Mater. Chem.* **2004**, *14*, 1219; P. Kirsch, M. Bremer, *Angew. Chem.* **2000**, *112*, 4384; *Angew. Chem. Int. Ed.* **2000**, *39*, 4216; T. Geelhaar, K. Griesar, B. Reckmann, *Angew. Chem.* **2013**, *125*, DOI: 10.1002/ange.201301457; *Angew. Chem. Int. Ed.* **2013**, *52*, DOI: 10.1002/anie.201301457
- [6] *Liquid Crystals. Materials Design and Self-assembly*, Vol. 318 of *Top. Curr. Chem.* (Ed.: C. Tschierske), Springer, New York, **2012**.
- [7] a) *Handbook of Liquid Crystals* (Eds.: D. Demus, J. Goodby, G. W. Gray, H.-W. Spiess, V. Vill), Wiley-VCH, Weinheim, **1998**; b) *Handbook of Liquid Crystals*, 2nd ed. (Eds.: J. W. Goodby, P. J. Collings, H. Gleeson, P. Raynes, T. Kato, C. Tschierske), Wiley-VCH, Weinheim, **2013**.
- [8] F. Stoddart, *Nat. Chem.* **2009**, *1*, 14.
- [9] a) J. Israelachvili, *Intermolecular and Surface Forces*, 3rd ed., Academic Press, Burlington, **2010**; b) S. Hassan, W. Rowe, G. J. T. Tiddy, *Handbook of Applied Surface and Colloid Chemistry*, Vol. 1 (Ed.: K. Holmberg), Wiley-VCH, Chichester, **2002**, p. 465.
- [10] Birefringent textures were observed by Virchow for myelin in contact with water, and thus lyotropic LC phases have already been reported before the thermotropic LCs: R. Virchow, *Virchows Arch. Pathol. Anat. Physiol.* **1854**, *6*, 562.
- [11] V. S. K. Balagurusamy, G. Ungar, V. Percec, G. Johansson, *J. Am. Chem. Soc.* **1997**, *119*, 1539.
- [12] a) D. J. P. Yearley, G. Ungar, V. Percec, N. M. Holerca, G. Johansson, *J. Am. Chem. Soc.* **2000**, *122*, 1684; b) H. Duan, S. D. Hudson, G. Ungar, M. N. Holerca, V. Percec, *Chem. Eur. J.* **2001**, *7*, 4134.
- [13] F. Liu, R. Kieffer, X.-B. Zeng, K. Pelz, M. Prehm, G. Ungar, C. Tschierske, *Nat. Commun.* **2012**, *3*, 1104.
- [14] G. Ungar, F. Liu, X. B. Zeng, B. Glettner, M. Prehm, R. Kieffer, C. Tschierske, *J. Phys. Conf. Ser.* **2010**, *247*, 012032.
- [15] F. Reinitzer, *Monatsh. Chem.* **1888**, *9*, 421.
- [16] a) T. J. Sluckin, D. A. Dunmur, H. Stegemeyer, *Crystals that flow: Classic Papers from the History of Liquid Crystals*, Taylor & Francis, London, **2004**; b) D. Dunmur, T. Sluckin, *Soap, Science and Flat-Screen TVs, A History of Liquid Crystals*, Oxford University Press, New York, **2011**.
- [17] H. Stegemeyer, *Bunsen-Magazin* **2007**, *9*, 120.
- [18] D. Vorländer, *Z. Phys. Chem.* **1923**, *105*, 211; D. Vorländer, *Chemische Kristallographie der Flüssigkeiten*, Akademische Verlagsgesellschaft, Leipzig, **1924**.

- [19] C. Weygand, *Ber. Dtsch. Chem. Ges. A* **1943**, 76, A41.
- [20] J. Billard, *Liq. Cryst.* **1998**, 24, 99.
- [21] H. Kelker, *Mol. Cryst. Liq. Cryst.* **1973**, 21, 1; H. Kelker, *Mol. Cryst. Liq. Cryst.* **1988**, 165, 1; D. Demus, *Mol. Cryst. Liq. Cryst.* **1988**, 165, 45; H. Kelker, P. M. Knoll, *Liq. Cryst.* **1989**, 5, 19.
- [22] D. Demus, *Mol. Cryst. Liq. Cryst.* **2001**, 364, 25.
- [23] D. W. Bruce, K. Heyns, V. Vill, *Liq. Cryst.* **1997**, 23, 813; V. Vill, *Liq. Cryst.* **1998**, 24, 21.
- [24] The logic depth of a structure is used here as a measure of how difficult it is to construct this structure, or how difficult it is to predict, understand, and simulate it (based on the current state of knowledge).
- [25] M. Mitchell, *Complexity, a Guided Tour*, Oxford University Press, Oxford, **2009**; F. Heylighen in *The Evolution of Complexity* (Eds.: F. Heylighen, J. Bollen, A. Riegler), Kluwer, Dordrecht, **1999**, p. 17–44.
- [26] D. Vorländer, *Ber. Dtsch. Chem. Ges.* **1907**, 40, 1970.
- [27] W. Weisswange, Ph.D.-Thesis Halle, **1925**; R. Kühnemann, Ph.D. Thesis Halle **1922**; D. Vorländer, *Ber. Dtsch. Chem. Ges.* **1925**, 58, 1893.
- [28] D. Vorländer, *Z. Phys. Chem.* **1923**, 105, 211.
- [29] *Metallomesogens: Synthesis Properties and Applications* (Ed.: J. L. Serrano), Wiley-VCH, Weinheim, **1996**.
- [30] M. E. Huth, Ph.D.-Thesis Halle, **1909**.
- [31] D. Vorländer, *Z. Phys. Chem.* **1919**, 105, 211.
- [32] P. Horbach, Ph.D.-Thesis, University Halle, **1924**.
- [33] G. Pelzl, I. Wirth, W. Weissflog, *Liq. Cryst.* **2001**, 28, 969.
- [34] R. Eidenschink, F.-H. Kreuzer, W. H. De Jeu, *Liq. Cryst.* **1990**, 8, 879.
- [35] a) J. Malthête, A.-M. Levelut, *Adv. Mater.* **1991**, 3, 94; b) J. Malthête, L. Leibert, A. M. Levelut, Y. Galerne, *C. R. Acad. Sci. Ser. II* **1986**, 303, 1073; c) J. Malthête, *New J. Chem.* **1996**, 20, 925.
- [36] a) A. Pegenau, P. Göring, C. Tschierske, *Chem. Commun.* **1996**, 2563; b) A. Pegenau, T. Hegmann, C. Tschierske, S. Diele, *Chem. Eur. J.* **1999**, 5, 1643.
- [37] M. Lehmann, *Chem. Eur. J.* **2009**, 15, 3638; M. Lehmann, *Top. Curr. Chem.* **2012**, 318, 193.
- [38] D. Vorländer, *Ber. Dtsch. Chem. Ges.* **1910**, 43, 3120.
- [39] T. Welton, *Chem. Rev.* **1999**, 99, 2071.
- [40] A. Skoulios, V. Luzzati, *Acta Crystallogr.* **1961**, 14, 278; V. Luzzati, L. H. Mustacchi, A. Skoulios, *Acta Crystallogr.* **1960**, 13, 660; V. Luzzati, A. Skoulios, *Nature* **1959**, 183, 1310; P. Mariani, V. Luzzati, H. Delacroix, *J. Mol. Biol.* **1988**, 204, 165.
- [41] K. Binnemans, *Chem. Rev.* **2005**, 105, 4148; K. V. Axenov, S. Laschat, *Materials* **2011**, 4, 206.
- [42] C. F. J. Faul, M. Antonietti, *Adv. Mater.* **2003**, 15, 673.
- [43] Y. Takagi, K. Ohta, S. Shimosugi, T. Fujii, E. Itoh, *J. Mater. Chem.* **2012**, 22, 14418.
- [44] T. Kato, *Science* **2002**, 295, 2414.
- [45] S. Chandrasekhar, B. K. Sadashiva, K. A. Suresh, *Pramana* **1977**, 9, 471.
- [46] It is interesting to note that in fact the homologous series of benzene hexaalkanoates has been synthesized about 40 years earlier, but their potential was not discovered at that time: H. J. Backer, S. van der Baan, *Recl. Trav. Chim. Pays-Bas* **1937**, 56, 1161; S. Chandrasekhar, *Philos. Trans. R. Soc. London Ser. A* **1983**, 309, 93.
- [47] a) S. Laschat, A. Baro, N. Steinke, F. Giesselmann, C. Hägele, G. Scalia, R. Judele, E. Kapatsina, S. Sauer, A. Schreivogel, M. Tosoni, *Angew. Chem.* **2007**, 119, 4916; *Angew. Chem. Int. Ed.* **2007**, 46, 4832; *Angew. Chem.* **2007**, 119, 4916; b) S. Kumar, *Chemistry of discotic liquid crystals—From monomers to polymers*, CRC, Taylor & Francis Group, Boca-Raton, **2011**; c) B. Roy, N. De, K. C. Majumdar, *Chem. Eur. J.* **2012**, 18, 14560.
- [48] a) F. Würthner, C. Thalacker, S. Diele, C. Tschierske, *Chem. Eur. J.* **2001**, 7, 2245; b) S. Sergeyev, W. Pisula, Y. H. Geerts, *Chem. Soc. Rev.* **2007**, 36, 1902; c) W. Pisula, M. Zorn, J. Y. Chang, K. Müllen, R. Zentel, *Macromol. Rapid Commun.* **2009**, 30, 1179; d) M. O'Neill, S. M. Kelly, *Adv. Mater.* **2011**, 23, 566; e) L. Maggini, D. Bonifazi, *Chem. Soc. Rev.* **2012**, 41, 211; f) *Self-organized Organic Semiconductors – From Materials to Device Applications* (Ed.: Q. Li), Wiley, Hoboken, **2011**; g) D. Görl, X. Zhang, F. Würthner, *Angew. Chem.* **2012**, 124, 6434; *Angew. Chem. Int. Ed.* **2012**, 51, 6328.
- [49] a) J. Malthête, A. M. Levelut, N. H. Tinh, *J. Phys. Lett.* **1985**, 46, L875; b) H.-T. Nguyen, C. Destrade, J. Malthête, *Adv. Mater.* **1997**, 9, 375; c) M. , Gharbia, A. Gharbi, H. T. Nguyen, J. Malthête, *Curr. Opin. Colloid Interface Sci.* **2002**, 7, 312.
- [50] W. Weissflog, G. Pelzl, I. Letko, S. Diele, *Mol. Cryst. Liq. Cryst.* **1995**, 260, 157.
- [51] M. Herrmann-Schönherr, O. Ebert, J. H. Wendorff, H. Ringsdorf, P. Tschirner, *Liq. Cryst.* **1990**, 7, 63.
- [52] a) G. R. Luckhurst, *Thin Solid Films* **2001**, 393, 40; b) C. Tschierske, D. J. Photinos, *J. Mater. Chem.* **2010**, 20, 4263.
- [53] D. W. Bruce, *Acc. Chem. Res.* **2000**, 33, 831; D. Fazio, C. Mongin, B. Donnio, Y. Galerne, D. Guillon, D. W. Bruce, *J. Mater. Chem.* **2001**, 11, 2852.
- [54] V. Luzzati, P. A. Spegt, *Nature* **1967**, 215, 701.
- [55] G. W. Gray, B. Jones, F. Marson, *J. Chem. Soc.* **1957**, 393.
- [56] D. Demus, G. Kunicke, J. Neelsen, H. Sackmann, *Z. Naturforsch. A* **1968**, 23, 84; S. Diele, P. Brand, H. Sackmann, *Mol. Cryst. Liq. Cryst.* **1972**, 17, 163.
- [57] G. Etherington, A. J. Leadbetter, X. J. Wang, G. W. Gray, A. Tajbakhsh, *Liq. Cryst.* **1986**, 1, 209.
- [58] Recent review: S. Kutsumizu, *Isr. J. Chem.* **2012**, 52, 844.
- [59] H. Schubert, J. Hauschild, D. Demus, S. Hoffmann, *Z. Chem.* **1978**, 18, 256; D. Demus, A. Gloza, H. Hartung, A. Hauser, I. Raphtel, A. Wiegeleben, *Cryst. Res. Technol.* **1981**, 16, 1445.
- [60] Early theoretical concepts unifying thermotropic and lyotropic mesophase formation considering the curvature of aggregates (R-theory): P. A. Winsor in *Liquid Crystals and Plastic Crystals, Vol. 1* (Eds.: G. W. Gray, P. A. Winsor), Ellis Horwood, Chichester, **1974**, p. 199.
- [61] Analogies of the cubic LC phases with cubic plastic crystals, formed by molecules, of more or less globular shape, were also discussed (however, as the individual molecules have fixed positions on the crystal lattice they are not considered as LC phases): J. Timmermans, *J. Chim. Phys.* **1938**, 35, 331; P. A. Winsor in *Liquid Crystals and Plastic Crystals, Vol. 1* (Eds.: G. W. Gray, P. A. Winsor), Wiley, New York, **1974**, p. 48.
- [62] I. W. Hamley, *The physics of block-copolymers*, Oxford University Press, Oxford, **1998**.
- [63] Y. , Hendrikx, A. M. Levelut, *Mol. Cryst. Liq. Cryst.* **1988**, 165, 233.
- [64] a) A. Skoulios in *Advances in Liquid Crystals* (Ed.: G. H. Brown), Academic Press, New York, **1975**, p. 169; b) A. Skoulios, D. Guillon, *Mol. Cryst. Liq. Cryst.* **1988**, 165, 317.
- [65] J. Charvolin, *J. Chim. Phys.* **1983**, 80, 15.
- [66] B. I. Ostrovskii, *Struct. Bonding (Berlin)* **1999**, 94, 199.
- [67] S. Diele, S. Oelsner, F. Kuschel, B. Hisgen, H. Ringsdorf, R. Zentel, *Makromol. Chem.* **1987**, 188, 1993.
- [68] Concept of generalized dipoles and multipoles: A. G. Petrov, A. Derzhanski, *Mol. Cryst. Liq. Cryst.* **1987**, 151, 303.
- [69] A Voronoi tessellation is a tessellation of a plane obtained by choosing a discrete set of points around which the plane is partitioned into polygonal cells containing the part of the plane that is closer to the cell point than to any other point; the Voronoi honeycomb is considered as the extension of the Voronoi tessellation into the third dimension; the Voronoi foam is the corresponding partition of 3D space into polyhedra (see Figure 7c,d, bottom).

- [70] Interaggregate and intermaterial interfaces can be distinguished. Interaggregate interfaces represent planes (Sm), infinite minimal surfaces (Cub_V), Voronoi honeycombs (Col) or Voronoi polyhedra (Cub_I), separating the aggregates and in most cases located between the ends of the alkyl chains. Intermaterial interfaces separate the distinct segregated regions, that is, the layers, columns, spheroids formed by the one of the incompatible molecular parts from the layers or the continuum surrounding columns and spheres, formed by the other molecular parts. It must be considered that in the Col and Cub_I phases the interaggregate interfaces (Voronoi-cells) and in the Cub_V phases the intermaterial interfaces (bicontinuous nets) do not have a uniform curvature (planes, edges, and column segments and nodes, respectively). As the two types of these interfaces are almost parallel to each other and have the same type of curvature, they are not always strictly distinguished. One measure of the curvature is the Gauss curvature K , which is the product of the two main curvatures k_1 and k_2 ; it is positive if both are on the same side, as in paraboloids; it is negative if they are on opposite sides, as in the saddle-splay of the infinite minimal surfaces in bicontinuous cubic phases. Another measure of the curvature is the mean curvature H , which is the arithmetic average of the two main curvatures k_1 and k_2 . Thus for the LC phases of binary amphiphiles: Sm $H = K = 0$; Cub_V $H = 0$, $K < 0$; Col $H > 0$, $K = 0$; and Cub_I $H > 0$, $K > 0$.
- [71] a) S. Diele, *Curr. Opin. Colloid Interface Sci.* **2002**, 7, 333; b) M. Imp  rator-Clerc, *Curr. Opin. Colloid Interface Sci.* **2005**, 9, 370; c) S. Kutsumizu, *Curr. Opin. Solid State Mater. Sci.* **2002**, 6, 537.
- [72] Cub_V und Cub_I were introduced in lyotropic LCs as abbreviations for bicontinuous and discontinuous cubic phases, respectively^[9] and are also used herein. Alternatively, the assignments Cub_{bi} und Cub_{mic} are occasionally used for Cub_V und Cub_I, respectively.
- [73] A. H. Schoen, *Interface Focus* **2012**, 2, 658.
- [74] Y. Nakazawa, Y. Yamamura, S. Kutsumizu, K. Saito, *J. Phys. Soc. Jpn.* **2012**, 81, 094601.
- [75] N. Lindner, M. K  lbel, C. Sauer, S. Diele, J. Jokiranta, C. Tschierske, *J. Phys. Chem. B* **1998**, 102, 5261.
- [76] K. Hatsusaka, K. Ohta, I. Yamamoto, H. Shirai, *J. Mater. Chem.* **2001**, 11, 423.
- [77] J. Motoyanagi, T. Fukushima, T. Aida, *Chem. Commun.* **2005**, 101.
- [78] M. A. Alam, J. Motoyanagi, Y. Yamamoto, T. Fukushima, J. Kim, K. Kato, M. Takata, A. Saeki, S. Seki, S. Tagawa, T. Aida, *J. Am. Chem. Soc.* **2009**, 131, 17722.
- [79] > a) A.-M. Levelut, M. Clerc, *Liq. Cryst.* **1998**, 24, 105; b) S. Kutsumizu, K. Morita, S. Yano, S. Nijima, *Liq. Cryst.* **2002**, 29, 1459; c) K. Saito, M. Sorai, *Chem. Phys. Lett.* **2002**, 366, 56; d) W. T. Gozdoz, R. Holyst, *Phys. Rev. E* **1996**, 54, 5012.
- [80] a) X. Zeng, G. Ungar, M. Imp  rator-Clerc, *Nat. Mater.* **2005**, 4, 562; b) X. Zeng, L. Cseh, G. H. Mehl, G. Ungar, *J. Mater. Chem.* **2008**, 18, 2953.
- [81] K. Ozawa, Y. Yamamura, S. Yasuzuka, H. Mori, S. Kutsumizu, K. Saito, *J. Phys. Chem. B* **2008**, 112, 12179.
- [82] X. Cheng, X. Bai, S. Jing, H. Ebert, M. Prehm, C. Tschierske, *Chem. Eur. J.* **2010**, 16, 4588.
- [83] M. Peterca, M. R. Imam, P. Leowanawat, B. M. Rosen, D. A. Wilson, C. J. Wilson, X. Zeng, G. Ungar, P. A. Heiney, V. Percec, *J. Am. Chem. Soc.* **2010**, 132, 11288.
- [84] Recently another new bicontinuous or multicontinuous cubic phase with the space group $Pm\bar{3}m$ has been identified for an imidazolium salt, but the precise structure of this cubic phase is still unclear: K. Goossens, S. Wellens, K. Van Hecke, L. Van Meervelt, T. Cardinaels, K. Binnemans, *Chem. Eur. J.* **2011**, 17, 4291.
- [85] J. Malthete, A. Collet, A.-M. Levelut, *Liq. Cryst.* **1989**, 5, 123.
- [86] D. M. Kok, H. Wynberg, W. H. De Jeu, *Mol. Cryst. Liq. Cryst.* **1985**, 129, 53.
- [87] B. M. Rosen, C. J. Wilson, D. A. Wilson, M. Peterca, M. R. Imam, V. Percec, *Chem. Rev.* **2009**, 109, 6275.
- [88] E. Nishikawa, E. T. Samulski, *Liq. Cryst.* **2000**, 27, 1457.
- [89] E. Nishikawa, J. Yamamoto, H. Yokoyama, *Liq. Cryst.* **2003**, 30, 785; E. Nishikawa, J. Yamamoto, H. Yokoyama, *J. Mater. Chem.* **2003**, 13, 1887.
- [90] A. Kohlmeier, D. Janietz, *Liq. Cryst.* **2007**, 34, 65.
- [91] Y. Takanishi, T. Ogasawara, A. Yoshizawa, J. Umezawa, T. Kusumoto, T. Hiyama, K. Ishikawa, H. Takezoe, *J. Mater. Chem.* **2002**, 12, 1325.
- [92] J.-H. Ryu, M. Lee, *Struct. Bonding (Berlin)* **2008**, 128, 63; M. Lee, Y.-S. Yoo, *J. Mater. Chem.* **2002**, 12, 2161; M. Lee, B.-K. Cho, W.-C. Zin, *Chem. Rev.* **2001**, 101, 3869; H.-J. Kim, T. Kim, M. Lee, *Acc. Chem. Res.* **2011**, 44, 72.
- [93] T. Kato, N. Mizoshita, K. Kanie, *Macromol. Rapid Commun.* **2001**, 22, 797; T. Kato, *Struct. Bonding (Berlin)* **2000**, 96, 96; C. M. Paleos, D. Tsiourvas, *Curr. Opin. Colloid Interface Sci.* **2001**, 6, 257.
- [94] U. Beginn, *Prog. Polym. Sci.* **2003**, 28, 1049.
- [95] D. W. Bruce, *Struct. Bonding (Berlin)* **2008**, 126, 161.
- [96] M. SuTrez, J.-M. Lehn, S. C. Zimmerman, A. Skoulios, B. Heinrich, *J. Am. Chem. Soc.* **1998**, 120, 9526.
- [97] T. Akutagawa, K. Iuchi, Y. Matsunaga, *Liq. Cryst.* **2000**, 27, 1399.
- [98] M. A. J. Veld, D. Haveman, A. R. A. Palmans, E. W. Meijer, *Soft Matter* **2011**, 7, 524.
- [99] H. M. Keizer, R. P. Sijbesma, *Chem. Soc. Rev.* **2005**, 34, 226.
- [100] U. Beginn, G. Lattermann, *Mol. Cryst. Liq. Cryst.* **1994**, 241, 215; G. Stauffer, M. Schellhorn, G. Lattermann, *Liq. Cryst.* **1995**, 18, 519.
- [101] K. Borisch, S. Diele, P. G  ring, H. Kresse, C. Tschierske, *J. Mater. Chem.* **1998**, 8, 529.
- [102] G. Lattermann, G. Stauffer, *Mol. Cryst. Liq. Cryst.* **1990**, 191, 199.
- [103] B. Pfannem  ller, W. Welthe, E. Chin, J. W. Goodby, *Liq. Cryst.* **1986**, 1, 357; J. W. Goodby, *Mol. Cryst. Liq. Cryst.* **1984**, 110, 205.
- [104] K. Praefcke, A.-M. Levelut, B. Kohne, A. Echert, *Liq. Cryst.* **1989**, 6, 263.
- [105] S. Fischer, H. Fischer, S. Diele, G. Pelzl, K. Jankowski, R. R. Schmidt, V. Vill, *Liq. Cryst.* **1994**, 17, 855; V. Vill, R. Hashim, *Curr. Opin. Colloid Interface Sci.* **2002**, 7, 395.
- [106] K. Borisch, S. Diele, P. G  ring, H. M  ller, C. Tschierske, *Liq. Cryst.* **1997**, 22, 427.
- [107] J. W. Goodby, V. G  rtz, S. J. Cowling, G. Mackenzie, P. Martin, D. Plusquellec, T. Benvegnu, P. Boullanger, D. Lafont, Y. Queneau, S. Chambert, J. Fitremann, *Chem. Soc. Rev.* **2007**, 36, 1971.
- [108] K. Praefcke, P. Marquard, B. Kohne, W. Stephan, *J. Carbohydr. Chem.* **1991**, 10, 539; K. Praefcke, D. Blunk, *Liq. Cryst.* **1993**, 14, 1181.
- [109] C. Tschierske, *Prog. Polym. Sci.* **1996**, 21, 775.
- [110] Diisobutylsilanediol is probably the first example for this type of self-assembly: J. D. Bunning, J. E. Lydon, C. Eaborn, P. M. Jackson, J. W. Goodby, G. W. Gray, *J. Chem. Soc. Faraday Trans. 1* **1982**, 78, 713.
- [111] T. Ichikawa, M. Yoshio, A. Hamasaki, S. Taguchi, F. Liu, X.-B. Zeng, G. Ungar, H. Ohno, T. Kato, *J. Am. Chem. Soc.* **2012**, 134, 2634; X. Zhu, B. Tartsch, U. Beginn, M. M  ller, *Chem. Eur. J.* **2004**, 10, 3871.
- [112] K. Borisch, S. Diele, P. G  ring, C. Tschierske, *Chem. Commun.* **1996**, 237.
- [113] K. Borisch, S. Diele, P. G  ring, H. Kresse, C. Tschierske, *Angew. Chem.* **1997**, 109, 2188; *Angew. Chem. Int. Ed. Engl.* **1997**, 36, 2087.

- [114] R. Germer, F. Giesselmann, P. Zugenmaier, C. Tschierske, *Mol. Cryst. Liq. Cryst.* **1999**, *331*, 643.
- [115] S. Yazaki, Y. Kamikawa, M. Yoshio, A. Hamasaki, T. Mukai, H. Ohno, T. Kato, *Chem. Lett.* **2008**, *37*, 538.
- [116] P. Fuchs, C. Tschierske, K. Raith, K. Das, S. Diele, *Angew. Chem.* **2002**, *114*, 650; *Angew. Chem. Int. Ed.* **2002**, *41*, 628.
- [117] K. Borisch, C. Tschierske, P. Göring, S. Diele, *Chem. Commun.* **1998**, 2711.
- [118] K. Borisch, C. Tschierske, P. Göring, S. Diele, *Langmuir* **2000**, *16*, 6701.
- [119] Normal type Cub_v phase formed by ionic amphiphiles: T. Ichikawa, T. Kato, H. Ohno, *J. Am. Chem. Soc.* **2012**, *134*, 11354.
- [120] a) C. Tschierske, *J. Mater. Chem.* **1998**, *8*, 1485; b) C. Tschierske, *J. Mater. Chem.* **2001**, *11*, 2647; c) C. Tschierske, *Annu. Rep. Prog. Chem. Sect. C* **2001**, *97*, 191; d) C. Tschierske, *Isr. J. Chem.* **2012**, *52*, 935.
- [121] U. Beginn, S. Keinath, M. Möller, *Liq. Cryst.* **1997**, *23*, 35.
- [122] X. H. Cheng, M. K. Das, S. Diele, C. Tschierske, *Langmuir* **2002**, *18*, 6521.
- [123] a) D. Janietz, A. Kohlmeier, *Liq. Cryst.* **2009**, *36*, 685; b) A. Kohlmeier, D. Janietz, *Chem. Eur. J.* **2010**, *16*, 10453.
- [124] Y. Sagara, T. Kato, *Angew. Chem.* **2008**, *120*, 5253; *Angew. Chem. Int. Ed.* **2008**, *47*, 5175.
- [125] a) B.-K. Cho, A. Jain, S. M. Gruner, U. Wiesner, *Science* **2004**, *305*, 1598; b) B. K. Cho, A. Jain, S. M. Gruner, U. Wiesner, *Chem. Commun.* **2005**, 2143; c) B.-K. Cho, *Polym. J.* **2012**, *44*, 475.
- [126] T. Hatano, T. Kato, *Tetrahedron* **2008**, *64*, 8368.
- [127] S. Kohmoto, Y. Hara, K. Kishikawa, *Tetrahedron Lett.* **2010**, *51*, 1508.
- [128] J. Song, B.-K. Cho, *Soft Matter* **2012**, *8*, 3419.
- [129] T. Hatano, T. Kato, *Chem. Commun.* **2006**, 1277.
- [130] J. Jiménez, A. Laguna, A. M. Molter, J. L. Serrano, J. Barberá, L. Oriol, *Chem. Eur. J.* **2011**, *17*, 1029.
- [131] M. R. Imam, M. Peterca, U. Edlund, V. S. K. Balagurusamy, V. Percec, *J. Polym. Sci. Part A* **2009**, *47*, 4165.
- [132] V. Percec, M. N. Holerca, S. Uchida, W. D. Cho, G. Ungar, Y. S. Lee, D. J. P. Yeardley, *Chem. Eur. J.* **2002**, *8*, 1106.
- [133] D. Kim, S. Jon, H.-K. Lee, K. Baek, N.-K. Oh, W.-C. Zin, K. Kim, *Chem. Commun.* **2005**, 5509.
- [134] J.-K. Kim, M.-K. Hong, J.-H. Ahn, M. Lee, *Angew. Chem.* **2005**, *117*, 332; *Angew. Chem. Int. Ed.* **2005**, *44*, 328.
- [135] U. Beginn, L. Yan, S. N. Chvalun, M. A. Shcherbina, A. Bakirov, M. Möller, *Liq. Cryst.* **2008**, *35*, 1073.
- [136] D. R. Dukeson, G. Ungar, V. S. K. Balagurusamy, V. Percec, G. A. Johansson, M. Glodde, *J. Am. Chem. Soc.* **2003**, *125*, 15974.
- [137] G. Ungar, X. B. Zeng, *Soft Matter* **2005**, *1*, 95.
- [138] a) M. Lee, Y.-S. Jeong, B.-K. Cho, N.-K. Oh, W.-C. Zin, *Chem. Eur. J.* **2002**, *8*, 876; b) B.-K. Cho, Y.-W. Chung, M. Lee, *Macromolecules* **2005**, *38*, 10261.
- [139] T. Yasuda, H. Ooi, J. Morita, Y. Akama, K. Minoura, M. Funahashi, T. Shimomura, T. Kato, *Adv. Funct. Mater.* **2009**, *19*, 411.
- [140] A. Głębowska, P. Przybylski, M. Winek, P. Krzyczkowska, A. Krówczyński, J. Szydłowska, D. Pocięcha, E. Górecka, *J. Mater. Chem.* **2009**, *19*, 1395.
- [141] T. Hegmann, F. Peides, S. Diele, C. Tschierske, *Liq. Cryst.* **2000**, *27*, 1261; B. Bilgin-Eran, C. Tschierske, S. Diele, U. Baumeister, *J. Mater. Chem.* **2006**, *16*, 1145.
- [142] B. Kohne, K. Praefcke, J. Billard, *Z. Naturforsch. B* **1986**, *41*, 1036.
- [143] J. Billard, H. Zimmermann, P. Poupko, Z. Luz, *J. Phys.* **1989**, *50*, 539.
- [144] S. Diele, P. Göring, *Handbook of Liquid Crystals, Vol. 2B* (Eds.: D. Demus, J. Goodby, G. W. Gray, H.-W. Spiess, V. Vill), Wiley-VCH, Weinheim, **1998**, p. 887.
- [145] M. Ariyoshi, M. Sugibayashi-Kajita, A. Suzuki-Ichihara, T. Kato, T. Kamei, E. Itoh, K. Ohta, *J. Porphyrins Phthalocyanines* **2012**, *16*, 1114; M. Ichihara, A. Suzuki, K. Hatsusaka, K. Ohta, *J. Porphyrins Phthalocyanines* **2007**, *11*, 503.
- [146] a) H. Mukai, M. Yokokawa, M. Ichihara, K. Hatsusaka, K. Ohta, *J. Porphyrins Phthalocyanines* **2010**, *14*, 188; b) H. Mukai, K. Hatsusaka, K. Ohta, *J. Porphyrins Phthalocyanines* **2007**, *11*, 846; c) M. Ichihara, A. Suzuki, K. Hatsusaka, K. Ohta, *Liq. Cryst.* **2007**, *34*, 555.
- [147] T. Kato, T. Matsuoka, M. Nishii, Y. Kamikawa, K. Kanie, T. Nishimura, E. Yashima, S. Ujiie, *Angew. Chem.* **2004**, *116*, 2003; *Angew. Chem. Int. Ed.* **2004**, *43*, 1969.
- [148] V. Percec, M. R. Imam, M. Peterca, D. A. Wilson, R. Graf, H. W. Spiess, V. S. K. Balagurusamy, P. A. Heiney, *J. Am. Chem. Soc.* **2009**, *131*, 7662.
- [149] V. Percec, M. R. Imam, M. Peterca, D. A. Wilson, P. A. Heiney, *J. Am. Chem. Soc.* **2009**, *131*, 1294.
- [150] M. Seitz, T. Plesnivý, K. Schimossek, M. Edelmann, H. Ringsdorf, H. Fischer, H. Uyama, S. Kobayashi, *Macromolecules* **1996**, *29*, 6560.
- [151] U. Stebani, G. Lattermann, M. Wittenberg, J. H. Wendorff, *J. Mater. Chem.* **1997**, *7*, 607.
- [152] In analogy, smectic phases were found for molecules incorporating only one aromatic ring in combination with a semi-perfluorinated alkyl chain.^[159a]
- [153] Remarkably, in the series of compounds **35**, the Cub_v phase is found for **35b** with the shorter fluorinated segment, whereas compound **35a** with the longer R_F segments, and thus the larger chain volume, forms a SmA phase. In this case, the lamellar phase is stabilized by elongation of the rigid and linear R_F chain, which disfavours curved interfaces (see Section 3.5).
- [154] A. Pegenau, X. H. Cheng, C. Tschierske, P. Göring, S. Diele, *New J. Chem.* **1999**, *23*, 465.
- [155] X. H. Cheng, S. Diele, C. Tschierske, *Angew. Chem.* **2000**, *112*, 605; *Angew. Chem. Int. Ed.* **2000**, *39*, 592.
- [156] It is likely that also for the benzene hexaalkanoates reported by Chandrasekhar et al.^[45] the formation of columnar phases is due more to the segregation of the polar cores from the lipophilic chains than to a disc-like molecular shape.
- [157] CED values can be calculated from tabulated group contributions of the molar vaporization energy and the molar volume.^[120d,165]
- [158] There is also an influence of the linking units on the molecular flexibility (CH₂O > COO > CONH), but this effect is thought to be opposite to the effect of segregation, as the higher the flexibility, the easier the tetrahedral molecules can adopt to the curved interfaces in the Col_{hex} phases, hence increased molecular flexibility should lead to enhanced mesophase stability in this case.
- [159] a) S. Takenaka, *J. Chem. Soc. Chem. Commun.* **1992**, 1748; b) T. Doi, Y. Sakurai, A. Tamatani, S. Takenaka, S. Kusabayashi, Y. Nishihata, H. Terauchi, *J. Mater. Chem.* **1991**, *1*, 169.
- [160] a) V. Percec, G. Johansson, G. Ungar, J. Zhou, *J. Am. Chem. Soc.* **1996**, *118*, 9855; b) G. Johansson, V. Percec, G. Ungar, J. P. Zhou, *Macromolecules* **1996**, *29*, 646.
- [161] C. Tschierske, *Top. Curr. Chem.* **2012**, *318*, 1.
- [162] M. P. Krafft, J. G. Riess, *Chem. Rev.* **2009**, *109*, 1714.
- [163] J. H. Cameron, A. Facher, G. Lattermann, S. Diele, *Adv. Mater.* **1997**, *9*, 398.
- [164] K. Lorenz, H. Frey, B. Stühn, R. Mülhaupt, *Macromolecules* **1997**, *30*, 6860.
- [165] D. W. Van Krevelen, *Properties of Polymers, 3rd ed.*, Elsevier, Amsterdam, **1990**, p. 189.
- [166] E. Białecka-Florjanczyk, *J. Phys. Chem. B* **2006**, *110*, 2582.

- [167] M. Yoneya, K. Araya, E. Nishikawa, H. Yokoyama, *J. Phys. Chem. B* **2004**, *108*, 8099.
- [168] M. Yoneya, *Chem. Rec.* **2011**, *11*, 66.
- [169] W. Chen, B. Wunderlich, *Macromol. Chem. Phys.* **1999**, *200*, 283.
- [170] Z. Xu, S. Lee, E. B. Lobkovsky, Y.-H. Kiang, *J. Am. Chem. Soc.* **2002**, *124*, 123; S. Lee, A. B. Mallik, Z. Xu, E. B. Lobkovsky, L. Tran, *Acc. Chem. Res.* **2005**, *38*, 251; H. G. von Schnering, R. Nesper, *Angew. Chem.* **1987**, *99*, 1097; *Angew. Chem. Int. Ed. Engl.* **1987**, *26*, 1059.
- [171] a) A.-M. Giroud-Godquin, A. Rassat, *C. R. Seances Acad. Sci. Ser. 2* **1982**, *294*, 241; b) H. Zheng, T. M. Swager, *J. Am. Chem. Soc.* **1994**, *116*, 761.
- [172] G. Lattermann, *Liq. Cryst.* **1987**, *2*, 723.
- [173] B. Donnio, D. Guillon, *Adv. Polym. Sci.* **2006**, *201*, 45; B. Donnio, S. Buathong, I. Bury, D. Guillon, *Chem. Soc. Rev.* **2007**, *36*, 1495.
- [174] a) D. W. Bruce, D. A. Dummur, S. A. Hudson, E. Lalinde, P. M. Maitlis, M. P. McDonald, R. Orr, P. Styring, *Mol. Cryst. Liq. Cryst.* **1991**, *206*, 79; b) D. W. Bruce, B. Donnio, S. A. Hudson, A.-M. Levelut, S. Megtert, D. Petermann, M. Veber, *J. Phys. II* **1995**, *5*, 289.
- [175] D. J. Wales, *Philos. Trans. R. Soc. London Ser. A* **2012**, *370*, 2877.
- [176] L. Cademartiri, K. J. M. Bishop, P. W. Snyder, G. A. Ozin, *Philos. Trans. R. Soc. London Ser. A* **2012**, *370*, 2824.
- [177] J. H. E. Cartwright, A. L. Mackay, *Philos. Trans. R. Soc. London Ser. A* **2012**, *370*, 2807.
- [178] B. Donnio, B. Heinrich, H. Allouchi, J. Kain, S. Diele, D. Guillon, D. W. Bruce, *J. Am. Chem. Soc.* **2004**, *126*, 15258.
- [179] V. Percec, M. Glodde, G. Johansson, V. S. K. Balagurusamy, P. A. Heiney, *Angew. Chem.* **2003**, *115*, 4474; *Angew. Chem. Int. Ed.* **2003**, *42*, 4338.
- [180] C. H. M. Weber, F. Liu, X. B. Zeng, G. Ungar, N. Mullin, J. K. Hobbs, M. Jahr, M. Lehmann, *Soft Matter* **2010**, *6*, 5390.
- [181] C. Tschierske in *Chirality at the Nanoscale* (Ed.: D. B. Amabilino), Wiley-VCH, Weinheim, **2009**, p. 271.
- [182] D. Weaire, R. Phelan, *Philos. Mag. Lett.* **1994**, *69*, 107; D. Weaire, R. Phelan, *Philos. Trans. R. Soc. London Ser. A* **1996**, *354*, 1989.
- [183] a) P. Zihlerl, R. D. Kamien, *J. Phys. Chem. B* **2001**, *105*, 10147; b) G. M. Grason, R. D. Kamien, *Phys. Rev. E* **2005**, *71*, 051801.
- [184] G. Ungar, Y. S. Liu, X. B. Zeng, V. Percec, W.-D. Cho, *Science* **2003**, *299*, 1208.
- [185] Recently the $P4_2/mnm$ lattice was also observed for block copolymer morphologies: S. Lee, M. J. Bluemle, F. S. Bates, *Science* **2010**, *330*, 349.
- [186] $P4_2/mnm$ in lyotropic systems: C. Gao, Y. Sakamoto, O. Terasaki, S. Che, *Chem. Eur. J.* **2008**, *14*, 11423; A. E. Garcia-Bennett, N. Kupferschmidt, Y. Sakamoto, S. Che, O. Terasaki, *Angew. Chem.* **2005**, *117*, 5451; *Angew. Chem. Int. Ed.* **2005**, *44*, 5317.
- [187] a) X. B. Zeng, G. Ungar, Y. S. Liu, V. Percec, A. E. Dulcey, J. K. Hobbs, *Nature* **2004**, *428*, 157; b) G. Ungar, V. Percec, X. B. Zeng, P. Leowanawat, *Isr. J. Chem.* **2011**, *51*, 1206.
- [188] A. K. Sinha, *Topologically Closed Packed Structures in Transition Metal Alloys*, Pergamon, Oxford, **1972**.
- [189] F. C. Frank, J. S. Kasper, *Acta Crystallogr.* **1958**, *11*, 184; F. C. Frank, J. S. Kasper, *Acta Crystallogr.* **1959**, *12*, 483; D. X. Li, K. H. Kuo, *Acta Crystallogr. Sect. B* **1986**, *42*, 152.
- [190] Y. Li, S.-T. Lin, W. A. Goddard III, *J. Am. Chem. Soc.* **2004**, *126*, 1872.
- [191] I. Bury, B. Heinrich, C. Bourgogne, D. Guillon, B. Donnio, *Chem. Eur. J.* **2006**, *12*, 8396.
- [192] S. Coco, C. Cordovilla, B. Donnio, P. Espinet, M. J. Garcia-Casas, D. Guillon, *Chem. Eur. J.* **2008**, *14*, 3544.
- [193] C.-J. Jang, J.-H. Ryu, J.-D. Lee, D. Sohn, M. Lee, *Chem. Mater.* **2004**, *16*, 4226.
- [194] B. M. Rosen, M. Peterca, C. Huang, X. Zeng, G. Ungar, V. Percec, *Angew. Chem.* **2010**, *122*, 7156; *Angew. Chem. Int. Ed.* **2010**, *49*, 7002.
- [195] E. Lee, J.-H. Ryu, M.-H. Park, M. Lee, K.-H. Han, Y.-W. Chung, B.-K. Cho, *Chem. Commun.* **2007**, 2920.
- [196] B. Donnio, P. García-Vázquez, J.-L. Gallani, D. Guillon, E. Terazzi, *Adv. Mater.* **2007**, *19*, 3534.
- [197] T. H. Jordan, W. E. Streib, W. N. Lipscomb, *J. Chem. Phys.* **1964**, *41*, 760; T. H. Jordan, W. E. Streib, H. W. Smith, W. N. Lipscomb, *Acta Crystallogr.* **1964**, *17*, 777; D. T. Cromer, R. L. Mills, D. Schiferl, L. A. Schwalbe, *Acta Crystallogr. Sect. B* **1981**, *37*, 8.
- [198] K. Fontell, K. K. Fox, E. Hansson, *Mol. Cryst. Liq. Cryst. Lett. Sect.* **1985**, *1*, 9; K. Fontell, *Colloid Polym. Sci.* **1990**, *268*, 264.
- [199] G. C. Shearman, A. I. I. Tyler, N. J. Brooks, R. H. Templer, O. Ces, R. V. Law, J. M. Seddon, *Liq. Cryst.* **2010**, *37*, 679.
- [200] A. Gulik, H. Delacroix, G. Kirschner, V. Luzzati, *J. Phys.* **1995**, *5*, 445.
- [201] M. O'Keeffe, S. Andersson, *Acta Crystallogr. Sect. A* **1977**, *33*, 914.
- [202] This structure should be recognized by XRD, as in this organization the ($h \pm k \pm l = 0$) reflections in the XRD pattern should become weaker: V. Luzzati, A. Tardieu, T. Gulik-Krzywichei, *Proc. Natl. Acad. Sci. USA* **1981**, *78*, 4683.
- [203] a) D. C. Wright, N. D. Mermin, *Rev. Mod. Phys.* **1989**, *61*, 385; b) P. P. Crooker, *Liq. Cryst.* **1989**, *5*, 751.
- [204] M. Oxborrow, C. L. Henley, *Phys. Rev. B* **1993**, *48*, 6966; M. O'Keeffe, M. M. J. Treacy, *Acta Crystallogr. Sect. A* **2010**, *66*, 5; M. N. van der Linden, J. P. K. Doye, A. A. Louis, *J. Chem. Phys.* **2012**, *136*, 054904.
- [205] M. Baake, R. Klitzling, M. Schlottmann, *Phys. A* **1992**, *191*, 554; P. Stampfli, *Helv. Phys. Acta* **1986**, *59*, 1260.
- [206] T. Dotera, *J. Polym. Sci. Part B* **2012**, *50*, 155; K. Hayashida, T. Dotera, A. Takano, Y. Matsushita, *Phys. Rev. Lett.* **2007**, *98*, 195502; T. Dotera, *Isr. J. Chem.* **2011**, *51*, 1197.
- [207] D. Shechtman, I. Blech, D. Gratias, J. W. Cahn, *Phys. Rev. Lett.* **1984**, *53*, 1951.
- [208] T. Ishimasa, H.-U. Nissen, Y. Fukano, *Phys. Rev. Lett.* **1985**, *55*, 511; T. Ishimasa, *Isr. J. Chem.* **2011**, *51*, 1216.
- [209] C. R. Iacovella, A. S. Keys, S. C. Glotzer, *Proc. Natl. Acad. Sci. USA* **2011**, *108*, 20935.
- [210] K. Barkan, H. Diamant, R. Lifshitz, *Phys. Rev. B* **2011**, *83*, 172201; R. Lifshitz, H. Diamant, *Philos. Mag.* **2007**, *87*, 3021.
- [211] a) V. Percec, W. D. Cho, G. Ungar, D. J. P. Yearlley, *J. Am. Chem. Soc.* **2001**, *123*, 1302; b) V. Percec, M. Peterca, M. J. Sienkowska, M. A. Ilies, E. Aqad, J. Smidrkal, P. A. Heiney, *J. Am. Chem. Soc.* **2006**, *128*, 3324; c) B. M. Rosen, D. A. Wilson, C. J. Wilson, M. Peterca, B. C. Won, C. Huang, L. R. Lipski, X. Zeng, G. Ungar, P. A. Heiney, V. Percec, *J. Am. Chem. Soc.* **2009**, *131*, 17500.
- [212] J. Zhang, F. S. Bates, *J. Am. Chem. Soc.* **2012**, *134*, 7636.
- [213] S. Fischer, A. Exner, K. Zielske, J. Perlich, S. Deloudi, W. Steurer, P. Lindner, S. Förster, *Proc. Natl. Acad. Sci. USA* **2011**, *108*, 1810.
- [214] C. Xiao, N. Fujita, K. Miyasaka, Y. Sakamoto, O. Terasaki, *Nature* **2012**, *487*, 349.
- [215] D. V. Talapin, E. V. Shevchenko, M. I. Bodnarchuk, X. Ye, J. Chen, C. B. Murray, *Nature* **2009**, *461*, 964.
- [216] Y. Yang, Y. Wang, H. Li, W. Li, L. Wu, *Chem. Eur. J.* **2010**, *16*, 8062; Y. Wang, X. Wang, X. Zhang, N. Xia, B. Liu, J. Yang, W. Yu, M. Hu, M. Yang, W. Wang, *Chem. Eur. J.* **2010**, *16*, 12545; S. Floquet, E. Terazzi, A. Hijazi, L. Guenee, C. Pigué, E. Cadot, *New J. Chem.* **2012**, *36*, 865.
- [217] E. Terazzi, C. Bourgogne, R. Welter, J.-L. Gallani, D. Guillon, G. Rogez, B. Donnio, *Angew. Chem.* **2008**, *120*, 500; *Angew.*

- Chem. Int. Ed.* **2008**, *47*, 490; G. Rogez, B. Donnio, E. Terazzi, J.-L. Gallani, J.-P. Kappler, J.-P. Bucher, M. Drillon, *Adv. Mater.* **2009**, *21*, 4323; Y. Molard, F. Dorson, V. Circu, T. Roisnel, F. Artzner, S. Cordier, *Angew. Chem.* **2010**, *122*, 3423; *Angew. Chem. Int. Ed.* **2010**, *49*, 3351; Y. Molard, A. Ledneva, M. Amela-Cortes, V. Circu, N. G. Naumov, C. Meriadec, F. Artzner, S. Cordier, *Chem. Mater.* **2011**, *23*, 5122.
- [218] R. Deschenaux, B. Donnio, D. Guillon, *New J. Chem.* **2007**, *31*, 1064.
- [219] G. H. Mehl, I. M. Saez, *Appl. Organomet. Chem.* **1999**, *13*, 261; I. M. Saez, J. W. Goodby, *Liq. Cryst.* **1999**, *26*, 1101.
- [220] X. Wang, C. M. Cho, W. Y. Say, A. Y. X. Tan, C. He, H. S. O. Chan, J. Xu, *J. Mater. Chem.* **2011**, *21*, 5248.
- [221] R. Elsäßer, G. H. Mehl, J. W. Goodby, D. J. Photinos, *Chem. Commun.* **2000**, 851; I. Saez, J. W. Goodby, *Struct. Bonding (Berlin)* **2008**, *128*, 1.
- [222] H. Mamlouk-Chaouachi, B. Heirich, C. Bourgogne, D. Guillon, B. Donnio, D. Felder-Flesch, *J. Mater. Chem.* **2011**, *21*, 9121.
- [223] a) J. W. Goodby, I. M. Saez, S. J. Cowling, V. Görtz, M. Draper, A. W. Hall, S. Sia, G. Cosquer, S.-E. Lee, E. P. Raynes, *Angew. Chem.* **2008**, *120*, 2794; *Angew. Chem. Int. Ed.* **2008**, *47*, 2754; b) J. W. Goodby, I. M. Saez, S. J. Cowling, J. S. Gasowska, R. A. MacDonald, S. Sia, P. Watson, K. J. Toyne, M. Hird, R. A. Lewis, S.-E. Lee, V. Vaschenko, *Liq. Cryst.* **2009**, *36*, 567.
- [224] I. M. Saez, J. W. Goodby, R. M. Richardson, *Chem. Eur. J.* **2001**, *7*, 2758.
- [225] P. K. Karahaliou, P. H. J. Kouwer, T. Meyer, G. H. Mehl, D. J. Photinos, *Soft Matter* **2007**, *3*, 857; P. K. Karahaliou, P. H. J. Kouwer, T. Meyer, G. H. Mehl, D. J. Photinos, *J. Phys. Chem. B* **2008**, *112*, 6550.
- [226] E.-K. Fleischmann, R. Zentel, *Angew. Chem.* **2013**, *125*, DOI: 10.1002/ange.201300371; *Angew. Chem. Int. Ed.* **2013**, *52*, DOI: 10.1002/anie.201300371; *J. Mater. Chem.* **2008**, *18*, No. 25, Theme issue: Liquid Crystals Beyond Display Applications, S. 2857–3060.
- [227] K. Kanie, M. Matsubara, X. Zeng, F. Liu, G. Ungar, H. Nakamura, A. Muramatsu, *J. Am. Chem. Soc.* **2012**, *134*, 808.
- [228] G. L. Nealon, R. Greget, C. Dominguez, Z. T. Nagy, D. Guillon, J.-L. Gallani, B. Donnio, *Beilstein J. Org. Chem.* **2012**, *8*, 349; O. Stamatoiu, J. Mirzaei, X. Feng, T. Hegmann, *Top. Curr. Chem.* **2012**, *318*, 331.
- [229] M. Brust, M. Walker, D. Bethell, D. J. Schiffrin, R. Whyman, *J. Chem. Soc. Chem. Commun.* **1994**, 801.
- [230] H. Qi, T. Hegmann, *Liq. Cryst. Today* **2011**, *20*, 102.
- [231] H. K. Bisoyi, S. Kumar, *Chem. Soc. Rev.* **2011**, *40*, 306.
- [232] S. I. Stoeva, B. L. V. Prasad, U. Sitharaman, P. Stoimenov, V. Zaikovski, C. M. Sorensen, K. J. Klabunde, *J. Phys. Chem. B* **2003**, *107*, 7441.
- [233] L. Rossi, S. Sacanna, W. T. M. Irvine, P. M. Chaikin, D. J. Pine, A. P. Philipse, *Soft Matter* **2011**, *7*, 4139.
- [234] Other reported $Pm\bar{3}m$ type cubic phases seem to be bicontinuous cubic phases.^[77,84,129]
- [235] M. Draper, I. M. Saez, S. J. Cowling, P. Gai, B. Heinrich, B. Donnio, D. Guillon, J. W. Goodby, *Adv. Funct. Mater.* **2011**, *21*, 1260.
- [236] S. Mischler, S. Guerra, R. Deschenaux, *Chem. Commun.* **2012**, *48*, 2183.
- [237] a) M. M. Wojcik, M. Kolpaczynska, D. Pocięcha, J. Mieczkowski, E. Gorecka, *Soft Matter* **2010**, *6*, 5397; b) M. M. Wojcik, M. Gora, J. Mieczkowski, J. Romiszewski, E. Gorecka, D. Pocięcha, *Soft Matter* **2011**, *7*, 10561; c) M. M. Wojcik, W. Lewandowski, J. Matraszek, J. Mieczkowski, J. Borysiuk, D. Pocięcha, E. Gorecka, *Angew. Chem.* **2009**, *121*, 5269; *Angew. Chem. Int. Ed.* **2009**, *48*, 5167.
- [238] a) X. Zeng, F. Liu, A. G. Fowler, G. Ungar, L. Cseh, G. H. Mehl, J. E. Macdonald, *Adv. Mater.* **2009**, *21*, 1746; b) X. Mang, X. Zeng, B. Tang, F. Liu, G. Ungar, R. Zhang, L. Cseh, G. H. Mehl, *J. Mater. Chem.* **2012**, *22*, 11101.
- [239] C. H. Yu, C. P. J. Schubert, C. Welch, B. J. Tang, M.-G. Tamba, G. H. Mehl, *J. Am. Chem. Soc.* **2012**, *134*, 5076; J. Dintinger, B.-J. Tang, X. Zeng, F. Liu, T. Kienzler, G. H. Mehl, G. Ungar, C. Rockstuhl, T. Scharf, *Adv. Mater.* **2013**, *25*, 1999.
- [240] H. Chen, *J. Mater. Chem.* **2011**, *21*, 6452; H. Chen, C. T. Chan, P. Sheng, *Nat. Mater.* **2010**, *9*, 387.
- [241] V. Luzzati, H. Mustacchi, A. Skoulios, *Discuss. Faraday Soc.* **1958**, *25*, 43.
- [242] H.-J. Kim, F. Liu, J.-H. Ryu, S.-K. Kang, X. Zeng, G. Ungar, J. K. Lee, W.-C. Zin, M. Lee, *J. Am. Chem. Soc.* **2012**, *134*, 13871.
- [243] X. Li, S. Kang, S. K. Lee, M. Tokita, J. Watanabe, *Jpn. J. Appl. Phys. Part 1* **2010**, *49*, 121701; X. Li, M. Zhan, K. Wang, H. Zhou, *Chem. Lett.* **2011**, *40*, 820; S. Kang, M. Harada, X. Li, M. Tokita, J. Watanabe, *Soft Matter* **2012**, *8*, 1916.
- [244] S. Kang, R. Ishige, E.-W. Lee, M. Tokita, J. Watanabe, *J. Mater. Chem.* **2012**, *22*, 21448.
- [245] S. Sioula, N. Hadjichristidis, E. L. Thomas, *Macromolecules* **1998**, *31*, 8419; V. Abetz, P. F. W. Simon, *Adv. Polym. Sci.* **2005**, *189*, 125; K. Aissou, H. K. Choi, A. Nunnes, I. Manners, C. A. Ros, *Nano Lett.* **2013**, *13*, 835; J. J. K. Kirkensgaard, *Interface Focus* **2012**, *2*, 602.
- [246] Y. Matsushita, K. Hayashida, A. Takano, *Macromol. Rapid Commun.* **2010**, *31*, 1579.
- [247] G. Starkulla, M. Kaller, W. Frey, K. V. Axenov, S. Laschat, *Liq. Cryst.* **2011**, *38*, 1515; H. Müller, C. Tschierske, *J. Chem. Soc. Chem. Commun.* **1995**, 645; K. Ema, K. Takekoshi, H. Yao, S. T. Wang, C. C. Huang, *Phys. Rev. E* **2005**, *71*, 031706; C.-T. Liano, J.-Y. Lee, C.-C. Lai, *Mol. Cryst. Liq. Cryst.* **2011**, *534*, 3.
- [248] J. Newton, H. Coles, P. Hodge, J. Hannington, *J. Mater. Chem.* **1994**, *4*, 869.
- [249] F. Tournilhac, L. M. Blinov, J. Simon, S. V. Yablonsky, *Nature* **1992**, *359*, 621.
- [250] B. Bilgin-Eran, C. Yörür, C. Tschierske, M. Prehm, U. Baumeister, *J. Mater. Chem.* **2007**, *17*, 2319.
- [251] A. Zelcer, B. Donnio, C. Bourgogne, F. D. Cukiernik, D. Guillon, *Chem. Mater.* **2007**, *19*, 1992; R. Zniber, R. Achour, M. Z. Cherkaoui, B. Donnio, L. Gehringer, D. Guillon, *J. Mater. Chem.* **2002**, *12*, 2208; L. Cui, J. P. Collet, G. Xu, L. Zhu, *Chem. Mater.* **2006**, *18*, 3503.
- [252] S. Sauer, N. Steinke, A. Baro, S. Laschat, F. Giesselmann, W. Kantlehner, *Chem. Mater.* **2008**, *20*, 1909.
- [253] I. Paraschiv, M. Giesbers, B. van Lagen, F. C. Grozema, R. D. Abellon, L. D. A. Siebbeles, A. T. M. Marcelis, H. Zuilhof, E. J. R. Sudhölter, *Chem. Mater.* **2006**, *18*, 968; C. F. C. Fitié, I. Tomatsu, D. Byelov, W. H. de Jeu, R. P. Sijbesma, *Chem. Mater.* **2008**, *20*, 2394; M. D. McKenna, J. Barbera, M. Marcos, J. L. Serrano, *J. Am. Chem. Soc.* **2005**, *127*, 619.
- [254] V. Percec, T. K. Bera, M. Glodde, Q. Fu, V. S. K. Balagurusamy, P. A. Heiney, *Chem. Eur. J.* **2003**, *9*, 921.
- [255] V. Percec, C.-H. Ahn, T. K. Bera, G. Ungar, D. J. P. Yeadley, *Chem. Eur. J.* **1999**, *5*, 1070.
- [256] L. Cui, J. Miao, L. Zhu, *Macromolecules* **2006**, *39*, 2536; U. Dahn, C. Erdelen, H. Ringsdorf, R. Festag, J. H. Wendorff, P. A. Heiney, N. C. Maliszewskyj, *Liq. Cryst.* **1995**, *19*, 759.
- [257] T. Sakurai, K. Tashiro, Y. Honsho, A. Saeki, S. Seki, A. Osuka, A. Muranaka, M. Uchiyama, J. Kim, S. Ha, K. Kato, M. Takata, T. Aida, *J. Am. Chem. Soc.* **2011**, *133*, 6537.
- [258] M. Lehmann, M. Jahr, J. Gutmann, *J. Mater. Chem.* **2008**, *18*, 2995.
- [259] X. Feng, V. Marcon, W. Pisula, M. R. Hansen, J. Kirkpatrick, F. Grozema, D. Andrienko, K. Kremer, K. Müllen, *Nat. Mater.* **2009**, *8*, 421.

- [260] L. de Campo, T. Varslot, M. J. Moghaddam, J. J. K. Kirkensgaard, K. Mortensen, S. T. Hyde, *Phys. Chem. Chem. Phys.* **2011**, *13*, 3139.
- [261] S. Sioula, N. Hadjichristidis, E. L. Thomas, *Macromolecules* **1998**, *31*, 5272.
- [262] V. Percec, M. R. Imam, T. K. Bera, V. S. K. Balagurusamy, M. Peterca, P. A. Heiney, *Angew. Chem.* **2005**, *117*, 4817; *Angew. Chem. Int. Ed.* **2005**, *44*, 4739.
- [263] I. Bury, B. Heinrich, C. Bourgonne, G. H. Mehl, D. Guillon, B. Donnio, *New J. Chem.* **2012**, *36*, 452.
- [264] Polyphilic dendrimers formed by ionic self-assembly of perfluorinated benzoic acids with amine based dendrimers: S. Hernández-Ainsa, J. Barberá, M. Marcos, J. L. Serrano, *Chem. Mater.* **2010**, *22*, 4762.
- [265] Related polar/apolar Janus-type dendrimers form similar structures, see Ref. [191] and: B. Liu, M. Yang, N. Xia, P. Theng, W. Wang, C. Burger, *Soft Matter* **2012**, *8*, 9545; J.-W. Choi, M.-H. Ryu, E. Lee, B.-K. Cho, *Chem. Eur. J.* **2010**, *16*, 9006; M. Peterca, V. Percec, P. Leowanawat, A. Bertin, *J. Am. Chem. Soc.* **2011**, *133*, 20507.
- [266] W. Weissflog, D. Demus, *Cryst. Res. Technol.* **1984**, *19*, 55.
- [267] K. Leblanc, P. Berdague, J.-P. Bayle, P. Judeinstein, J. Rault, *Chem. Commun.* **2000**, 1291.
- [268] S. V. Arehart, C. Pugh, *J. Am. Chem. Soc.* **1997**, *119*, 3027; C. Pugh, J.-Y. Bae, J. Dharia, J. J. Ge, S. Z. D. Cheng, *Macromolecules* **1998**, *31*, 5188.
- [269] F. Hildebrandt, J. A. Schröter, C. Tschierske, R. Festag, R. Kleppinger, J. H. Wendorff, *Angew. Chem.* **1995**, *107*, 1780; *Angew. Chem. Int. Ed. Engl.* **1995**, *34*, 1631.
- [270] C. Tschierske, *Chem. Soc. Rev.* **2007**, *36*, 1930.
- [271] G. Ungar, C. Tschierske, V. Abetz, R. Holyst, M. A. Bates, F. Liu, M. Prehm, R. Kieffer, X. B. Zeng, M. Walker, B. Glettner, A. Zywockinski, *Adv. Funct. Mater.* **2011**, *21*, 1296.
- [272] C. Tschierske, C. Nürnberger, H. Ebert, B. Glettner, M. Prehm, F. Liu, X.-B. Zeng, G. Ungar, *Interface Focus* **2012**, *2*, 669.
- [273] R. Plehnert, J. A. Schröter, C. Tschierske, *J. Mater. Chem.* **1998**, *8*, 2611.
- [274] J.-H. Fuhrhop, T. Wang, *Chem. Rev.* **2004**, *104*, 2901.
- [275] M. Kölbels, T. Beyersdorff, X. H. Cheng, C. Tschierske, J. Kain, S. Diele, *J. Am. Chem. Soc.* **2001**, *123*, 6809.
- [276] X. Cheng, M. Prehm, M. K. Das, J. Kain, U. Baumeister, S. Diele, D. Leine, A. Blume, C. Tschierske, *J. Am. Chem. Soc.* **2003**, *125*, 10977.
- [277] X. Cheng, F. Liu, X.-B. Zeng, G. Ungar, J. Kain, S. Diele, M. Prehm, C. Tschierske, *J. Am. Chem. Soc.* **2011**, *133*, 7872.
- [278] X. Cheng, X. Dong, R. Huang, X. Zeng, G. Ungar, M. Prehm, C. Tschierske, *Chem. Mater.* **2008**, *20*, 4729.
- [279] X. Cheng, X. Dong, G. Wei, M. Prehm, C. Tschierske, *Angew. Chem.* **2009**, *121*, 8158; *Angew. Chem. Int. Ed.* **2009**, *48*, 8014.
- [280] M. Prehm, G. Götz, P. Bäuerle, F. Liu, X. Zeng, G. Ungar, C. Tschierske, *Angew. Chem.* **2007**, *119*, 8002; *Angew. Chem. Int. Ed.* **2007**, *46*, 7856.
- [281] X. Cheng, H. Gao, W. Bu, X. Tan, M. Prehm, H. Ebert, C. Tschierske, *Chem. Sci.* **2013**, *4*, 3317.
- [282] H. Gao, Y. Ye, L. Kong, X. Cheng, M. Prehm, H. Ebert, C. Tschierske, *Soft Matter* **2012**, *8*, 10921.
- [283] W. Bu, H. Gao, X. Tan, X. Dong, X. Cheng, M. Prehm, C. Tschierske, *Chem. Commun.* **2013**, *49*, 1756.
- [284] B. Glettner, F. Liu, X.-B. Zeng, M. Prehm, U. Baumeister, M. A. Bates, M. Walker, P. Boesecke, G. Ungar, C. Tschierske, *Angew. Chem.* **2008**, *120*, 9203; *Angew. Chem. Int. Ed.* **2008**, *47*, 9063.
- [285] X. B. Zeng, R. Kieffer, B. Glettner, C. Nürnberger, F. Liu, K. Pelz, M. Prehm, U. Baumeister, H. Hahn, H. Lang, G. A. Gehring, C. H. M. Weber, J. K. Hobbs, C. Tschierske, G. Ungar, *Science* **2011**, *331*, 1302.
- [286] R. Kieffer, M. Prehm, K. Pelz, U. Baumeister, F. Liu, H. Hahn, H. Lang, G. Ungar, C. Tschierske, *Soft Matter* **2009**, *5*, 1214.
- [287] Q. Zhou, T. Chen, J. Zhang, L. Wan, P. Xie, C. C. Han, S. Yan, R. Zhang, *Tetrahedron Lett.* **2008**, *49*, 5522.
- [288] X. Cheng, M. K. Das, U. Baumeister, S. Diele, C. Tschierske, *J. Am. Chem. Soc.* **2004**, *126*, 12930.
- [289] M. Prehm, C. Enders, M. Y. Anzahae, B. Glettner, U. Baumeister, C. Tschierske, *Chem. Eur. J.* **2008**, *14*, 6352.
- [290] X. H. Cheng, M. K. Das, S. Diele, C. Tschierske, *Angew. Chem.* **2002**, *114*, 4203; *Angew. Chem. Int. Ed.* **2002**, *41*, 4031.
- [291] M. Prehm, X. H. Cheng, S. Diele, M. K. Das, C. Tschierske, *J. Am. Chem. Soc.* **2002**, *124*, 12072.
- [292] M. Prehm, S. Diele, M. K. Das, C. Tschierske, *J. Am. Chem. Soc.* **2003**, *125*, 614.
- [293] F. Hentrich, C. Tschierske, H. Zschke, *Angew. Chem.* **1991**, *103*, 429; *Angew. Chem. Int. Ed. Engl.* **1991**, *30*, 440.
- [294] F. Hentrich, S. Diele, C. Tschierske, *Liq. Cryst.* **1994**, *17*, 827.
- [295] a) H. S. Frank, W.-Y. Wen, *Discuss. Faraday Soc.* **1957**, *24*, 133; b) L. J. Bellamy, R. L. Pace, *Spectrochim. Acta* **1966**, *22*, 525; c) H. Kleeberg in *Intermolecular Forces. An Introduction to Modern Methods and Results* (Eds.: P. L. Huyskens, W. A. P. Luck, T. Zeegers), Springer, Berlin, **1999**, p. 251.
- [296] M. Sorai, K. Saito, *Chem. Rev.* **2003**, *3*, 29.
- [297] A. Lehmann, A. Diploma Thesis, Halle, **2008**.
- [298] M. O'Keeffe, B. G. Hyde, *Philos. Trans. R. Soc. London Ser. A* **1980**, *295*, 553; O. Delgado-Friedrichs, M. O'Keeffe, O. M. Yagi, *Phys. Chem. Chem. Phys.* **2007**, *9*, 1035.
- [299] B. Grünbaum, G. C. Shephard, *Tilings and Patterns*, W. H. Freeman, New York, **1987**.
- [300] B. Chen, X. Zeng, U. Baumeister, G. Ungar, C. Tschierske, *Science* **2005**, *307*, 96.
- [301] a) M. A. Bates, M. Walker, *Soft Matter* **2009**, *5*, 346; b) M. A. Bates, M. Walker, *Mol. Cryst. Liq. Cryst.* **2010**, *525*, 204; c) M. A. Bates, M. Walker, *Liq. Cryst.* **2011**, *38*, 1749.
- [302] A. J. Crane, F. J. Martinez-Veracoechea, F. A. Escobedo, E. A. Müller, *Soft Matter* **2008**, *4*, 1820; A. J. Crane, E. A. Müller, *J. Phys. Chem. B* **2011**, *115*, 4592.
- [303] S. D. Peroukidis, *Soft Matter* **2012**, *8*, 11062.
- [304] C.-A. Palma, M. Cecchini, P. Samori, *Chem. Soc. Rev.* **2012**, *41*, 3713.
- [305] M. Prehm, F. Liu, U. Baumeister, X. Zeng, G. Ungar, C. Tschierske, *Angew. Chem.* **2007**, *119*, 8118; *Angew. Chem. Int. Ed.* **2007**, *46*, 7972.
- [306] N. M. Patel, M. R. Dodge, M. H. Zhu, R. G. Petschek, C. Rosenblatt, M. Prehm, C. Tschierske, *Phys. Rev. Lett.* **2004**, *92*, 015501; N. M. Patel, I. M. Syed, C. Rosenblatt, M. Prehm, C. Tschierske, *Liq. Cryst.* **2005**, *32*, 55.
- [307] N. Chattham, C. Zhu, X. Cheng, J. Limtrakul, C. Tschierske, J. E. MacLennan, N. A. Clark, *Soft Matter* **2011**, *7*, 9978.
- [308] A. Facchetti, *Chem. Mater.* **2011**, *23*, 733.
- [309] K. Fu, N. Sekine, M. Sone, M. Tokita, J. Watanabe, *Polym. J.* **2002**, *34*, 291.
- [310] B. Carbonnier, T. Pakula, D. A. M. Egbe, *J. Mater. Chem.* **2005**, *15*, 880.
- [311] T. Kim, L. Arnt, E. Atkins, G. N. Tew, *Chem. Eur. J.* **2006**, *12*, 2423.
- [312] P. Riala, A. Andreopoulou, J. Kallitsis, A. Gitsas, G. Floudas, *Polymer* **2006**, *47*, 7241.
- [313] B. Carbonnier, A. K. Andreopoulou, T. Pakula, J. K. Kallitis, *Macromolecules* **2004**, *37*, 3576; B. Carbonnier, A. K. Andreopoulou, T. Pakula, J. K. Kallitis, *Macromol. Chem. Phys.* **2005**, *206*, 66.
- [314] J. Watanabe, N. Sekine, T. Nematsu, M. Sone, H. R. Kricheldorf, *Macromolecules* **1996**, *29*, 4816.
- [315] R. Kieffer, M. Prehm, B. Glettner, K. Pelz, U. Baumeister, F. Liu, X. Zeng, G. Ungar, C. Tschierske, *Chem. Commun.* **2008**, 3861.

- [316] M. Prehm, F. Liu, X. Zeng, G. Ungar, C. Tschierske, *J. Am. Chem. Soc.* **2008**, *130*, 14922.
- [317] M. Prehm, F. Liu, X. Zeng, G. Ungar, C. Tschierske, *J. Am. Chem. Soc.* **2011**, *133*, 4906.
- [318] F. Liu, M. Prehm, X.-B. Zeng, G. Ungar, C. Tschierske, *Angew. Chem.* **2011**, *123*, 10787; *Angew. Chem. Int. Ed.* **2011**, *50*, 10599.
- [319] M. Prehm, Ph.D. Thesis, Halle, **2006**.
- [320] F. Lui, Ph.D. Thesis, Sheffield, **2009**.
- [321] B. Glettner, F. Liu, X. Zeng, M. Prehm, U. Baumeister, G. Ungar, C. Tschierske, *Angew. Chem.* **2008**, *120*, 6169; *Angew. Chem. Int. Ed.* **2008**, *47*, 6080.
- [322] a) H.-J. Kim, Y.-H. Jeong, E. Lee, M. Lee, *J. Am. Chem. Soc.* **2009**, *131*, 17371; b) Z. Huang, S.-K. Kang, M. Banno, T. Yamaguchi, D. Lee, C. Seok, E. Yashima, M. Lee, *Science* **2012**, *337*, 1521.
- [323] W. Li, J. Zhang, B. Li, M. Zhang, L. Wu, *Chem. Commun.* **2009**, 5269; J. Zhang, M. Zhou, S. Wang, J. Carr, W. Li, L. Wu, *Langmuir* **2011**, *27*, 4134; T. Nishizawa, K. Tajima, K. Hashimoto, *J. Mater. Chem.* **2007**, *17*, 2440.
- [324] F. Liu, B. Chen, U. Baumeister, X. B. Zeng, G. Ungar, C. Tschierske, *J. Am. Chem. Soc.* **2007**, *129*, 9578.
- [325] F. Hildebrandt, J. A. Schröter, C. Tschierske, R. Festag, M. Wittenberg, J. H. Wendorff, *Adv. Mater.* **1997**, *9*, 564.
- [326] B. Chen, U. Baumeister, S. Diele, M. K. Das, X. Zeng, G. Ungar, C. Tschierske, *J. Am. Chem. Soc.* **2004**, *126*, 8608.
- [327] B. Chen, U. Baumeister, G. Pelzl, M. K. Das, X. Zeng, G. Ungar, C. Tschierske, *J. Am. Chem. Soc.* **2005**, *127*, 16578.
- [328] J. A. Schröter, C. Tschierske, M. Wittenberg, J. H. Wendorff, *J. Am. Chem. Soc.* **1998**, *120*, 10669.
- [329] F. Liu, B. Chen, B. Glettner, M. Prehm, M. K. Das, U. Baumeister, X. Zeng, G. Ungar, C. Tschierske, *J. Am. Chem. Soc.* **2008**, *130*, 9666.
- [330] B. Chen, X. B. Zeng, U. Baumeister, S. Diele, G. Ungar, C. Tschierske, *Angew. Chem.* **2004**, *116*, 4721; *Angew. Chem. Int. Ed.* **2004**, *43*, 4621.
- [331] A. G. Cook, U. Baumeister, C. Tschierske, *J. Mater. Chem.* **2005**, *15*, 1708.
- [332] J. A. Schröter, C. Tschierske, M. Wittenberg, J. H. Wendorff, *Angew. Chem.* **1997**, *109*, 1160; *Angew. Chem. Int. Ed. Engl.* **1997**, *36*, 1119.
- [333] X.-F. Chen, Z. Shen, X.-H. Wan, X.-H. Fan, E.-Q. Chen, Y. Ma, Q.-F. Zhou, *Chem. Soc. Rev.* **2010**, *39*, 3072.
- [334] I. Tahar-Djebbar, F. Nekelson, B. Heinrich, B. Donnio, D. Guillon, D. Kreher, F. Mathevet, A.-J. Attias, *Chem. Mater.* **2011**, *23*, 4653.
- [335] S. Valkama, T. Ruotsalainen, A. Nykänen, A. Laiho, H. Kosonen, G. ten Brinke, O. Ikkala, J. Ruokolainen, *Macromolecules* **2006**, *39*, 9327.
- [336] R. Mosseri, *C. R. Chim.* **2008**, *11*, 192.
- [337] Simulations^[301c] gave only the smaller tiling by 8-octagons and 4-squares: M. A. Bates, M. Walker, *Phys. Chem. Chem. Phys.* **2009**, *11*, 1893.
- [338] Y. Matsushita, *Polym. J.* **2008**, *40*, 177.
- [339] A. Takano, W. Kawashima, A. Noro, Y. Isono, N. Tanaka, T. Dotera, Y. Matsushita, *J. Polym. Sci. Part B* **2005**, *43*, 2427.
- [340] L. Bartels, *Nat. Chem.* **2010**, *2*, 87; T. Kudernac, S. Lei, J. A. A. W. Elemans, S. De Feyter, *Chem. Soc. Rev.* **2009**, *38*, 402; D. Bonifazi, S. Mohnani, A. Llanes-Pallas, *Chem. Eur. J.* **2009**, *15*, 7004.
- [341] M. Lackinger, W. M. Heckl, *Langmuir* **2009**, *25*, 11307.
- [342] S. Klyatskaya, F. Klappenberger, U. Schlickum, D. Kühne, M. Marschall, J. Reichert, R. Decker, W. Krenner, G. Zoppellaro, H. Brune, J. V. Barth, M. Ruben, *Adv. Funct. Mater.* **2011**, *21*, 1230.
- [343] K. S. Mali, J. Adisojoso, E. Ghijsens, I. de Cat, S. De Feyter, *Acc. Chem. Res.* **2012**, *45*, 1309; K. Tahara, S. Lei, J. Adisojoso, S. De Feyter, Y. Tobe, *Chem. Commun.* **2010**, *46*, 8507; J. A. A. W. Elemans, S. Lei, S. De Feyter, *Angew. Chem.* **2009**, *121*, 7434; *Angew. Chem. Int. Ed.* **2009**, *48*, 7298; S. De Feyter, H. Xu, K. Mali, *Chimia* **2012**, *66*, 38.
- [344] a) K. Tahara, S. Okuhata, J. Adisojoso, S. Lei, T. Fujita, S. De Feyter, Y. Tobe, *J. Am. Chem. Soc.* **2009**, *131*, 17583; b) J. Adisojoso, K. Tahara, S. Lei, P. Szabelski, W. Rzyzsko, K. Inukai, M. O. Blunt, Y. Tobe, S. De Feyter, *ACS Nano* **2012**, *6*, 897.
- [345] J. Carrasco, A. Michaelides, M. Forster, S. Haq, R. Raval, A. Hodgson, *Nat. Mater.* **2009**, *8*, 427.
- [346] J. Liu, T. Lin, Z. Shi, F. Xia, L. Dong, P. N. Liu, N. Lin, *J. Am. Chem. Soc.* **2011**, *133*, 18760.
- [347] K. Tahara, T. Balandina, S. Furukawa, S. De Feyter, Y. Tobe, *CrystEngComm* **2011**, *13*, 5551.
- [348] C. Ren, F. Zhou, B. Qin, R. Ye, S. Shen, H. Su, H. Zeng, *Angew. Chem.* **2011**, *123*, 10800; *Angew. Chem. Int. Ed.* **2011**, *50*, 10612.
- [349] I. Nierengarten, S. Guerra, M. Holler, J.-F. Nierengarten, R. Deschenaux, *Chem. Commun.* **2012**, *48*, 8072.
- [350] S.-S. Jester, E. Sigmund, S. Höger, *J. Am. Chem. Soc.* **2011**, *133*, 11062.
- [351] D. Écija, J. I. Urgel, A. C. Papageorgiou, S. Joshi, W. Auwärter, A. P. Seitsonen, S. Klyatskaya, M. Ruben, S. Fischer, S. Vijayaraghavan, J. Reichert, J. V. Barth, *Proc. Natl. Acad. Sci. USA* **2013**, *110*, 6678.
- [352] H. Zhou, H. Dang, J.-H. Yi, A. Nanci, A. Rochefort, J. D. Wuest, *J. Am. Chem. Soc.* **2007**, *129*, 13774; M. Blunt, X. Lin, M. D. Gimenez-Lopez, M. Schröder, N. R. Champness, P. H. Beton, *Chem. Commun.* **2008**, 2304.
- [353] U. Schlickum, R. Decker, F. Klappenberger, G. Zoppellaro, S. Klyatskaya, W. Auwärter, S. Neppel, K. Kern, H. Brune, M. Ruben, J. V. Barth, *J. Am. Chem. Soc.* **2008**, *130*, 11778.
- [354] J. Adisojoso, K. Tahara, S. Okuhata, S. Lei, Y. Tobe, S. De Feyter, *Angew. Chem.* **2009**, *121*, 7403; *Angew. Chem. Int. Ed.* **2009**, *48*, 7267.
- [355] Other filled 2D nets: S. Furukawa, K. Tajara, F. C. De Schryver, M. Van der Auweraer, Y. Tobe, S. De Feyter, *Angew. Chem.* **2007**, *119*, 2889; *Angew. Chem. Int. Ed.* **2007**, *46*, 2831; Y. Li, Z. Ma, K. Deng, S. Lei, Q. Zeng, X. Fan, S. De Feyter, W. Huang, C. Wang, *Chem. Eur. J.* **2009**, *15*, 5418; T. Balandina, K. Tahara, N. Sändig, M. O. Blunt, J. Adisojoso, S. Lei, F. Zerbetto, Y. Tobe, S. De Feyter, *ACS Nano* **2012**, *6*, 8381.
- [356] Other examples of complex multicomponent tiling patterns: S.-S. Jester, E. Sigmund, L. M. Röck, S. Höger, *Angew. Chem.* **2012**, *124*, 8683; *Angew. Chem. Int. Ed.* **2012**, *51*, 8555; J. Liu, T. Chen, X. Deng, D. Wang, J. Pei, L.-J. Wan, *J. Am. Chem. Soc.* **2011**, *133*, 21010.
- [357] S. H. Ko, M. Su, C. Zhang, A. E. Ribbe, W. Jiang, C. Mao, *Nat. Chem.* **2010**, *2*, 1050; W. Liu, H. Zhong, R. Wang, N. C. Seeman, *Angew. Chem.* **2011**, *123*, 278; *Angew. Chem. Int. Ed.* **2011**, *50*, 264; J. Malo, J. C. Mitchell, A. J. Turberfield, *J. Am. Chem. Soc.* **2009**, *131*, 13574.
- [358] A. L. Boyle, E. H. C. Bromley, G. J. Bartlett, R. B. Sessions, T. H. Sharp, C. L. Williams, P. M. G. Curmi, N. R. Forde, H. Linke, D. N. Woolfson, *J. Am. Chem. Soc.* **2012**, *134*, 15457.
- [359] D. Maspoch, D. Ruiz-Molina, J. Vecian, *Chem. Soc. Rev.* **2007**, *36*, 770; J. J. Perry IV, J. A. Perman, M. J. Zaworotko, *Chem. Soc. Rev.* **2009**, *38*, 1400.
- [360] A. P. Cote, A. I. Benin, N. W. Ockwig, M. O'Keeffe, A. J. Matzger, O. M. Yaghi, *Science* **2005**, *310*, 1166; X. Feng, X. Ding, D. Jiang, *Chem. Soc. Rev.* **2012**, *41*, 6010; E. L. Spitzer, J. W. Colson, F. J. Uribe-Romo, A. R. Woll, M. R. Giovino, A. Saldivar, W. R. Dichtel, *Angew. Chem.* **2012**, *124*, 2677; *Angew. Chem. Int. Ed.* **2012**, *51*, 2623.
- [361] M. A. Horsch, Z. Zhang, S. C. Glotzer, *Nano Lett.* **2006**, *6*, 2406; T. D. Nguyen, S. C. Glotzer, *ACS Nano* **2010**, *4*, 2585.
- [362] a) G. Pelzl, S. Diele, W. Weissflog, *Adv. Mater.* **1999**, *11*, 707; b) R. A. Reddy, C. Tschierske, *J. Mater. Chem.* **2006**, *16*, 907;

- c) H. Takezoe, Y. Takanishi, *Jpn. J. Appl. Phys. Part I* **2006**, *45*, 597; d) J. Etxebarria, M. B. Ros, *J. Mater. Chem.* **2008**, *18*, 2919; e) G. Pelzl, W. Weissflog, *Thermotropic Liquid Crystals: Recent Advances* (Ed.: A. Ramamoorthy), Springer, Berlin, **2007**, pp. 1–58; f) A. Eremin, A. Jakli, *Soft Matter* **2013**, *9*, 615.
- [363] L. E. Hough, H. T. Jung, D. Krüerke, M. S. Heberling, M. Nakata, C. D. Jones, D. Chen, D. R. Link, J. Zasadzinski, G. Heppke, J. P. Rabe, W. Stocker, E. Körblova, D. M. Walba, M. A. Glaser, N. A. Clark, *Science* **2009**, *325*, 456.
- [364] C. Keith, A. Lehmann, U. Baumeister, M. Prehm, C. Tschierske, *Soft Matter* **2010**, *6*, 1704.
- [365] T. Niori, F. Sekine, J. Watanabe, T. Furuwara, H. Takezoe, *J. Mater. Chem.* **1996**, *6*, 1231.
- [366] G. Dantlgraber, A. Eremin, S. Diele, A. Hauser, H. Kresse, G. Pelzl, C. Tschierske, *Angew. Chem.* **2002**, *114*, 2514; *Angew. Chem. Int. Ed.* **2002**, *41*, 2408; C. Keith, R. A. Reddy, A. Hauser, U. Baumeister, C. Tschierske, *J. Am. Chem. Soc.* **2006**, *128*, 3051.
- [367] a) C. Keith, R. A. Reddy, H. Hahn, H. Lang, C. Tschierske, *Chem. Commun.* **2004**, 1898; b) Y. Zhang, U. Baumeister, C. Tschierske, M. J. O'Callaghan, C. Walker, *Chem. Mater.* **2010**, *22*, 2869; c) R. A. Reddy, C. Zhu, R. Shao, E. Körblova, T. Gong, Y. Shen, E. Garcia, M. A. Glaser, J. E. MacLennan, D. M. Walba, N. A. Clark, *Science* **2011**, *332*, 72.
- [368] A. Jakli, I. C. Pintre, J. L. Serrano, M. B. Ros, M. R. de la Fuente, *Adv. Mater.* **2009**, *21*, 3784.
- [369] a) E. Gorecka, D. Pociecha, F. Araoka, D. R. Link, M. Nakata, J. Thisayukta, Y. Takanishi, K. Kishikawa, J. Watanabe, H. Takezoe, *Phys. Rev. E* **2000**, *62*, R4524; b) M. Nakata, D. R. Link, J. Thisayukta, Y. Takanishi, K. Ishikawa, J. Watanabe, H. Takezoe, *J. Mater. Chem.* **2001**, *11*, 2694.
- [370] D. M. Walba, E. Körblova, R. Shao, J. E. MacLennan, D. R. Link, M. A. Glaser, N. A. Clark, *Science* **2000**, *288*, 2181.
- [371] R. A. Reddy, B. K. Sadashiva, *Liq. Cryst.* **2003**, *30*, 1031.
- [372] Ferroelectric and antiferroelectric LCs were also reported for chiral rod-like molecules organized in SmC phases. In this case, the reduction of the symmetry and polar order are due to the molecular chirality; however, as molecular chirality supports the formation of helical superstructures these LC phases represent helielectric phases: A. Fukuda, Y. Takanishi, T. Isozaki, K. Lshikawa, H. Takezoe, *J. Mater. Chem.* **1994**, *4*, 997; S. T. Lagerwall, *Ferroelectric and Antiferroelectric Liquid Crystals*, Wiley-VCH, Weinheim, **1999**.
- [373] Ferroelectricity in columnar phases: D. Miyajima, F. Araoka, H. Takezoe, J. Kim, K. Kato, M. Takata, T. Aida, *Science* **2012**, *336*, 209.
- [374] D. A. Coleman, J. Fernsler, N. Chattham, M. Nakata, Y. Takanishi, E. Körblova, D. R. Link, R.-F. Shao, W. G. Jang, J. E. MacLennan, O. Mondainn-Monval, C. Boyer, W. Weissflog, G. Pelzl, L.-C. Chien, J. Zasadzinski, J. Watanabe, D. M. Walba, H. Takezoe, N. A. Clark, *Science* **2003**, *301*, 1204.
- [375] N. Vaupotic, D. Pociecha, E. Gorecka, *Top. Curr. Chem.* **2012**, *318*, 281.
- [376] D. R. Link, G. Natale, R. Shao, J. E. MacLennan, N. A. Clark, E. Körblova, D. M. Walba, *Science* **1997**, *278*, 1924; D. M. Walba in *Materials-Chirality*, Vol. 24 of *Top. Stereochem.* (Eds.: M. M. Green, R. J. M. Nolte, E. W. Meijer), Wiley, New York, **2003**.
- [377] L. Pérez-García, D. B. Amabilino, *Chem. Soc. Rev.* **2002**, *31*, 342; L. Pérez-García, D. B. Amabilino, *Chem. Soc. Rev.* **2007**, *36*, 941; *Chirality at the Nanoscale* (Ed.: D. B. Amabilino), Wiley-VCH, Weinheim, **2009**; Y. Wang, J. Xu, Y. Wang, H. Chen, *Chem. Soc. Rev.* **2013**, *42*, 2930.
- [378] Supramolecular tilt chirality of 2_1 helical arrangements has been recently discussed: I. Hisaki, T. Sasaki, N. Tohnai, M. Miyata, *Chem. Eur. J.* **2012**, *18*, 10066.
- [379] J. P. Bedel, J. C. Rouillon, J. P. Mercierou, H. T. Nguyen, M. F. Achard, *Phys. Rev. E* **2004**, *69*, 061702; M. Nakata, R.-F. Shao, J. E. MacLennan, W. Weissflog, N. A. Clark, *Phys. Rev. Lett.* **2006**, *96*, 067802; M. W. Schröder, S. Diele, G. Pelzl, W. Weissflog, *ChemPhysChem* **2004**, *5*, 99.
- [380] J. Szydłowska, J. Mieczkowski, J. Matraszek, D. W. Bruce, E. Gorecka, D. Pociecha, D. Guillon, *Phys. Rev. E* **2003**, *67*, 031702.
- [381] a) C. Keith, R. A. Reddy, U. Baumeister, C. Tschierske, *J. Am. Chem. Soc.* **2004**, *126*, 14312; b) C. Keith, R. A. Reddy, M. Prehm, U. Baumeister, H. Kresse, J. L. Chao, H. Hahn, H. Lang, C. Tschierske, *Chem. Eur. J.* **2007**, *13*, 2556.
- [382] H. Ocak, B. Bilgin-Eran, M. Prehm, S. Schymura, J. P. F. Lagerwall, C. Tschierske, *Soft Matter* **2011**, *7*, 8266.
- [383] G. Pelzl, S. Diele, A. Jakli, C. Lischka, I. Wirth, W. Weissflog, *Liq. Cryst.* **1999**, *26*, 135.
- [384] J. P. F. Lagerwall, F. Giesselmann, *ChemPhysChem* **2010**, *11*, 975.
- [385] H. Takezoe, *Top. Curr. Chem.* **2012**, *318*, 303.
- [386] L. E. Hough, M. Spannuth, M. Nakata, D. A. Coleman, C. D. Jones, G. Dantlgraber, C. Tschierske, J. Watanabe, E. Körblova, D. M. Walba, J. E. MacLennan, M. A. Glaser, N. A. Clark, *Science* **2009**, *325*, 452; D. Chen, Y. Shen, C. Zhu, L. E. Hough, N. Gimeno, M. A. Glaser, J. E. MacLennan, M. B. Ros, N. A. Clark, *Soft Matter* **2011**, *7*, 1879.
- [387] L. Pasteur, *C. R. Hebd. Seances Acad. Sci.* **1848**, *26*, 535.
- [388] H. Ocak, B. Bilgin-Eran, M. Prehm, C. Tschierske, *Soft Matter* **2012**, *8*, 7773.
- [389] D. J. Earl, M. A. Osipov, H. Takezoe, Y. Takanishi, M. R. Wilson, *Phys. Rev. E* **2005**, *71*, 021706; S. Kawauchi, S.-W. Choi, K. Fukuda, K. Kishikawa, J. Watanabe, H. Takezoe, *Chem. Lett.* **2007**, *36*, 750; S.-W. Choi, S. Kang, Y. Takanishi, K. Ishikawa, J. Watanabe, H. Takezoe, *Chirality* **2007**, *19*, 250; F. Yan, C. A. Hixson, D. J. Earl, *Soft Matter* **2009**, *5*, 4477.
- [390] H. Niwano, M. Nakata, J. Thisayukta, D. R. Link, H. Takezoe, J. Watanabe, *J. Phys. Chem. B* **2004**, *108*, 14889.
- [391] T. Otani, F. Araoka, K. Ishikawa, H. Takezoe, *J. Am. Chem. Soc.* **2009**, *131*, 12368.
- [392] J. Thisayukta, Y. Nakayama, S. Kawauchi, H. Takezoe, J. Watanabe, *J. Am. Chem. Soc.* **2000**, *122*, 7441.
- [393] M. Alaasar, M. Prehm, M. Nagaraj, J. K. Vij, C. Tschierske, *Adv. Mater.* **2013**, *25*, 2186.
- [394] A. de Vries, *J. Mol. Liq.* **1986**, *31*, 193; P. Sarkar, P. K. Sarkar, S. Paul, P. Mandal, *Phase Transitions* **2000**, *71*, 1; I. G. Chistyakov, W. M. Chaikowsky, *Mol. Cryst. Liq. Cryst.* **1969**, *7*, 269; G. W. Stewart, R. M. Morrow, *Phys. Rev.* **1927**, *30*, 232.
- [395] G. Pelzl, A. Eremin, S. Diele, H. Kresse, W. Weissflog, *J. Mater. Chem.* **2002**, *12*, 2591; V. Görtz, *Liq. Cryst. Today* **2010**, *19*, 37.
- [396] V. P. Panov, M. Nagaraj, J. K. Vij, Y. P. Panarin, A. Kohlmeier, M. G. Tamba, R. A. Lewis, G. H. Mehl, *Phys. Rev. Lett.* **2010**, *105*, 167801; M. Cestari, S. Diez-Berart, D. A. Dunmur, A. Ferrarini, M. R. de la Fuente, D. A. Jackson, D. O. Lopez, G. R. Luckhurst, M. A. Perez-Jubindo, R. M. Richardson, J. Salud, B. A. Timimi, H. Zimmermann, *Phys. Rev. E* **2011**, *84*, 031704; P. A. Henderson, C. T. Imrie, *Liq. Cryst.* **2011**, *38*, 1407.
- [397] I. Dozov, *Europhys. Lett.* **2001**, *56*, 247.
- [398] D. M. Walba, L. Eshdat, E. Körblova, R. K. Shoemaker, *Cryst. Growth Des.* **2005**, *5*, 2091.
- [399] H. S. Jeong, S. Tanaka, D. K. Yoon, S.-W. Choi, Y. H. Kim, S. Kawauchi, F. Araoka, H. Takezoe, H. T. Jung, *J. Am. Chem. Soc.* **2009**, *131*, 15055.
- [400] H. Nagayama, S. K. Varshney, M. Goto, F. Araoka, K. Ishikawa, V. Prasad, H. Takezoe, *Angew. Chem.* **2010**, *122*, 455; *Angew. Chem. Int. Ed.* **2010**, *49*, 445.
- [401] T. Kajitani, S. Kohmoto, M. Yamamoto, K. Kishikawa, *Chem. Mater.* **2005**, *17*, 3812.
- [402] S. A. Kauffmann, *The Origins of Order*, Oxford University Press, New York, **1993**.

- [403] H. S. Kitzerow, C. Bahr, *Chirality in Liquid Crystals*, Springer, New York, **2001**; I. Nishiyama, *Chem. Rec.* **2009**, *9*, 340.
- [404] a) *Liquid Crystalline Functional Assemblies and their Supramolecular Structures*, Vol. 128 of *Struct. Bond.* (Ed.: T. Kato), Springer, Berlin, **2008**; b) R. D. Costa, F. Werner, X. Wang, P. Grönninger, S. Feihl, F. T. U. Kohler, P. Wasserscheid, S. Hibler, R. Beranek, K. Meyer, D. M. Guldi, *Adv. Energy Mater.* **2013**, *3*, 657.
- [405] J. P. F. Lagerwall, G. Scalia, *Curr. Appl. Phys.* **2012**, *12*, 1387; L. C. Palmer, S. I. Stupp, *Acc. Chem. Res.* **2008**, *41*, 1674.
- [406] O. Stamatoiu, J. Mirzaei, X. Feng, T. Hegmann, *Top. Curr. Chem.* **2012**, *318*, 331.
- [407] E. van den Pol, A. V. Petukhov, D. M. E. Thies-Weesie, G. J. Vroege, *Langmuir* **2010**, *26*, 1579.
- [408] Y. Bouligand, *C. R. Chim.* **2008**, *11*, 281.
- [409] H. Ringsdorf, B. Schlarb, J. Venzmer, *Angew. Chem.* **1988**, *100*, 117; *Angew. Chem. Int. Ed. Engl.* **1988**, *27*, 113.
- [410] Z. Almsheerqi, S. Hyde, M. Ramachandran, Y. Deng, *J. R. Soc. Interface* **2008**, *5*, 1023; Z. Almsheerqi, F. Margadant, Y. Deng, *Interface Focus* **2012**, *2*, 539.
- [411] S. Hyde, S. Andersson, K. Larsson, Z. Blum, T. Landh, S. Lidin, B. W. Ninham, *The Language of Shape*, Elsevier, Amsterdam, **1997**.
- [412] F. Livolant, A. Leforestier, *Prog. Polym. Sci.* **1996**, *21*, 1115; F. Livolant, S. Mangelot, A. Leforestier, A. Bertin, M. de Frutos, E. Raspaud, D. Durand, *Philos. Trans. R. Soc. London Ser. A* **2006**, *364*, 2615.
- [413] S. Hoffmann, *Molekulare Matrizen I–IV*, Akademie-Verlag Berlin, Berlin, **1978**; S. Hoffmann, W. Witkowski, *Mesomorphic Order in Polymers and Polymerization in Liquid Crystalline Media*, Vol. 74 of *Am. Chem. Soc. Symp. Ser.* (Ed.: A. Blumstein), **1978**, p. 178; W.-V. Meister, S. Lindau, A. L. Hauser, C. Bohley, U. Gromann, S. Naumann, M. Madre, L. Kovalenko, G. Bischoff, R. Zhuk, S. Hoffmann, *J. Biomol. Struct. Dyn.* **2000**, *18*, 385.
- [414] G. T. Stewart, *Liq. Cryst.* **2004**, *31*, 443.
- [415] T. Bellini, G. Zanchetta, T. P. Fraccia, R. Cerbino, E. Tsai, G. P. Smith, M. J. Moran, D. M. Walba, N. A. Clark, *Proc. Natl. Acad. Sci. USA* **2012**, *109*, 1110; M. Nakata, G. Zanchetta, B. D. Chapman, C. D. Jones, J. O. Cross, R. Pindak, T. Bellini, N. A. Clark, *Science* **2007**, *318*, 1276.